POLITECNICO DI TORINO

Master of Science in Mechanical Engineering

Master's Degree Thesis

Study of Abusive Head Trauma: human body model and finite element analysis

Academic Supervisors: Candidate:

Prof. Giorgio Chiandussi   Gianmarco Cane
Prof. Alessandro Scattina

Academic Year 2019-2020

SUMMARY

ABSTRACT

The Abusive Head Trauma (AHT), which is also commonly known as Shaken Baby Syndrome (SBS), is represented by a severe set of injuries to a child's head and neck also without exterior signs and can be classified as a non-accidental or an accidental trauma, depending on the circumstances. This trauma type can bring various potential consequences and some among them can be serious. A shaking movement impressed from another person commonly causes this injury, and it may or may not include an impact with a surface.

The aim of the present thesis's work is to simulate the AHT phenomena thanks to the Finite Element Method (FEM), in order to evaluate the potential risks for child's health. The PIPER child model, a finite element model better described later, has been used. The software used to perform the simulation of the shaking action is LS-Dyna, with the aid of LS-PrePost. The first three chapters of the thesis recall various useful information found in literature: in the introduction, the trauma mechanism is presented, then injury criteria and the present state-of-the-art about AHT are introduced. Thereafter, several parameters taken into account in the shaking simulation (normally called pre-processing phase) are presented (chapter 4) and some are further analysed in order to evaluate the child's trauma thanks to several different criteria present in the biomedical literature. The most important outputs for this analysis are kinematic parameters as accelerations and velocities. Maximum values and injury damages have been evaluated and compared. The results are compared with those from other studies in order to verify their rightness.

1. DESCRIPTION OF THE PHENOMENON

1.1 DEFINITION

Abusive Head Trauma (AHT) concerns a set of injuries in charge of a child's neck and head (skull and intracranial contents) [1, 2] and they are caused by the movement imposed to the child body thus provoking an uncontrolled movement of the head, cause of severe injuries [3]. Most of times it is a non-accidental injury: whom shakes, provoking the damage, generally does not know that the medical (and sometimes legal) consequences can be very serious, possibly causing an important damage to the child. The phenomenon is schematically drawn in Figure 1.

Figure 1 – A child shacked by adult's hands at the thorax level: damages can be caused by brain movement inside the skull.

In the biomedical and biomechanical literature, the phenomenon has been named differently. Sometimes this differentiation may bring confusion to the reader. The terms most frequently used in literature and in clinical papers are:

- Shaken Baby Syndrome (SBS): this is the historical definition used starting from 1976, introduced by Caffey [4]. This termination describes a violent shaking, which can be related to different intracranial lesions caused by the acceleration the brain is subjected to.
- Shaken Impact Syndrome (SIS): includes in the abuse mechanism an impact with a surface, eventually with exterior signs of the collision.
- Abusive Head Trauma (AHT): is the generic terminology associated with this pathology, independently from the mechanism that has generated the injury.

- Non-Accidental Head Injury (NAHI): it is intended as non-accidental, so it can also not include an abuse made on purpose.

In 2009, the American Academy of Paediatrics (AAP) recommended in the medical field to use the unique terminology Abusive Head Trauma, independently from every possible difference between the episodes. From a medical point of view, AHT and SBS have the same pathogenic hypotheses [5]. The AAP proposes a definition for this pathology, to remove any possible misunderstanding: AHT is a "*well-recognized constellation of brain injuries caused by the directed application of force (shaking or direct impact) to an infant or young child, resulting in physical injury to the head and/or its contents*" [3].

1.2 RISK FACTORS

In the majority of the cases checked in clinical data, the victims of the Abusive Head Trauma are very young: the age of the children usually ranges from few months to one year. In addition, in general the AHT phenomenon is related to children younger than 4 years. Usually, there are some characteristics which are classifiable as principal risk factors for the child, because are typical peculiarities observed in several cases of abuse. Some of them are the following [2]:

- Male gender of the child
- Premature-born baby
- Handicap conditions
- Neonatal abstinence syndrome
- Several crying crises

The perpetrators of the abuse are often parents or caregivers. It is possible to list also some typical risk factors concerning them:

- Male gender of the perpetrator
- Young age (often younger than 24 years)
- State of depression
- Use of drugs
- Previous violet episodes
- Mental upsets and instability
- Impulsive behaviour

According to American studies, over a sample of 100.000 babies younger than 2 years, there are 17 cases of non-accidental trauma (0,017 %) and 15 cases (0,015 %) of accidental trauma. Between them, almost 25% of the victims die after few days or few weeks. In the remaining cases, almost the 75% of the children exhibit permanent damages, that can be both physical and psychological [6, 7]. The incidence of the phenomenon is similar in Europe, where is estimated almost 2,5 cases over 10.000 one-year old children [8]. These examples of data clearly state that the consequences aroused by this phenomenon can be really serious for the child's health, sometimes lethal.

1.3 DAMAGE MECHANISM

Head's injuries occur during a shaking episode (Figure 2) in which a child is usually taken from the thorax or from the arms and is strongly shaken. In this case, the head of the child rotates around the neck in an uncontrollable way, because the muscles of the infant are not developed enough to sustain well the head. This movement causes in baby's head abrupt angular accelerations: the resultant rotational forces may cause rupture in blood vessels, producing hematomas, cerebral contusion, haemorrhages (retinal and subdural) and, eventually, the fracture of the skull and injuries of the spine [9]. The brain mass bounces against the skull, moving backward and forward and, sometimes, this gives rise to the rupture of the blood vessels and nerves. The brain tissue can be teared. The brain may strike the inside of the skull, causing bruising and bleeding. The damage can be even more serious when a shaking episode ends with an impact against some surface (Figure 3), indeed in this case accelerations could be more critical [10]. However, the diagnosis of AHT can be formulated also if there are no impacts against any surface. In both cases (with or without impact) damages can occur for the same motivation: an unexpected acceleration of the brain.
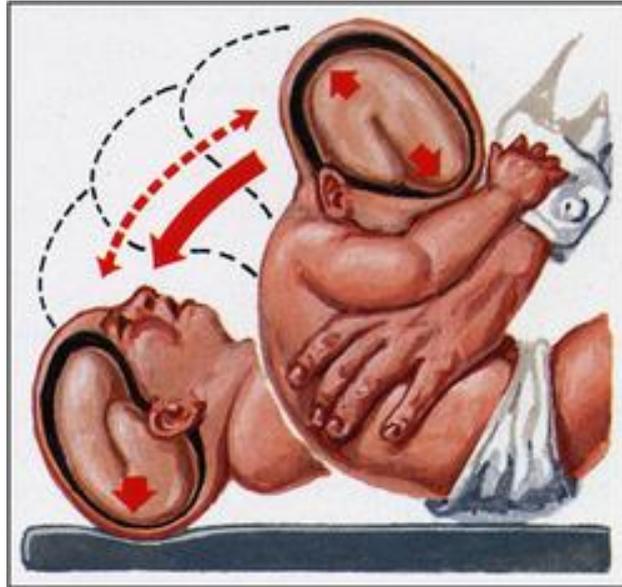
Figure 2 - A sketch of the damage mechanism with impact
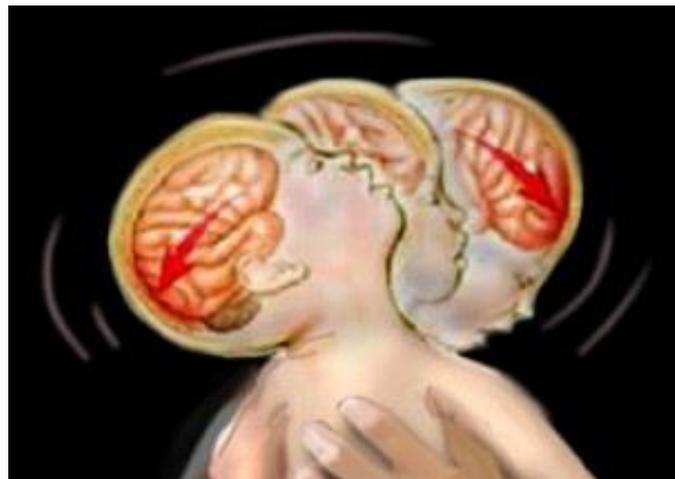
Figure 3 - A sketch of the damage mechanism without impact

Most of the victims of AHT are children younger than 1 year, even if the injuries can occur also in children up to 4 years. The anatomy of the infants is different from the adult's one: the volume and the mass of the head is relevant compared with the total mass of the body (about 15%). In addition, the skeletal structure is more vulnerable than the adult's one, the neurological system is not mature and it has a big content of water, moreover the head is delicate [11, 12]. The immature brain of a child requires a different balance of neurotransmission, blood and energy; so this may predispose to a poorer injury phenotype [3].

1.4 BRAIN CHARACTERISTICS

In the literature, there is a lot of information about brain injuries and how each damage can be quantified. However, there is not a unique mechanical property or a mathematical parameter which can be considered to quantify a brain damage (subdural hematoma, retinal bleeding, etc...). For this reason, it is difficult to define injury mechanisms in mathematical terms. According to the general medical outcome, the principal mechanism that should be considered is the bridging vein rupture that can be caused from shaking. Starting from it, some parameters have to be investigated in detail.

To understand brain injury, the principal physical properties of the brain should be figured out. According to the studies of AHS Holbourn, the brain has some basic properties:

- relatively uniform density;
- extreme incompressibility due to the large content of water (it is estimated that a force of 10000 t is required to reduce the brain's volume of a half);
- low module of stiffness (brain offers a little resistance to changes in shape compared to changes in size).

These three properties make the damage level proportional to the applied shearing stresses, bringing an important conclusion: generated rotational forces may produce a tissue injury through shearing within an intact skull. In opposition, usually the translational forces alone are not able to produce this effect, because they do not produce diffuse lesions [13].

1.5 INJURIES

The pathogenic effects of a shaking episode should be described in order to understand and associate the biomechanical parameters that have to be examined. The typical clinical consequences caused by the AHT have been mentioned in the previous paragraph. Herein a more detailed description is given.

- Subdural hematoma

This is the most frequent effect of the AHT, because it is the direct consequence of angular accelerations. It is usually abbreviated with the acronyms SDH. The rotational forces cause a rotation between the brain and the dura mater; the potential effect of this is the rupture of blood vessels. The blood may accumulate between the dura mater and the arachnoid mater of the meninges leading to the raise of a subdural hematoma. As shown in Figure 4, the subdural hematoma can be superficial

or not. Subdural hematomas can increase the pressure inside the skull, damaging the brain tissue [14]. The diagnosis can be defined thanks to a CT scan, as shown in Figure 5.
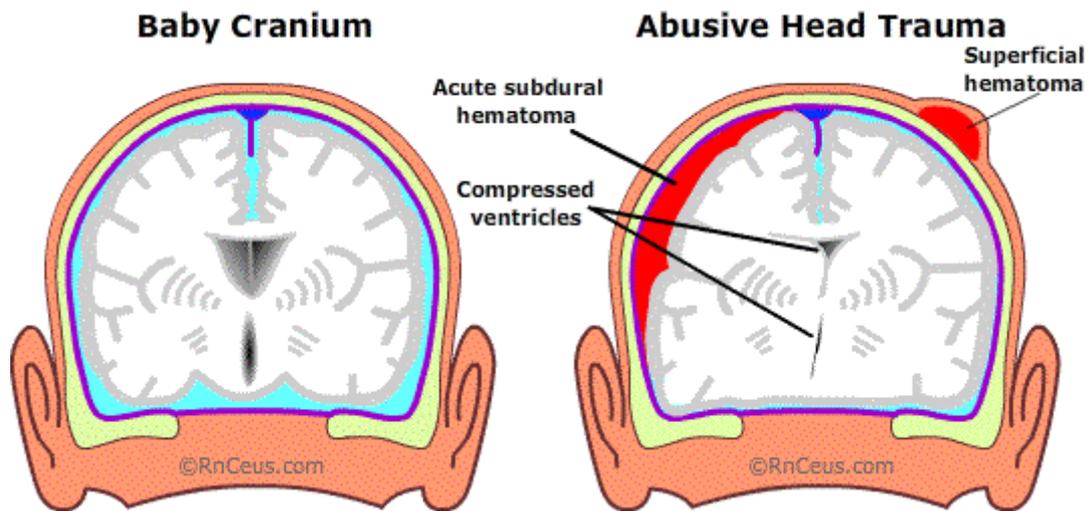

Figure 4 - The difference between a normal child's brain and an "abused" one

Figure 5 - Large left sided frontal parietal subdural hematoma with associated midline shift.

According to different studies, the rotational accelerations play an important role for SDH. Starting from 1960s, Ommaya described the potential danger of subdural haemorrhage also in the absence of any impact; this result was obtained from the analysis of primate experiments demonstrating the importance of sagittal plane rotational acceleration, noting that substantial SDHs were only seen after

the rotational component was introduced. As said previously, it should also be noted that in the biomedical literature there is not a specific mathematical quantity responsible for the head trauma. This means that for a complete comprehension of the phenomenon also other quantities should be considered, as velocity, strain rate, force, energy, or power, or some others [13].

- Retinal bleeding

Retinal bleeding represents a common symptom (50-100%) and for this reason it is important for the diagnosis. It consists of a blood lost from the retina provoked from a blockage of a vein. The importance of this injury in AHT was demonstrated in several studies, for example the one performed from Nadarasa et al. [15]. Using a 6-week-old dummy, they have carried out five simulations of impacts and three simulations of shaking episodes, comparing the results obtained from the two cases. The first ones simulate five different impacts: grass fall, lino fall, concrete fall, wall impact and a second concrete fall. The shaking episodes are performed with a frequency of excitation that ranges from 5 Hz to 6 Hz.

Results have shown that four parameters are relevant for shaking–fall comparison: these are pressure, Von Mises stress and strain, 1st principal stress. Also in this case is proofed the relevance of the rotational acceleration in the injury mechanism. For the selected parameters, it appears very clearly that the maxima registered values are much higher under shaking loading than for fall or wall impact, whereas the acceleration level an order of magnitude smaller in SBS events (Table 1).

Choroid	SBS	Fall	Ratio SBS/fall
Max pressure (kPa)	11.5	4.75	2.42
Max Von Mises stress (kPa)	32.3	7.53	4.29
Max 1st principal stress (kPa)	21.4	5.42	3.95
Max Von Mises strain	0.28	0.019	14.74
Retina	SBS	Fall	Ratio SBS/fall
Max pressure (kPa)	1.43	0.34	4.21
Max Von Mises stress (kPa)	2.35	0.55	4.27
Max 1st principal stress (kPa)	2.61	0.4	6.53
Max Von Mises strain	0.28	0.019	14.74

Table 1 - Comparison between shaken-baby cases and fall cases, for what concerns the eye damages

The conclusion of the comparison is yet simple: if moderate and severe falls can induce few retinal haemorrhages, shaking events are more likely to create these injuries than even severe falls.

- Encephalopathy

This term includes different neurological symptoms, some of them generic as vomit, convulsions, irritability or cerebral oedema. This last symptom is an alteration generally subsequent to a Diffuse Axonal Injury (DAI). DAI is for sure the principal aspect of encephalopathy that should be underlined. DAI (Figure 6) is associated with mechanical disruption of many axons in the cerebral hemispheres and subcortical white matter; lesions may occur over a widespread area in white matter tracts as well as grey matter. It can involve loss of consciousness lasting for days to weeks. Severe memory and motor deficits and posttraumatic amnesia may last for weeks. This injury can be caused from forces generated by rapid velocities or accelerations, referring to the centre of gravity of the head [16, 17].
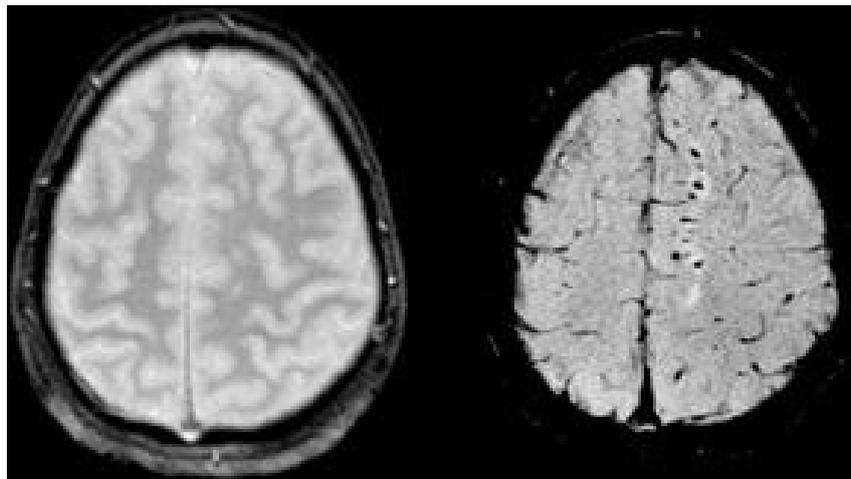

Figure 6 - Images from a magnetic resonance.

The biomechanical evaluation of DAI is associated with intracerebral stresses and strains, which can be linked to angular kinematic parameters according to several researchers (that will be introduced later) [17].

Another injury caused from AHT is the hyperextension or hyperflexion of the cervical spine. It is a consequence of the movement caused by shaking, colloquially called "whiplash". It can provoke damage in the nerve roots of some vertebrae, in particular C3, C4 and C5, shown in Figure 7 [18].

The parameter most useful for the evaluation of this damage is the rotational angle of the head around the neck.
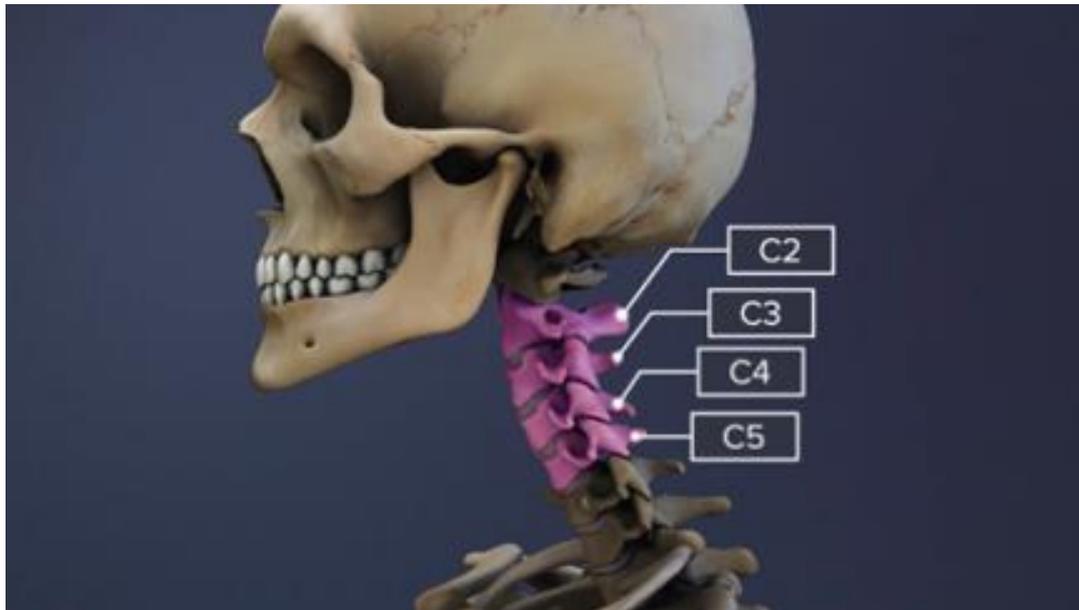

Figure 7 - Positions of vertebrae C2, C3, C4 and C5

1.6 LEGAL ASPECT AND PREVENCTION

Few words should be spent also about the legal perspective, often considered in various situations of AHT. The biomechanical study of the phenomenon of the Abusive Head Trauma can be relevant in two different ways: for medical knowledge and diagnosis, but also for a legal aspect. As a matter of the fact, the AHT is obviously considered a case of child abuse and it is, in this field, the prevalent cause of death in the most developed countries in the world [19]. The mechanical analysis of this kind of injury can be also useful in the real cases in which who made the abuse must be judged. A doctor, who understands that a child was subjected to an abuse after a medical analysis, is forced to report the fact to a competent authority (in general this is true also for adult victims of every kind of abuse). This is a juridical and deontological obligate [2]. An AHT diagnosis may bring serious consequences for the perpetrators, indeed they could be blamed for abuse. Actually, the differentiation between accidental or non-accidental trauma should be relevant especially in this case, but currently there is not a medical test that can certainly distinguish between the two cases. If the perpetrators are the parents, they can lose any right and authority over the child. Moreover, people, which are declared guilty, can be punished also with a period of detention in jail.

Preventing the phenomenon of abusive head trauma represents an important start point to reduce child abuse, maltreatment, and to increase the ethical education. Prevention includes public service

announcements, pamphlets, and brochures. Education is often focused on family resource centres, in particular in high-risk homes where parents are young and live in poverty conditions. Prevention programs can include mental and social services. It should be focalized in two areas: a parental education about crying and an information about the existence of AHT and its consequences. In few words, parents should be instructed in the danger of shaking a baby with an undeveloped brain and they need to learn how to deal with crying crises [20].

2. INJURY CRITERIA

Evaluating brain injuries is a difficult process, because there are many criteria and parameters that can be considered, each of them including different hypotheses and conditions. The literature presents many scientific articles and essays that debate AHT, sometimes making a comparison with the cases of impacts or falls. Moreover, the argument of head injury is generally discussed in many research works (for example about car accident or domestic accident) also for the adults, so the final conclusions can also be contemplated and adapted in the AHT case. Many studies underline the dangerousness of the shaking episode, finding possible injuries also in absence of any kind of collision.

According to the studies of many researchers, the kinematic parameters as velocities and accelerations (measured at the head's centre of gravity) assume an important role in the damage's evaluation. Most of criteria use angular velocities and accelerations because the rotational phenomena are the principle responsible factors for some damages of the AHT: the subdural hematoma and the diffuse axonal injury. In the case of SDH they are responsible for vein's rupture; in the DAI case, they are directly linked with stresses and strains. In the biomedical and biomechanical literature, as said, there are several criterions based on different hypothesis or experiments and a lot of aspects that are following described.

To evaluate the damage, it is convenient to use different criteria, comparing the differences between the resulting injury probabilities. In general, scientific articles regarding the shaken baby syndrome include both numerical and experimental researches, often comparing the two outputs. In the next paragraphs, some methods will be introduced. The evaluated factors are accelerations, velocities, stresses, strains and intracerebral pressure.

2.1 ANGULAR ACCELERATION

As reported in the previous paragraphs, the angular parameters are probably the most important because they are directly involved in the subdural hematoma, causing shearing on the brain and the consequent rupture of the veins. Different researchers suggested a threshold represented by the angular acceleration, beyond which the bridging veins may break. Nevertheless, data resulting from studies are various, depending on the conditions imposed in the analysis or in the experiments [13]:

1. Löwenhielm carried out the first cadaveric study in 1974. He proposed a threshold of 4500 rad/s² for occipital impacts with an impulse duration ranging from 15 to 44 ms.

2. In 2006, Depreitere et al. followed a complementary study, with a reduction in the duration time of the impact (less than 10 ms). They propose a limit of 10.000 rad/s².

3. Kleiven studied the problem thanks to a finite element analysis. The suggested threshold was 50 kW, correspondent to an acceleration of 34.000 rad/s² maintained for 5 ms and an angular velocity of 85 rad/s.

4. Huang et al. proposed another FEM analysis, proposing the acceleration threshold value of 71.200 rad/s².

AUTHOR	SDH THRESHOLD PROPOSED [rad/s²]
Löwenhielm	4.500
Depreitere et al.	10.000
Kleiven	34.000
Huang et al.	71.200

Table 2 - Summary of threshold proposed for bridging vein's rupture

All the proposed values are summarized in Table 2. These thresholds are more focused on the presence of impacts; in literature other research works exist more specifically focused on AHT.

Duhaime et al. studied specifically the shaken baby phenomenon in 1987 [21]. Their research started from the observation of 48 cases of infants and young children with this diagnosis. Collecting data, they tested their hypothesis constructing a 1-month-old model in which some accelerometers were implanted. This study proposes some thresholds for what concerns concussion, SDH and DAI: for SDH about 35.000 rad/s², for DAI almost 40.000 rad/s² (*Figure 8*).
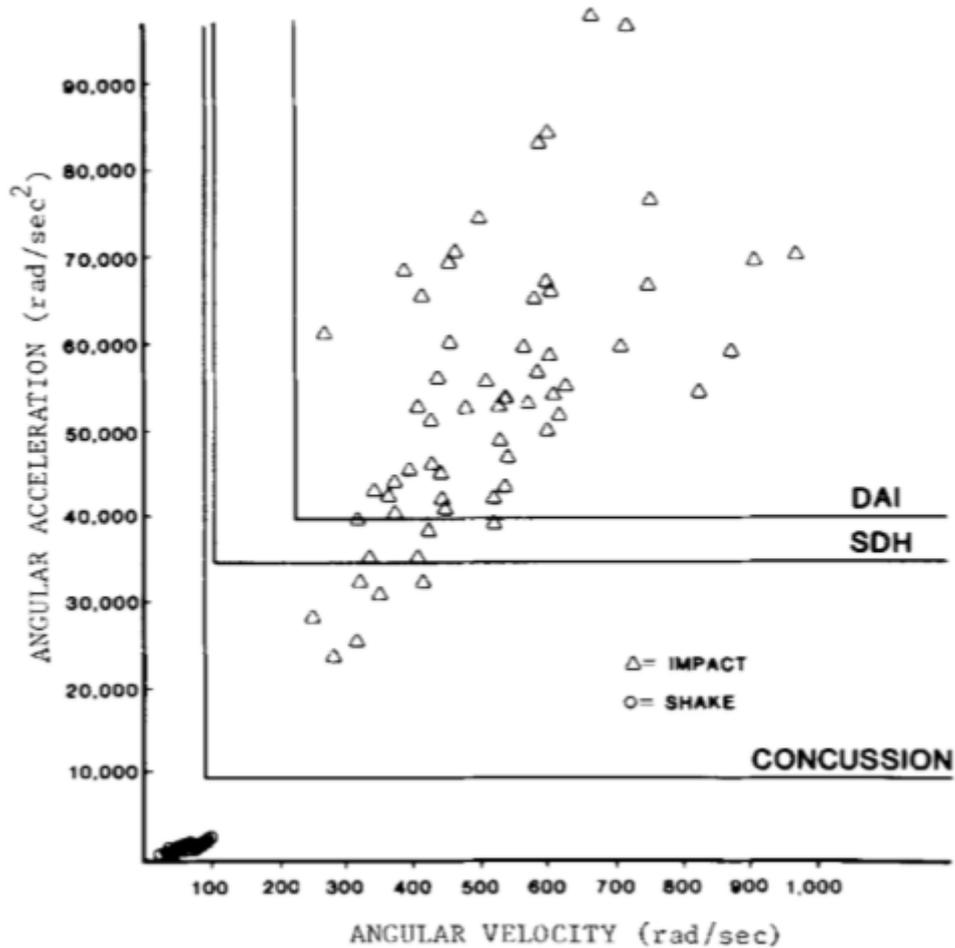
Figure 8 - Limits proposed related with angular velocity and angular acceleration. In the graph the experimental results of shaking and impact are reported.

A more recent work by Lloyd et al. uses a mannequin model of child, shaken by some adults. Data of angular accelerations were collected [22]. In their work, they propose the threshold given from Depreitere et al. (10.000 rad/s²); their results are compared to this limit.

Another study by Roth et al., more focused on child's head properties, compared experimental and numerical results obtained using a 3 years old FEM model [23]. Mechanical output parameters are taken from every simulation and classified in histograms leading to a specific injury risk curve, which allows estimating a threshold. For what concerns the angular acceleration, they built a curve, which links the head's angular acceleration to the probability of neurological injuries (Figure 9).
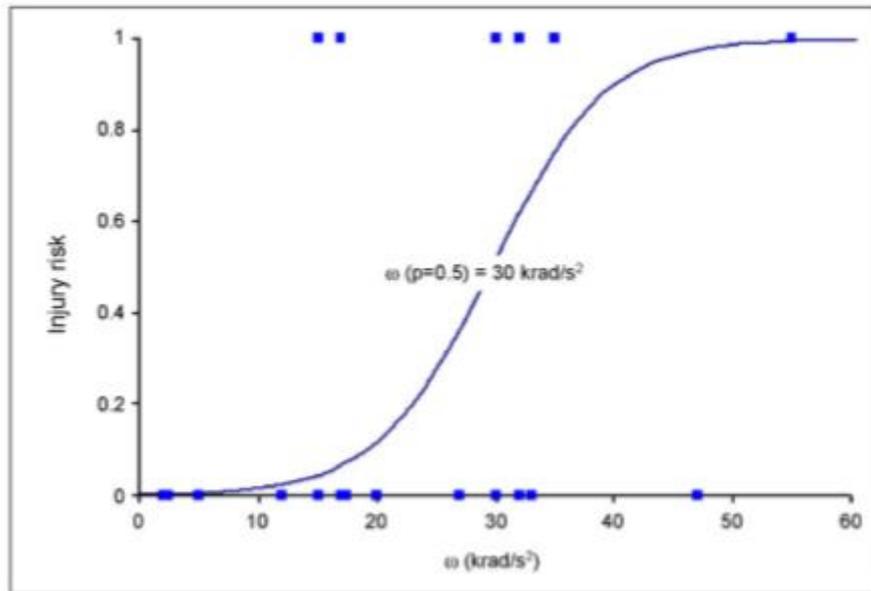
Figure 9 - The injury risk linked to angular accelerations

2.2 ANGULAR VELOCITY

A work by Takhounts et al. has focused the attention on another kinematic parameter: the angular velocity of the head. Doing this, they proposed the Brain Injury Criterion (BrIC) [24]. This criterion is based only on the values of angular velocities in each direction (x, y and z), which are related to lesions in the brain. A coefficient can be computed using the following relationship:

$$BrIC = \sqrt{\left(\frac{\omega_x}{\omega_{xcr}}\right)^2 + \left(\frac{\omega_y}{\omega_{ycr}}\right)^2 + \left(\frac{\omega_z}{\omega_{zcr}}\right)^2}$$

in which

- $\omega_x, \omega_y, \omega_z$ are the maxima values of angular velocities. They can be calculated in two ways: the maxima values independently from the instant of time in which they are registered or the values in each direction at the time that the maximum component x-, y- or z- of angular velocity is registered.

- $\omega_{xcr}, \omega_{ycr}, \omega_{zcr}$ are called critical values. They are calculated according to other criteria; in particular, the Cumulative Strain Damage Measure (CSDM) and the Maximum Principal Strain (MPS) are used in that sense. The critical values pretend to represent a probability of 50% of AIS4+ anatomic brain injury; this correspond to CSDM=0,49 or MPS=0,89. Using

these considerations, the critical velocities can be estimated using the two different ways. Table 3 shows the results.

Critical Max Angular Velocity	CSDM Based [rad/s]	MPS Based [rad/s]	Average [rad/s]
ω_{xcr}	66,20	66,30	66,25
ω_{ycr}	59,10	53,80	56,45
ω_{zcr}	44,25	41,50	42,87

Table 3 - Values of critical angular velocities

It is important to remember that these data are obtained from an experiment study focused on adult men; it is reasonable to think that values adapted for a baby's injury may be lower, because of the fragility of children's anatomic system compared with an adult's one. Then, once that the BrIC coefficient is obtained, the damage can be evaluated using some graphs, as the one shown in Figure 10.
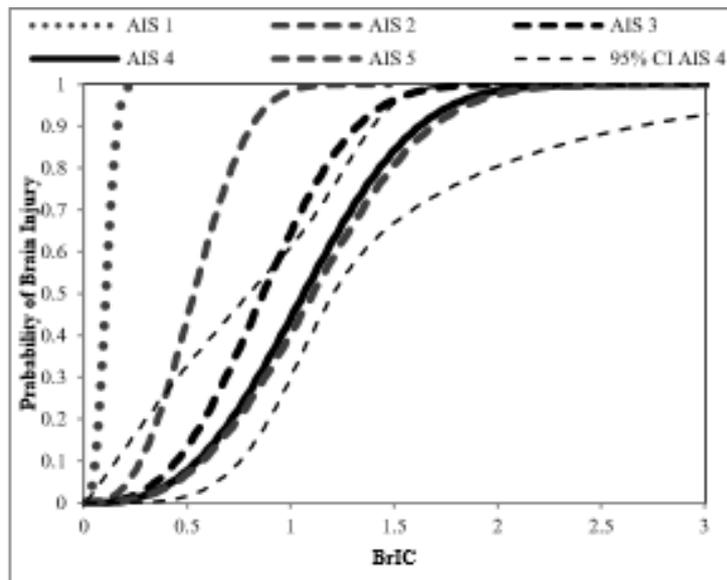

Figure 10 - Probability of brain injury associated with BrIC (MPS based). Different levels of AIS can be associated.

It is possible to see that in the previous image there are different curves, each of them linked with a grade of the AIS scale, that has to be introduced (Table 4). The Abbreviated Injury Scale (normally indicated with AIS) is a classification for the head's lesions which describes qualitatively the possible damages that can occur. Generally, it is used in the automotive field, for the biomechanical analysis of an accident; it has often a forensic aim [25].

AIS	Level	Description
1	Minor	Light brain lesions with possible headache, vertigo or lacking consciousness; light cervical lesion or contusions.
2	Moderate	Contusions with or without fracture of the skull, lacking consciousness for less than 15 minutes; eye's damages as corneal tiny cracks or detachment of the retina; face or noise fracture.
3	Serious	Contusions with or without fracture of the skull, lacking consciousness for more than 15 minutes without serious neurological damages.
4	Severe	Skull fracture with severe neurological injuries.
5	Critic	Concussion with possible skull fracture, lacking consciousness for more the 12 hours with haemorrhages.
6	Mortal	Death, partial or total cerebral damages.

Table 4 - Description of AIS levels

Another study comes by Marguiles and Thibault in 1992. Developed using experiments on primates, they estimated the DAI using both rotational velocities and accelerations (Figure 11). These curves correlate the change in angular velocity with the peak of angular acceleration. If there are small changes in angular velocities, the injury is less dependent on the peak angular acceleration; otherwise, if high values of peak change in angular velocity are registered, the injury is sensitive to the peak angular acceleration [17].
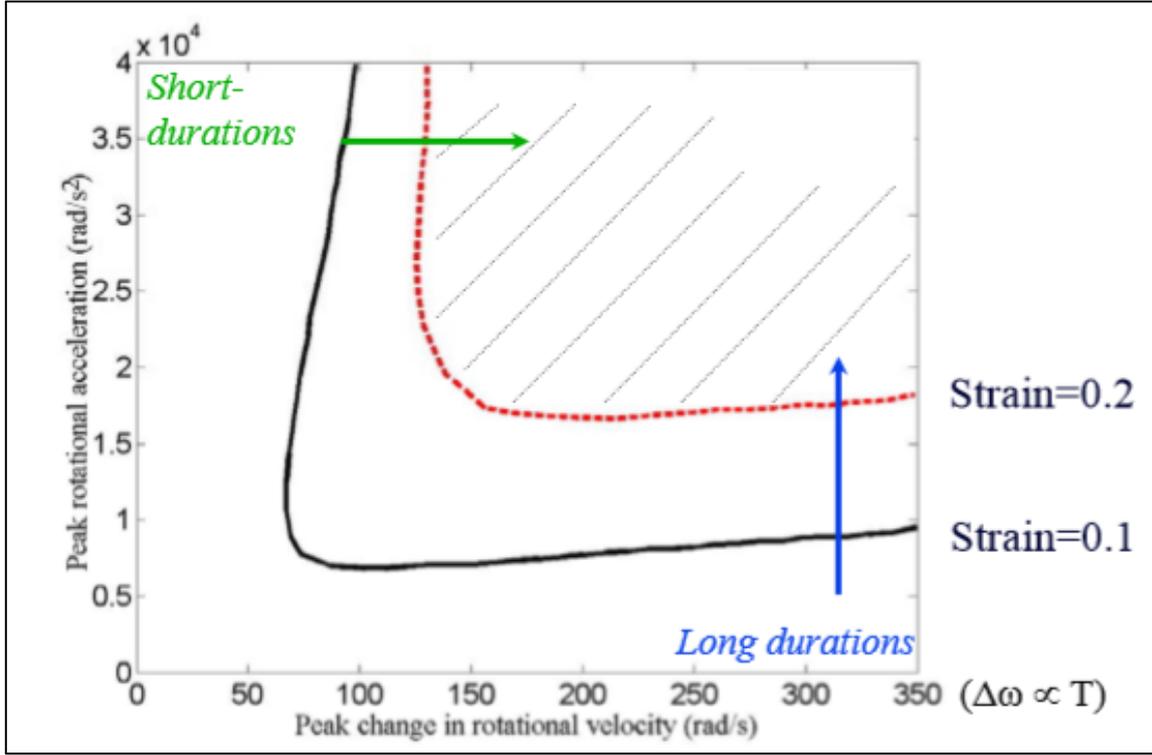
Figure 11 - DAI evaluation thanks to rotational acceleration and rotational velocity

2.3 LINEAR ACCELERATION

Linear kinematic parameters are not so relevant in the phenomenon of shaking; they are principally responsible for focal lesions [13]. Nevertheless, it is also convenient to mention in few words the Head Injury Criterion (HIC) because it is considered in many biomedical papers. It is a parameter used in general in the automotive field (for road accidents) and it is useful to evaluate cerebral lesions, that uses the maxima values of linear acceleration. The HIC depends not only from the maximum value of acceleration, but also from the time needed to reach it and from the time for which it is maintained [26]. The formula used is the next one:

$$HIC = max\left\{(t_2 - t_1) * \left(\frac{1}{t_2 - t_1}\int_{t_1}^{t_2} a_r(t)dt\right)^{2,5}\right\}$$

where

- t_2, t_1 are the extremes of the integration interval, and they should be expressed in seconds
- a_r is the resultant liner acceleration, computed as normally done with the three components in x, y and z direction, as $\sqrt{a_x^2 + a_y^2 + a_z^2}$

The HIC criterion can be applied with a maximum interval of 36 milliseconds. Usually, once the duration of the interval is chosen, the HIC can be computed for every interval of the simulation; then between all the obtained values, the maximum one should be considered. The resultant value of HIC quantifies the head's damage once is it correlated with the AIS scale thanks to some graphs (many graphs exist in literature, an example is provided in Figure 12).

This criterion is popular in the biomechanical literature and many papers describe it, but it has a limitation: it considers only the linear accelerations. As said, in the Abusive Head Trauma an important role is played by the rotational kinematic parameters that here are not taken into account. Moreover, HIC is based on skull fracture and not on brain injury; obviously, brain injury may happen also without any fracture [26].
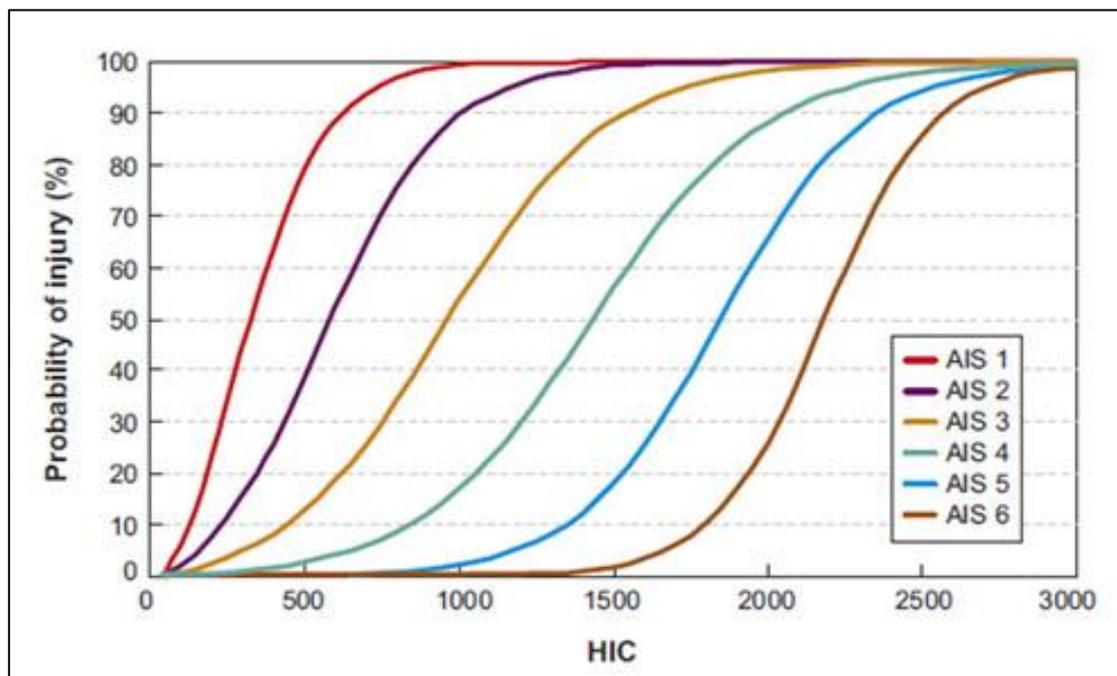

Figure 12 - Correlation between HIC and AIS grade

2.4 STRESS, STRAIN, PRESSURE

Other important parameters used to evaluate the damage can be stress, strain and pressure. These values can be registered in the brain and can be useful in order to evaluate the damage caused by the stretching of the tissue and by the relative movement between skull and dura mater. Several studies have tried to find a relationship between these numerical data and the probability that SDH or DAI can occur. Several experimental studies (mainly conducted on adult humans) use also the value of

angular accelerations and/or velocities as threshold linking them with the strain of brain tissue. Different authors estimate the probability of brain's injury associated with the deformations provoked by impacts or shaking.

Takhounts et al. resumed some possible solutions [27], studied for many years by different researcher, normally focused on adult men. Herein the proposed criteria to evaluate the brain's damage are presented:

- Cumulative Strain Damage Measure (CSDM). It is a criterion based on the concept that the diffuse axonal injury is associated with the cumulative volume of brain tissue experiencing tensile strains over a predefined critical level. To calculate the CSDM is necessary to compute the volume fraction of the brain, which during the event (impact or shaking) is experiencing strain levels greater than various specified levels.
- Relative Motion Damage Measure (RMDM). It is well correlated for acute subdural hematoma and it is used for the evaluation of injuries related to brain motion relative to the interior surface of the cranium. It allows taking into account for rupture of the bridging veins.

An experimental study accomplished using a logistic regression is done to link the CSDM to the injury probability. In Figure 13 some graphs are reported, depending on the strain level considered as limit (from ε=0,15 to ε=0,30).
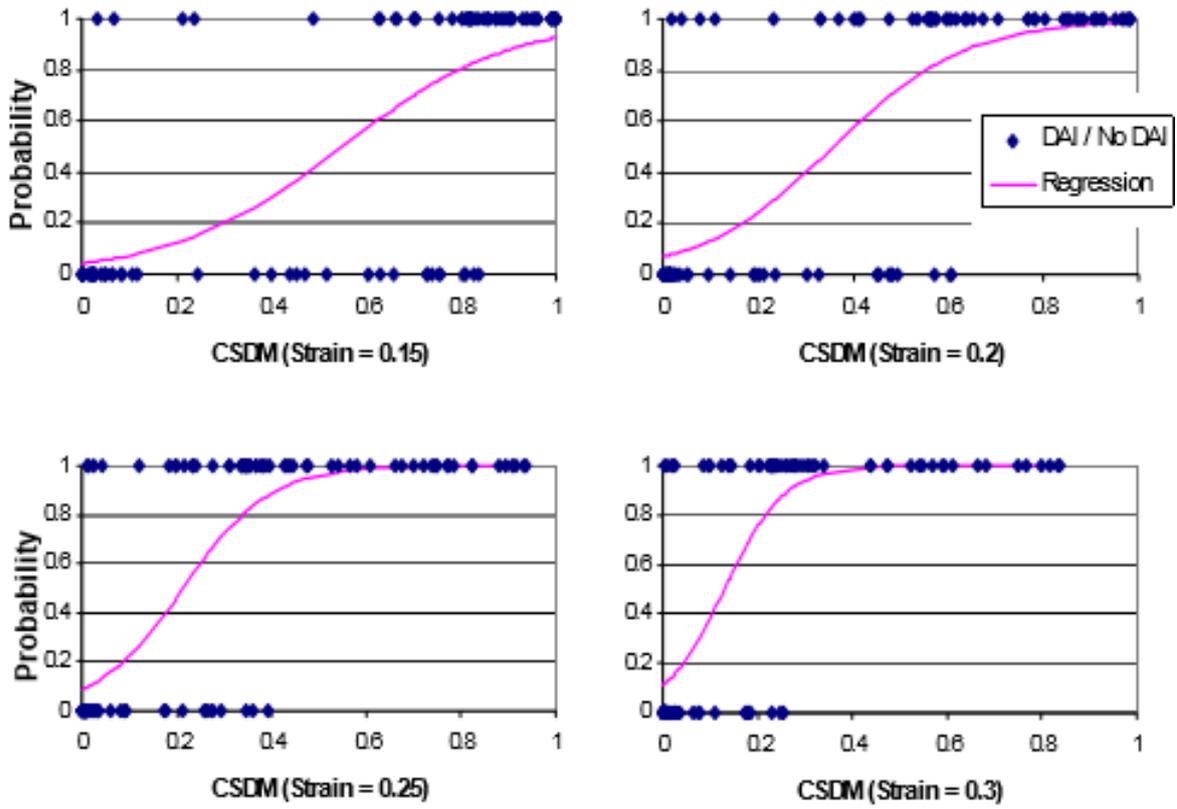
Figure 13 - Injury probability related with CSDM with different levels of strain

A similar outcome can be obtained for the case of RMDM; a similar procedure allows producing the relation with the injury, as depicted in Figure 14.
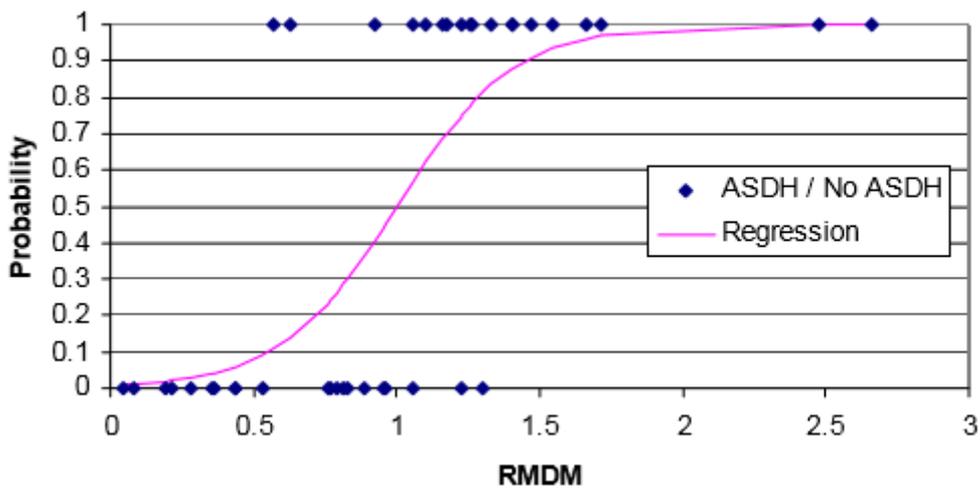

Figure 14 - Injury probability related with RMDM

A subsequent study [28], points out a relation between these parameters and the kinematic ones. From experimental data taken from American football players at collegiate level, they observed that the angular acceleration (or velocities) follow a linear relation with CSDM, RMDM and maximum principal strain; on the other side, liner accelerations and velocities does not have this kind of trend (Figure 15).
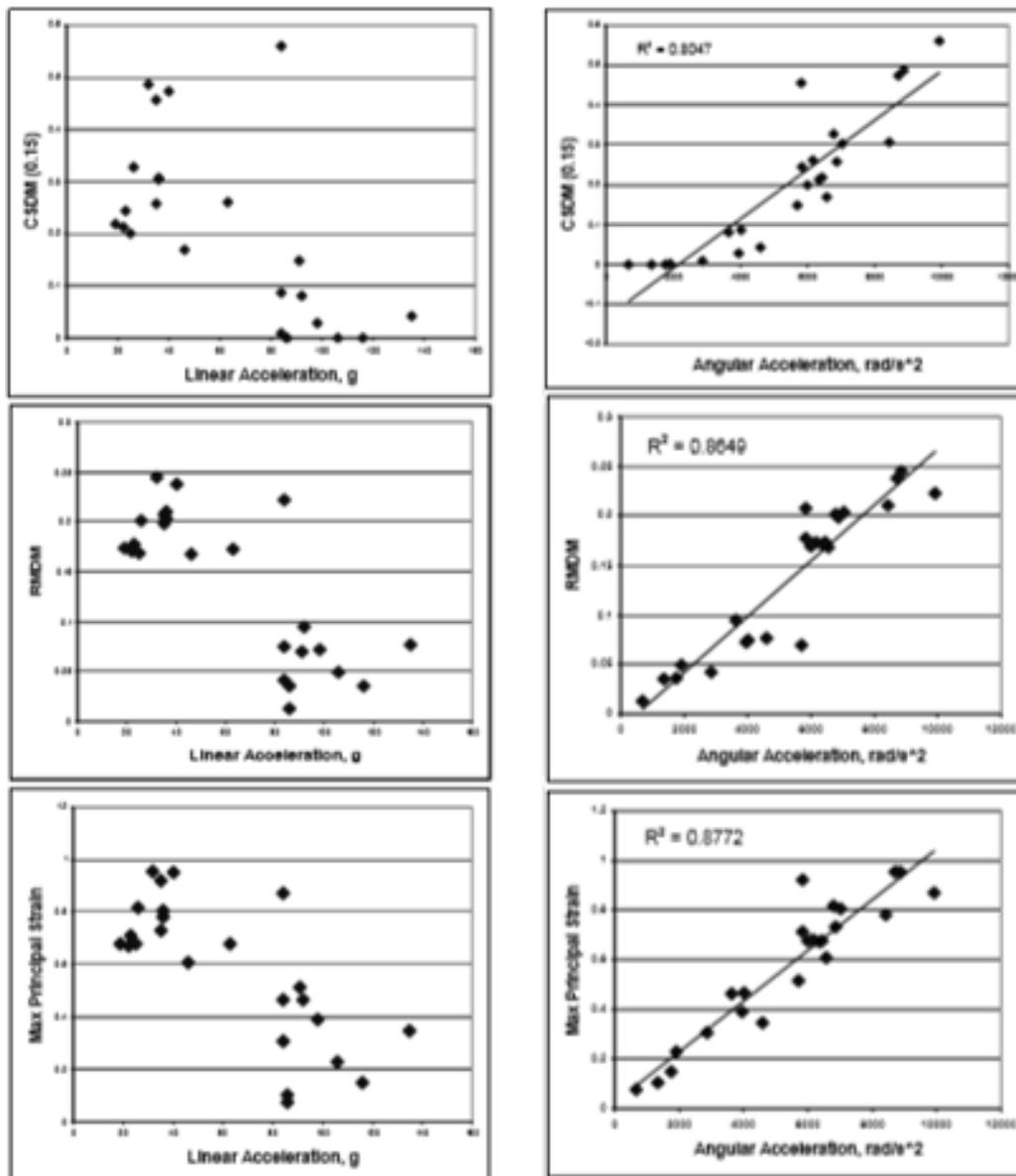

Figure 15 - Relationship between accelerations and CSDM (0,15), RMDM and Maximum Principal Strain

Using accelerations or velocities of the head is possible to evaluate the strain level of the brain and, consequently, an estimated probability of DAI.

Other projects have produced similar graphs. For example, the research of Roth et al. before mentioned [23] analysed the obtained data also for Von Mises stress (according on Stuck's constitutive law) and pressure. The resulting curves are plotted in Figure 16 and Figure 17.
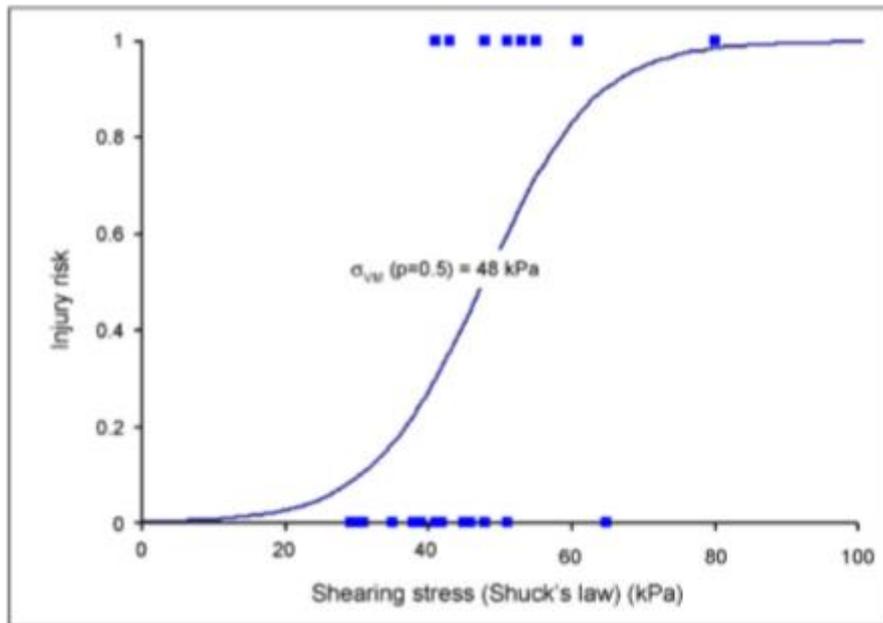

*Figure 16 - Shearing stress/Injury risk curve*
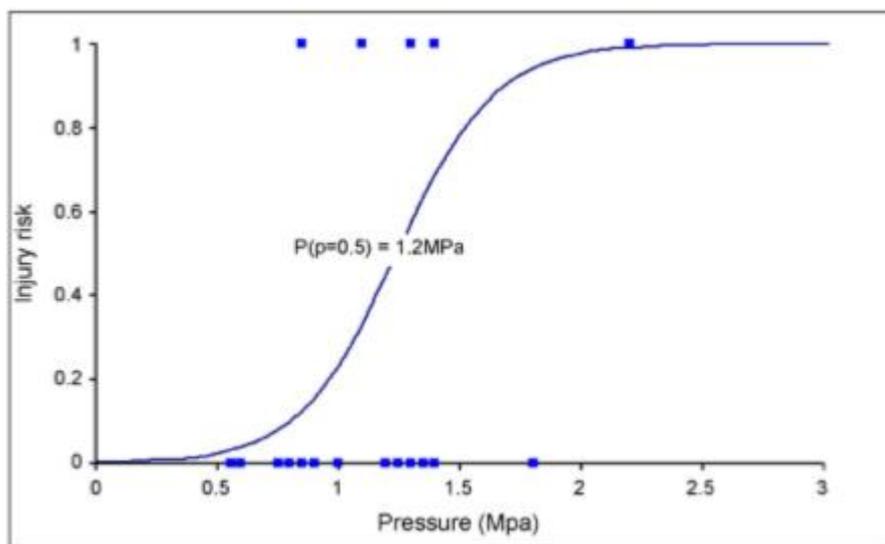
Figure 17 - Pressure/Injury risk curve

Another work has been conducted on car and domestic accidents involving children, therefore including impacts or violent movements [29]. The FE head-neck models used reproduce children 1, 3 and 6 years old. Twenty-two domestic accidents and nineteen road accident reconstructions were

collected from the paediatric emergency departments of different hospitals. Analysing the results, the authors proposed some thresholds for pressure and strain energy, schematically represented in Figure 18 taken to the referred article.

Concerning the 1-year-old model, a limit to predict skull failure and strain can be around 5 J but the lack of cases does not permit to establish clearly a limit.

For the 3-years-old model, the most relevant parameter registered was Von Mises stress, for which a threshold can be observed around 25 kPa. To predict skull failure the best parameter found is again the skull strain energy calculated with the finite element model. A limit can be observed around 7 J.

Finally, with the 6 years-old model the best candidate parameter to predict neurological injuries is again the brain Von Mises stress. A limit can be observed around 45 kPa.
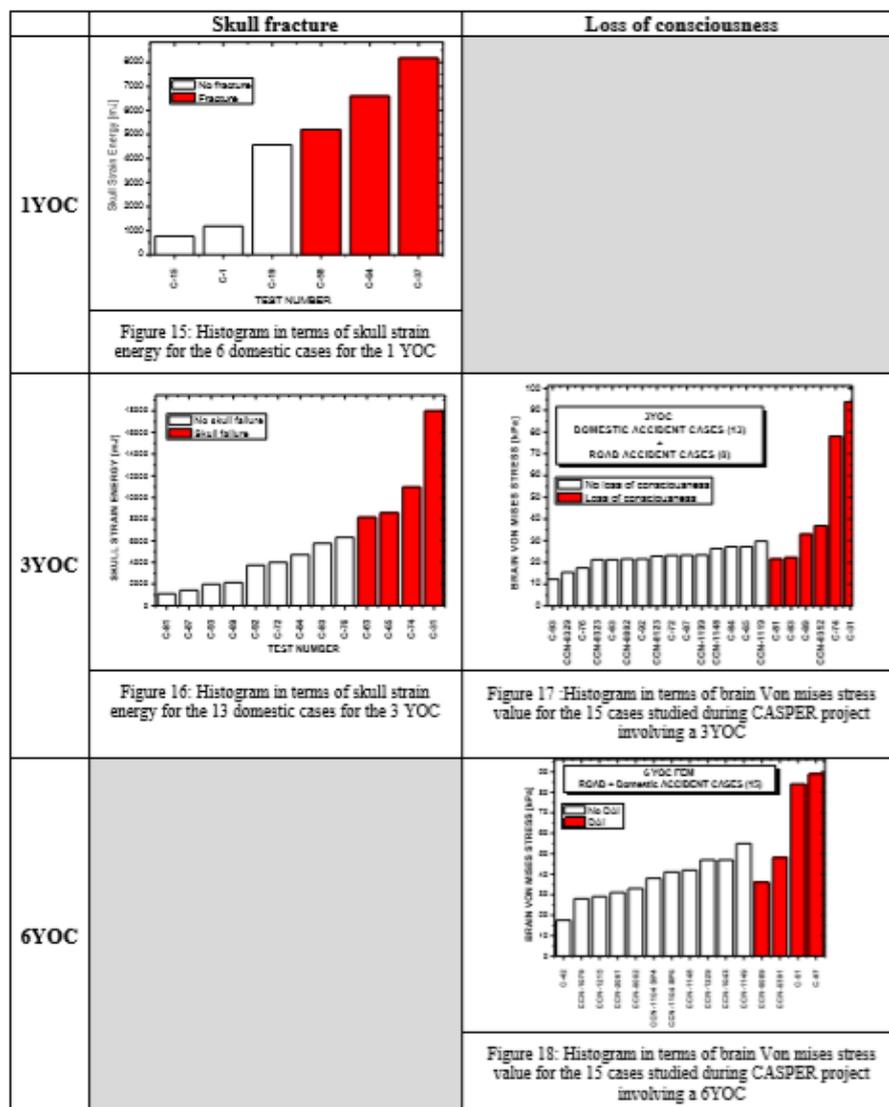

Figure 18 - Results of the analysis of Meyer et al

3. PRESENT STATE-OF-THE-ART

3.1 FEM ANALYSIS: A SHORT REVIEW

As said previously, the aim of this work is to study the mechanical aspect of the Abusive Head Trauma thanks to the finite element method, subsequently synthetically introduced.

The finite element method is a numerical technique used to perform finite element analysis of any given physical phenomenon, such as structural or fluid behaviour, thermal transport, wave propagation, calculation of mechanical stresses and deformations, biomechanical problems, etcetera [30]. Born during 1930s, it was developed during 1970s finding a large use. Nowadays it is commonly used in several engineering problems. Every FE analysis is divided into three parts:

- Pre-processing: it is the phase in which all the passages necessary to get start the real simulation are prepared. It includes the definition of the geometry, mesh, boundary conditions, loads and displacements
- Processing: the central part of the procedure, in which the solution is processed calculating the results
- Post-processing: once that the processing phase ended, the results can be visualized and analysed.

Nowadays there are many software's that are based on FEM method. In this analysis, the software LS-Dyna is used to run the simulation, thanks to the servers of Politecnico di Torino; instead the phases of pre-processing and post-processing are studied using LS-PrePost, a software freely released by LSCT. As schematically shown in Figure 19, the process passes between the two software's.
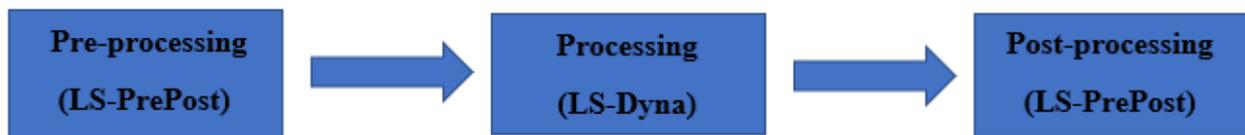

Figure 19 – FEM phases

Before to build any model or run any simulation, it is important to underline that this software requires a consistent set of units of measure. It means that is not possible to set in LS-PrePost which is the unit of measure that is used; every number should be put according to a consistent group of units. Herein

is shown a scheme taken from the official LS-Dyna website (Figure 20), which shows some acceptable combinations.

MASS	LENGTH	TIME	FORCE	STRESS	ENERGY	DENSITY	YOUNG's	35MPH 56.33KMPH	GRAVITY
kg	m	s	N	Pa	J	7.83e+03	2.07e+11	15.65	9.806
kg	cm	s	1.0e-02 N			7.83e-03	2.07e+09	1.56e+03	9.806e+02
kg	cm	ms	1.0e+04 N			7.83e-03	2.07e+03	1.56	9.806e-04
kg	cm	us	1.0e+10 N			7.83e-03	2.07e-03	1.56e-03	9.806e-10
kg	mm	ms	kN	GPa	kN-mm	7.83e-06	2.07e+02	15.65	9.806e-03
g	cm	s	dyne	dyne/cm²	erg	7.83e+00	2.07e+12	1.56e+03	9.806e+02
g	cm	us	1.0e+07 N	Mbar	1.0e+07 Ncm	7.83e+00	2.07e+00	1.56e-03	9.806e-10
g	mm	s	1.0e-06 N	Pa		7.83e-03	2.07e+11	1.56e+04	9.806e+03
g	mm	ms	N	MPa	N-mm	7.83e-03	2.07e+05	15.65	9.806e-03
ton	mm	s	N	MPa	N-mm	7.83e-09	2.07e+05	1.56e+04	9.806e+03
lbf-s²/in	in	s	lbf	psi	lbf-in	7.33e-04	3.00e+07	6.16e+02	386
slug	ft	s	lbf	psf	lbf-ft	1.52e+01	4.32e+09	51.33	32.17
kgf-s²/mm	mm	s	kgf	kgf/mm²	kgf-mm	7.98e-10	2.11e+04	1.56e+04	9.806e+03
kg	mm	s	mN	1.0e+03 Pa		7.83e-06	2.07e+08		9.806e+03
g	cm	ms	1.0e+1 N	1.0e+05 Pa		7.83e+00	2.07e+06		9.806e-04

Figure 20 - Sets of consistent units

3.2 PIPER CHILD BODY MODEL

Beillas et *al.* developed a finite element model, which replicates the geometry of a child, named PIPER. The PIPER Child model has been used in this thesis's work to simulate the Abusive Head Trauma mechanism. It was presented in 2016 in Munich (Germany) for the 14th International Conference Protection of Children in Cars. Document [31] contains a detailed description of all the parts, here synthetically reported in a general resume. The model is composed by several parts with specific properties. The model is continuously scalable between 18 months and 6 years of age, in its dimensions and in its properties. This is possible thanks to a tool developed for this purpose (PIPER tools). The final model with all validation simulations was released under an Open Source licence in 2017.

In this work, all the simulations were performed on the model representing a child 18 months old.

3.2.1 OVERVIEW

The complete human model is represented in an isometric view in Figure 21. It is composed of approximately 531.000 elements that are distributed in 353 parts and it is developed in the Ls-dyna explicit FE code. The internal geometry was created starting from CT scans obtained under agreement from a children hospital (Hospital HFME, Hospices Civilis de Lyon, Bron, France). Scans were obtained from children of different ages (1.5, 3 and 6 years). Bonds and main organs are modelled as shapes thanks to a semi-automatic segmentation of the scans; with the same method was defined the evolution of the growth cartilage. Other parts that are more difficult to scan, as the ligaments, were complemented by a detailed anatomical description. The only exception in this modelling process was the foot; its segmentation was difficult due to the large proportion of growth cartilage. For this reason, it was derived from the scan of an older subject and then it was scaled to the child size.

All the scans were done in a supine position. So, the developers of the model manually actuated postural adjustment of the thoracic and the lumbar spine. The same was made for the skin, also derived from several CT scans.
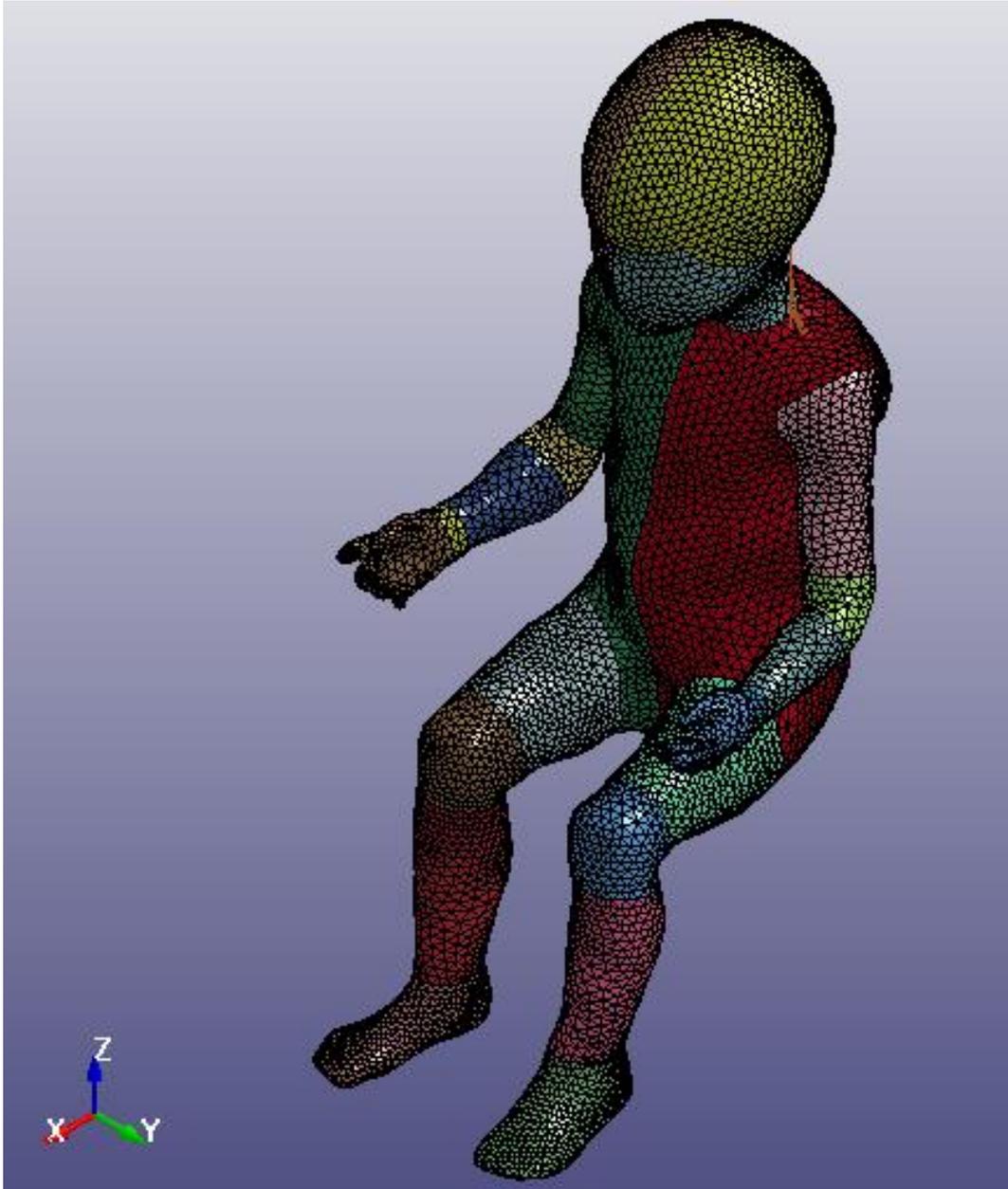
Figure 21 - PIPER child model, overview

The child model is complex, because it is composed by many detailed parts. In the subsequent paragraphs, some parts useful for this thesis's work will be described more in detail. It is also important to specify which is the units'system used, because, as said before, LS-Dyna requires a consistent set of them. It means that all the quantities should be expressed respecting this units'system. Therefore, in the Piper model the system used is:

- mass [kg]
- length [mm]
- time [ms]

Subsequently to this three, the other physical quantities will have these units:

- force [kN]
- stress [GPa]
- energy [kN*mm]
- density [kg/mm³]

The total mass of the model is 12,5 kg, instead the head's weight is 2,98 kg, representing the 24 % of the total weight.

3.2.2 HEAD

The current model of the head was realized continuing the one proposed in 2016 by Giordano and Klevein [32]. It is formed by more than 25.000 nodes, 40.000 solid elements and 12.000 shell elements. The typical spatial resolution ranges from 3 mm to 5 mm. The head's model includes the scalp, the skull, the cerebrum, the cerebellum, the meninges and the cerebrospinal fluid. Three different screenshots of the head are presented in Figure 22, in which are clearly visible the scalp and the brain.
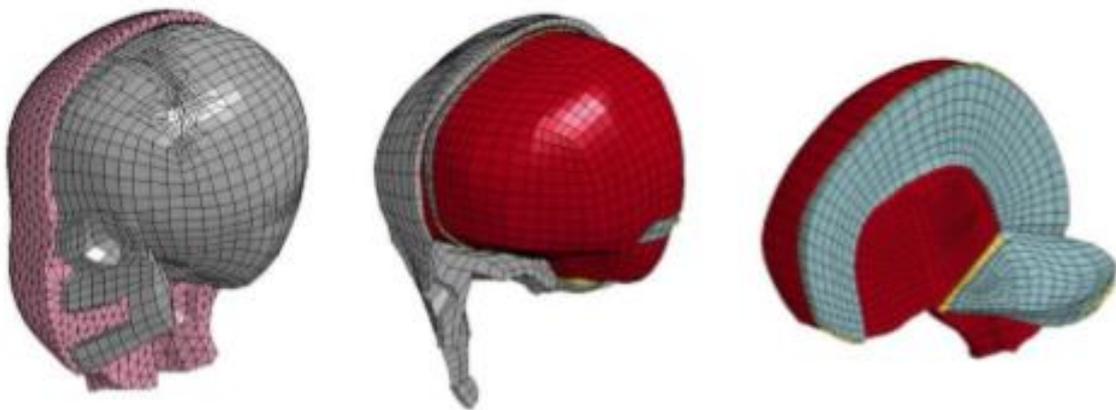

Figure 22 - Head model with open scalp (left); head model with open skull (centre); head model with open brain (right).

The mechanical properties of the materials were taken from previous studies [33, 34, 35, 36]. The skull's features are described by a linear isotropic elastic constitutive law. Differently, the brain tissue is constructed as a nonlinear viscoelastic model and it is characterized by an Ogden 2nd order constitutive law. The properties are originally defined for a 6-years old model but then they are adequately scaled if it is necessary. The principal properties (Young's modulus, density, Poisson's ratio or others) for the 18 months FEM model are resumed in Table 5.

TISSUE	YOUNG'S MODULUS	DENSITY [kg/m³]	POISSON'S RATIO
Scalp	Ogden 1st order + viscosity	1130	0,49
Outer Compact Bone	8,5 GPa	2000	0,22
Inner Compact Bone	8,5 GPa	2000	0,22
Porous Bone	1,0 GPa	1300	0,24
Brain Tissue	Orden 2nd order + viscosity	1040	≈0,5
Cerebrospinal Fluid	K = 2,1 GPa	1000	≈0,5
Dura Mater	Mooney - Rivlin	1130	0,45
Pia Mater	11,5 MPa	1130	0,45
Falx	31,5 MPa	1130	0,45
Tentorium	31,5 MPa	1130	0,45

Table 5 - Materials property of head model

3.2.3 A DETAIL ON THE TRUNK

It is also important to understand how is made the structure of the trunk, because is in that part that movement is applied. It is divided in a solid part (that stands for the flash) and an external shell (the skin). Obviously, the deeper part of the model is much more complicated, because it contains bonds and organs. Skin and flesh are only the external layers, but their features are important because they enter in contact with the shaker part. A section is presented in Figure 23.
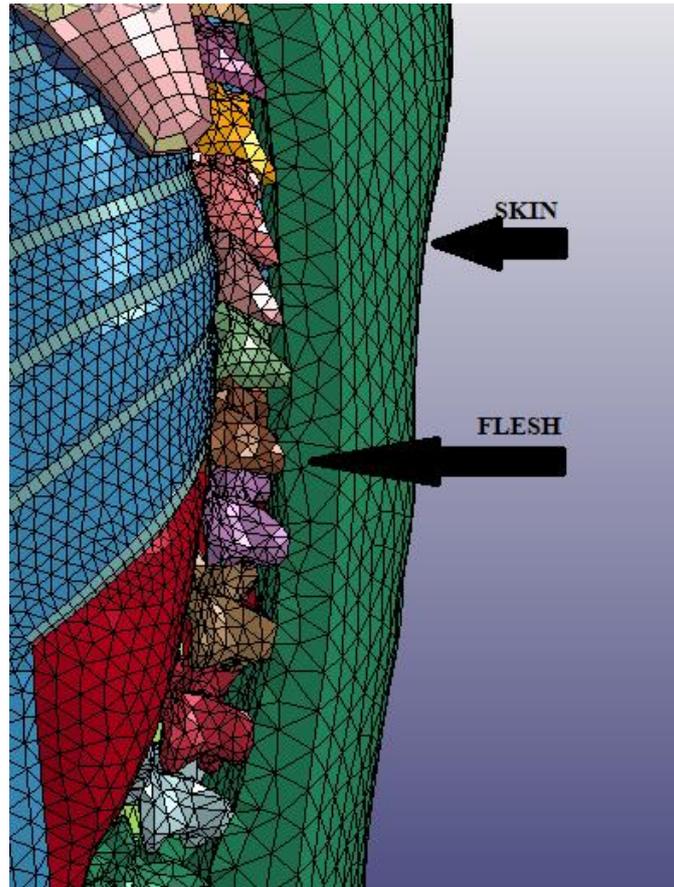
Figure 23 - A section showing how the trunk is made

The two parts present different sections (shell and solid) but also different kind of material: the skin is pretending to be an elastic material, instead the flesh is modelled in the software as a similar-rubber material. The principal characteristics are shown in Table 6.

PART	TYPE OF MATERIAL	DENSITY [kg/m³]	YOUNG'S MODULUS [GPa]	POISSON'S RATIO
Skin	Elastic	1000	0,0025	0,45
Flesh	Rubber	1050	K=2	

Table 6 - Mechanical properties of flesh and skin

In the deeper part of the trunk the pelvis is formed by deformable elements, instead the thoraco-lumbar spine is modelled using rigid bodies connected by 6 degrees of freedom beams. Deformable elements are used also for ribs, costal cartilage and sternum.

33

3.2.4 THE FILE'S STRUCTURE

The child human body model is developed in the Ls-Dyna explicit FE code and is possible to modify it under the terms of GNU General Public Licence. This can be done through the software LS-PrePost, that can be freely downloaded. The model is already very complex, and it is divided in many files, called *include files*. Each of them represents a part or a functionality of the body containing the geometrical description of the parts, the material, the contacts, etcetera. All these different codes are recalled together in a unique file called *main*, the one which is run in LS-Dyna. In the *main* is created a shell structure which simulates the activity of an arm that is moving and in addition is defined its interaction with the PIPER model.

All these files can be opened not only thanks to LS-PrePost, but also as text form, from where is also possible to modify them (Figure 24).

```
$  This file was generated by:
$ Piper application version 0.990
$ 04/23/17 15:51:58
*KEYWORD
*INCLUDE
main_Control.k
*INCLUDE
main_Interfaces.k
*INCLUDE
main_FleshSkin.k
*INCLUDE
main_Neck.k
*INCLUDE
NeckMuscles.k
*INCLUDE
main_Head_Brain.k
*INCLUDE
main_Head_Skull.k
*INCLUDE
main_FleshSkin_HeadNeck.k
*INCLUDE
main_Flesh_HeadNeck_InterfaceNodes.k
*INCLUDE
main_LEx.k
*INCLUDE
main_Trunk_UpperEx.k
*INCLUDE
mesh_PIPER_Body.k
*INCLUDE
main_Sensors.k
*END
```

Figure 24 – How the main file appears in text form. It is possible to see how all the include files are recalled, creating the child geometry

3.3 LITERATURE REVIEW: OTHER CHILD MODELS

In biomechanical and biomedical literature, a lot of material regarding AHT exists. Several authors proposed works in which the phenomenon is analysed thanks to experiments conducted on animals, child mannequins or on other kind of models. Some of these child-prototypes were born to evaluate the head's damage after a car accident, an impact or every possible injury's mechanism. Therefore, there are also many studies that uses the same prototypes applied and adapted for the AHT case.

A review of the literature allows to discuss differences and analogies between all the available studies, having in this way a comparison with the results of the simulations performed in this work. This may be an important point for the injury analysis. Several models are presented in literature; they vary a lot in terms of ages, weights, dimensions and boundary conditions imposed in the experiment. It is important to remember that weight and height in child's change a lot during the growth phase, especially in the first two years of child's life in which the growth rate is really fast [37]. Therefore, it is immediately understandable that not all the child's models present in literature can be compared, because anatomical differences can affect the phenomenon. To make a right comparison, weights (head's weight and total) and main boundary conditions should be similar. Here, some interesting works are introduced, in particular focalizing the attention for what concerns differences and analogies with the PIPER Child Model, used in this thesis's work; doing this the parameters resulted from simulations may be deeper analysed.

3.3.1 Q-DUMMY

The Q-series of child dummies is currently available after some projects started to develop acknowledges on child's behaviour when some kind of injury occurs [38]. The series include mannequins of various ages (starting from few weeks up to 6 years old). In a research work of Nadarasa et al, already mentioned [15], the Q0 mannequin was used to study the shaken-baby-syndrome especially for what concerns injury to the eye (retinal bleeding). A picture is shown in Figure 25.

Figure 25 - Q0 Dummy

A detail description of all the parts is available in the manual [39].

- Head: it is largely made from polyurethane synthetics; it presents a cavity that allows the use of accelerometers.
- Neck: it is flexible and allows shear and bending in all directions.
- Thorax: it is represented with the torso flesh, made of a PVC skin filled with polyurethane foam, instead the thoracic spine is made of hard polyurethane.
- Abdomen: it is represented integrally with the torso flesh.
- Lumbar Spine: it is made by a flexible rubber column (identical to the neck).
- Pelvis: it is represented integrally with the torso flesh made of a PVC skin filled with polyurethane foam.
- Arms and legs: they are integrally made of flexible solid polyurethane with a fixed angle between upper and lower parts

It is useful to relate the Q0 dummy's characteristics to the PIPER's one. It is done in Table 7, in which ages and weights are compared.

	Q0 DUMMY	PIPER
Simulated age	6 weeks	18 months
Head + Neck mass	1,13 kg	2,98 kg
Total mass	3,5 kg	12,5 kg
% (H+N mass / Tot. mass)	32 %	24 %

Table 7 - Comparison between Q0 Dummy and PIPER

The models present relevant differences, starting from the anatomical complexity of the structure (mannequin vs finite element model). Then, ages are very different: the dummy is representing a new-born, instead the FE model represents a child older than one year. The same difference is present for what concerns the weights: the total mass of the PIPER model is almost 4 times the total mass of the dummy. In percentage, the weight of the head is more influent in the dummy, in fact it is almost 1/3 of the total weight. So, it is difficult to make a comparison between these two cases; the difference given from the outputs of both experiments, in terms of velocities and accelerations, may be very relevant.

3.3.2 CRABI-12 MODEL

The CRABI-12 (standing for Child Restraint/Airbag-Interaction, displayed in Figure 26) is a mannequin replicating a 12 months-old child, developed by FTSS and Denton to evaluate small child restraint systems in automotive crash environments, in all directions of impact, with or without air bag interaction [40]. Also models of other ages exist.

Figure 26 - CRABI-12 Model

As done in the precedent paragraph, also this model can be compared with the PIPER model, as shown in Table 8.

	CRABI 12	PIPER
Simulated age	12 months	18 months
Head + Neck mass	2,64 kg	2,98 kg
Total mass	10 kg	12,5 kg
% (H+N mass / Tot. mass)	26,4 %	24 %

Table 8 - Comparison between CRABI-12 and PIPER

CRABI-12 is a mannequin, so its structure is much more simplified than the PIPER's one, which is a finite element model. In this case the simulated ages are similar and moreover also weights are similar; they can be compared. Lloyd et al. used this kind of mannequin to study Abusive Head Trauma, in an article published in 2011 [22]. They performed different shaking and fall proofs; nine adult volunteers grasped the mannequin and shook it, as illustrated in Figure 27.

Figure 27 - A volunteer grasps the child model

The nine volunteers shook the infant surrogate using three different techniques:

- mild shaking, used to simulate resuscitative efforts;
- gravity-assisted shaking, where the mannequin was swung forcefully towards the ground, but without any impact;
- aggressive shaking, which is a repetitive movement in the horizontal plane.

Most of the proofs were continued from 10 to 20 seconds of shaking at 3–5 Hz. Each volunteer repeated the shaking twice.

The results of the shaking episodes performed on the CRABI-12 are here reported. Subsequently Table 9 shows the values registered. Noises were eliminated using a pass filter with a cut-off frequency of 50 Hz. Angular accelerations were derived and from all the data root-mean-square values were calculated.

	Resuscitative shaking	Gravity-assisted shaking	Aggressive shaking
Angular Velocity [rad/s]	12,5	24,3	25,5

Angular Acceleration [rad/s²]	364,6	581,5	1068,3
Linear Acceleration [g]	3,2	7,2	7,6

Table 9 - Values registered in the experiments of Lloyd et al.

Authors concluded that angular accelerations of the head fall 84% below the scientifically accepted biomechanical threshold for bridging-vein rupture, which they considered 10.000 rad/s² according to the studies of Depreteire et al. [41]. They also stated that (although a shaking episode for an infant is potentially unsafe) according to the resulted data neither aggressive shaking is likely to be a primary cause of diffuse axonal injury, primary retinal haemorrhage or subdural hematoma in a previously healthy infant [22].

3.3.3 P-DUMMY

This dummy's series is similar to the Q series (actually Q series was developed later). It also includes mannequins which replicate children of different ages. An example of them is presented in *Figure 28*. One of these mannequins, specifically the P3/4 dummy, has been cited in the article of Cirovic et al., regarding the biomechanical aspects of AHT [42]. In this work it is used to evaluate the values assumed by kinematic parameters (accelerations and velocities) in the head, caused by a shaking-episode. The comparison between its characteristics and the PIPER model is following shown (Table 10).

Figure 28 - A mannequin of the P series

	P3/4 DUMMY	PIPER
Simulated age	9 months	18 months
Head + Neck mass	2,2 kg	2,98 kg
Total mass	9 kg	12,5 kg
% (H+N mass / Tot. mass)	24,4 %	24 %

Table 10 - Comparison between P3/4 Dummy and PIPER

The dimensions of the P3/4 dummy are based on the data for a 50th percentile child. The simulated ages in the two cases are different, but head's mass percentage is basically the same in both models. In addition, the weights are not so different.

The simulations have been performed at an average frequency of 3,9 Hz. The obtained values are shown in Table 11. In the article also some graphs are presented; in Figure 29 the components in three directions of linear acceleration are plotted.

Linear Acceleration [m/s²]	45 ± 12
Angular Velocity [rad/s]	25 ± 7

Angular Acceleration [rad/s²]	650 ± 180

Table 11 - Kinematic parameters resulted in the experiments
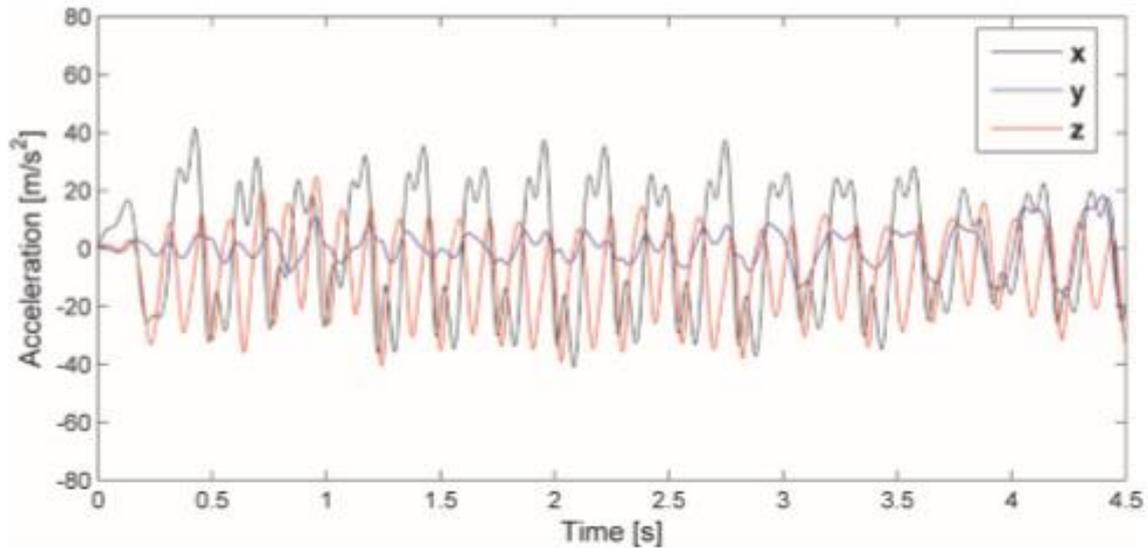
Figure 29 - Values of linear acceleration registered, in three components

An important point in this study is that the blood pressure in the veins increases during shaking. Even if this potential mechanism is not likely to contribute to the brain injuries leading to fatalities, it may contribute to eye haemorrhaging that is frequently found in the suspected cases of SBS.

3.3.4 OTHERS

Another work comes from a study of Wolfson et al. [43]. In this article is used a child model adapted from MADYMO CRABI 12 months model, introduced in the previous paragraphs. So, the characteristic in terms of mass will be almost the same. Experiments were conducted at shaking frequencies up to 5,5 Hz, considering 3,5 Hz as average value. Data are registered and evaluated thanks some injury criteria; all the values of angular acceleration registered are lower than 1000 rad/s². This work in particular is focalized on the influence of neck stiffness in kinematic parameters. The authors pointed out that in shaking episodes impact-type characteristics are required to exceed current injury criteria. In impacts only lower values for injury threshold were exceeded.

A more recent study of Jones et al. [44] uses a computational infant model (MD Adams; MSC Software Corp., Newport Beach, CA). It replicates a 9 months child and the head's weight is 2,3 kg. The experiments put attention also on the neck's stiffness influence. They are done with a shaking

frequency of 3 Hz with a maximum amplitude of 65 mm. Also in this work the pick values resulted have been reported, as shown in Table 12. This study demonstrated the importance of neck stiffness properties in shaking scenarios, because they are influent for peak vertex accelerations. Those values are below injury thresholds taken from other literature papers.

Linear Acceleration [m/s²]	95,73
Angular Velocity [rad/s]	17,17
Angular Acceleration [rad/s²]	1133

Table 12 – Values registered in the experiments

3.3.5 RESUME

All the introduced works may be subsequently used to make a comparison with the simulations' results. Obviously, other several researches exist. For example, some works studied the phenomenon using a younger and lighter child model [45]. The great difference in terms of mass brought to great difference in accelerations or velocity comparing them with the precedent studies (values of angular acceleration are almost 10.000 rad/s²). The models reported until now have been chosen generally because they have some similar characteristic with the PIPER model in terms of age, mass, head mass or boundary conditions. This makes possible a future results' comparison.

Here, a resume of the more interesting points written in precedent paragraphs is presented in Table 13. For each model discussed are reported again ages and masses. Then, the maxima kinematic parameters registered in each experiment are reported, in this way they can be recalled later one easily.

MODEL	AGE [months]	TOTAL MASS [kg]	HEAD MASS [kg]	HEAD/ TOTAL RATIO [%]	MAX LIN. ACCEL. [g]	MAX ANG. VEL. [rad/s]	MAX ANG. ACCEL. [rad/s²]
Q0 Dummy	≈2	3,5	1,13	32	12,2	\	4962
CRABI-12	12	10	2,64	26	7,6	25,5	1068

P3/4 Dummy	9	9	2,2	24	5,8	32	830
Comp. model	9	\	2,3	\	\	17,2	1133

Table 13 - Resume of some models

These are only some between the works that have been done in literature. It is possible to see that the data are more or less similar, except that the ones come out from the Q0 Dummy simulation, whose characteristics are totally different from the other models.

4. PRE-PROCESSING

4.1 SHAKING MATHEMATICAL LAW

The shaking movement law definition (in amplitude and period) is the starting point for present work. It is usually described with a wave function. The motion defined has a basic harmonic form in which the base of the neck is forced to follow the thorax, which is shaking. One oscillation is completed after a certain period [46]. The equations that can properly describe the shaking movement in its displacement, velocity and acceleration are typical of oscillations phenomena. In these cases, according to the reference system of the child model that will be used, the equation adopted for the displacement is, in its most generic form:

$$x(t) = B + \frac{A}{2}\sin(\omega t + \varphi)$$

in which:

- A is the amplitude of the curve.
- B is a parameter that can be chosen arbitrary.
- ω is the angular frequency, which is equal to $2\pi/T$, where T is representing the period.
- t is the generic instant of time.
- φ is the phase.

In the previous equation, once the amplitude and the period are chosen, it is possible to act on the phase and on the parameter B to impose the minimum value assumed and the rest position x=0.

Consequently, the equations for velocity and acceleration are obtained computing respectively the first and the second derivatives of the displacement's law.

$$v(t) = \frac{dx}{dt} = \frac{A}{2}\omega\cos(\omega t + \varphi)$$

$$a(t) = \frac{d^2x}{dt^2} = -\frac{A}{2}\omega^2\sin(\omega t + \varphi)$$

As the Hooke law states, these equations can be applied to every movement in which the force necessary to restore an equilibrium position is proportional to the displacement. An example of the displacement-time relationship is represented in Figure 30.
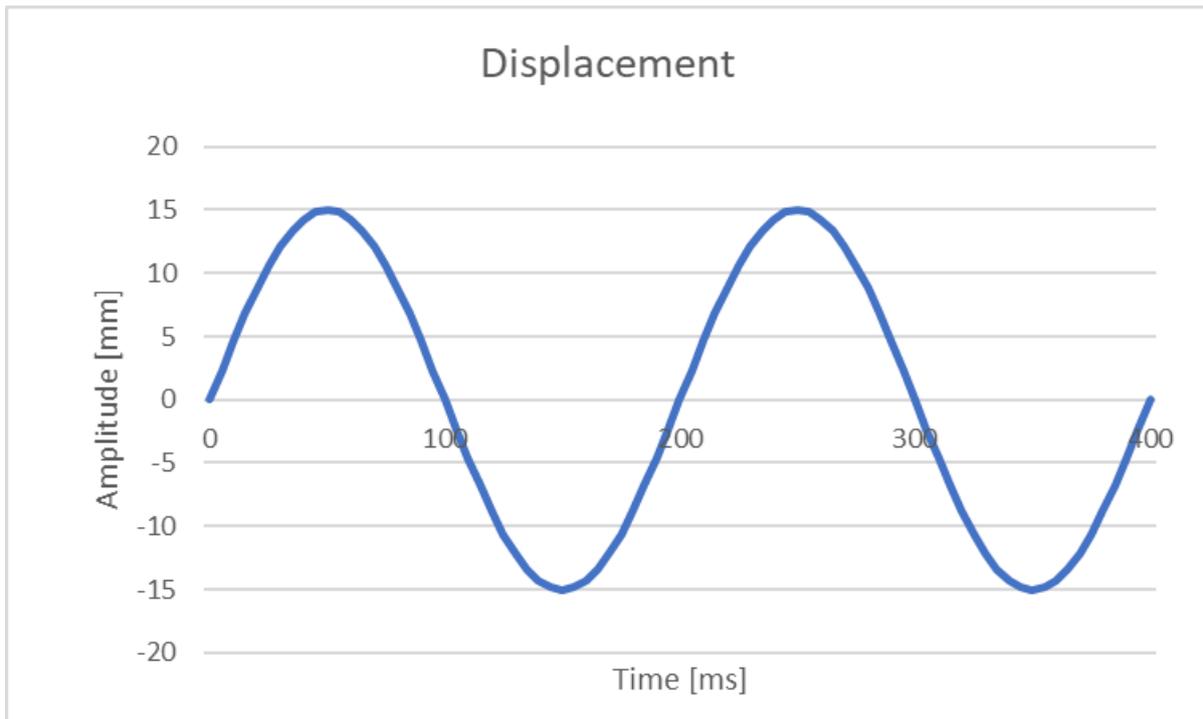
Figure 30 - An example that describes the evolution of displacement during the time

Studying how the head responds to this kind of movement is important in order to understand the Abusive Head Trauma. As said before, the base of the neck is forced to follow the chest, however the head may move uncontrollably backward and forward, depending on the frequency of excitation. It is also important to remember that the angular displacement of the head is limited in one side from the chin, in the other side from the neck's hyperextension.

Obviously, the period used is important because it is linked with the shaking frequency, that has to be chosen in order to replicate a verisimilar episode. They are directly connected from the equation:

$$f = \frac{1}{T}$$

According to Reimann [46], is difficult moving the hand backward and forward more than four times in a second, so actually it is improbable the possibility to shake a child to frequencies higher than 4 Hz, instead other authors as Nadarasa et al [47] simulated some shaking episodes with frequencies ranged from 5 Hz to 6 Hz.

4.2 MODEL'S PREPARATION

4.2.1 AN EXAMPLE TO START

In order to understand how the real child model could work and to get started with the complete problem and with the software, initially some simplified geometries were prepared and analysed, in particular for what concern the interaction between the bodies. Obviously, the episode that ought to be simulated is a shaking movement. Here, an easy model is presented as example to illustrate the first passages that brought to the complete simulation (Figure 31). The simplified model consists of a cylinder solid and a cylinder shell. The solid simulates the trunk of the baby; the shell represents the hand of a person which is moving with a sinusoidal movement law, shaking the cylinder. Different proofs where performed, changing the movement of the shell, the materials of the parts and the type of contact. The sample geometry little by little got more complicated in order to replicate the real phenomenon as similar as possible. The last simplified simulation done before to approach the real problem consists of a hollow cylinder which has two layers, one internal and one external.
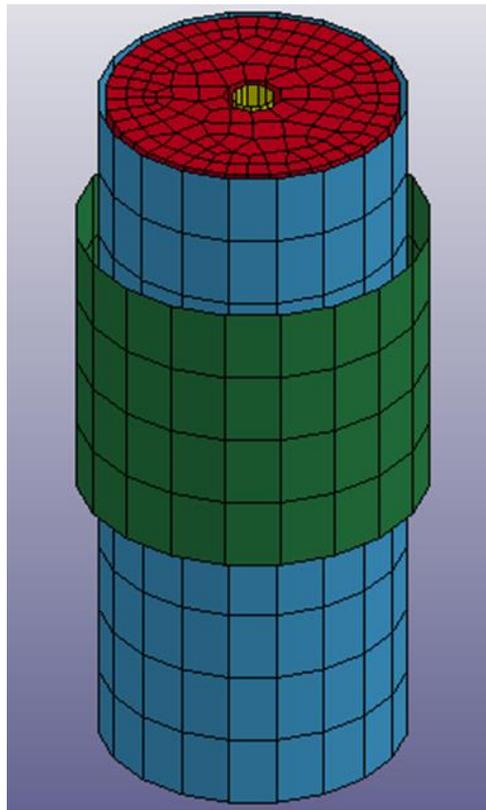
Figure 31 - Simplified geometry

The whole structure is composed of 4 parts that have been associated with a part of the human body to approach the real problem.

- A first external shell (green): it is simulating the hand of another person, which is moving shaking the cylinder.

- A second external shell (light blue): it represents the skin, which is the softest part of the whole structure.

- The cylinder (red): it stands for the flesh.

- The internal shell (yellow): a layer which is representing the internal bond

This model was initially studied and perfectioned in order to see how a shaking episode could work on LS-Dyna. Then the real child model was approached.

4.2.2 PRELIMINARY STEPS

The FEM model used in the simulations of the AHT is the PIPER's one, that is mainly presented in the previous paragraph. It is convenient to remind that the model is replicating 18 months-old child weighting 12,5 kilograms. According to weight-for-age curve presented by the World Health Organization [48] (reported in Figure 32, data referred to U.S. population) the PIPER child model replicates a baby at 85th percentile of the weight-growth.
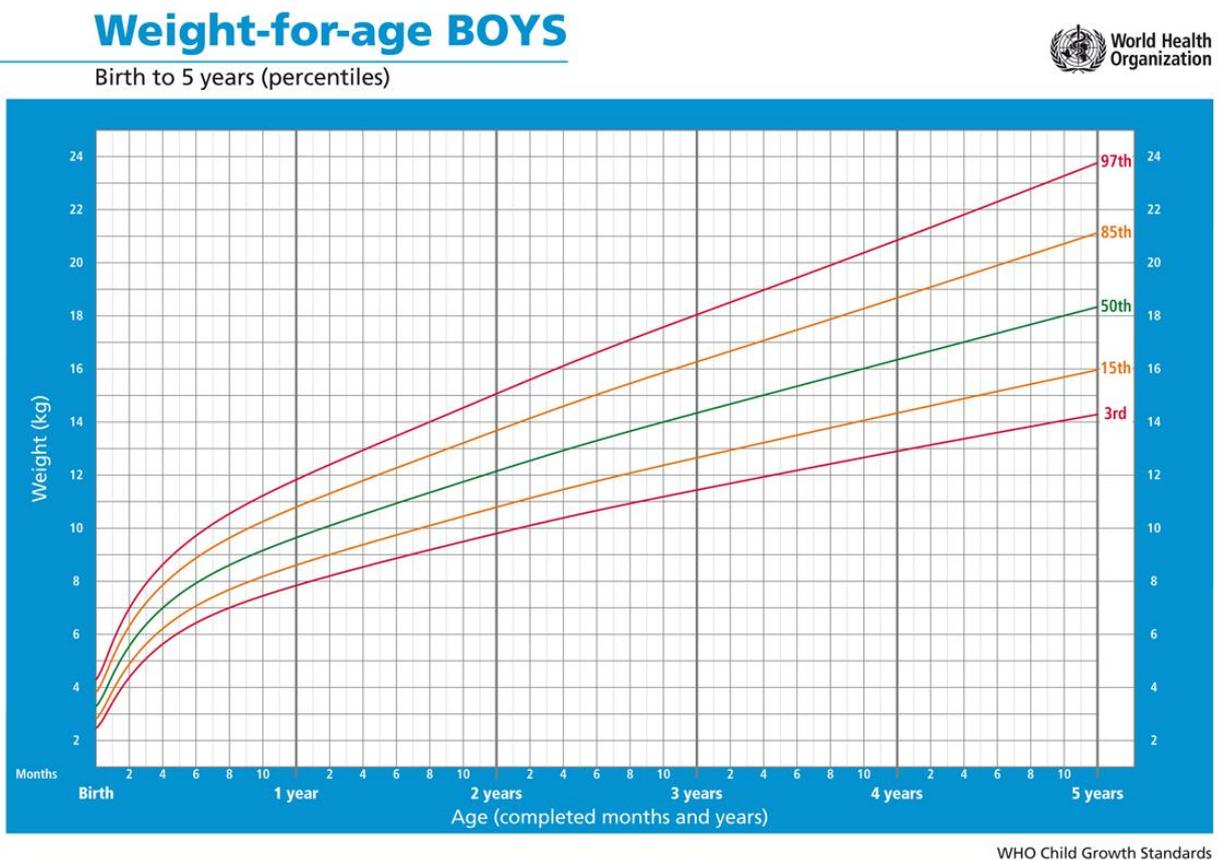
Figure 32 - Weight-for-age BOYS, growth percentiles

The model, freely available, was downloaded from the PIPER web site and then all the required modifications were introduced. In order to simulate the phenomenon in the best possible way, the necessary modifications were added step by step, performing various simulations and evaluating the outputs. The most important passages are successively described. Before, some general steps are introduced; they are valid for all the simulations done.

The shaking episode is simulated with a shell element that wraps the baby's model. It is pretending to replicate the arm and/or the hand of an adult person, so the dimensions must be verisimilar. The designed shell has an extension of almost 85 millimetres, according to the measure of the length of an adult's man hand illustrated in Figure 33 [49].
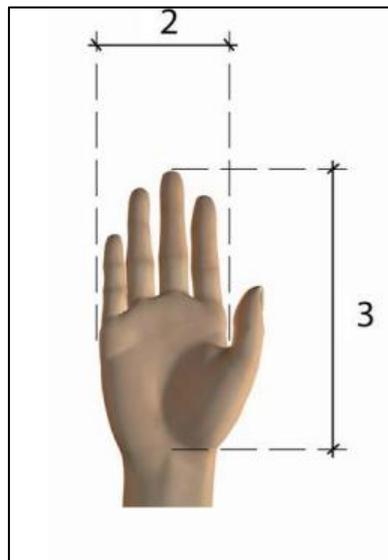
Figure 33 – Hand's measures, the referred extension is the number 2

In LS-PrePost a new part is created. In every part definition two important parameter must be set: the section (SECID) and the material (MID). They should be put in the space shown in Figure 34.
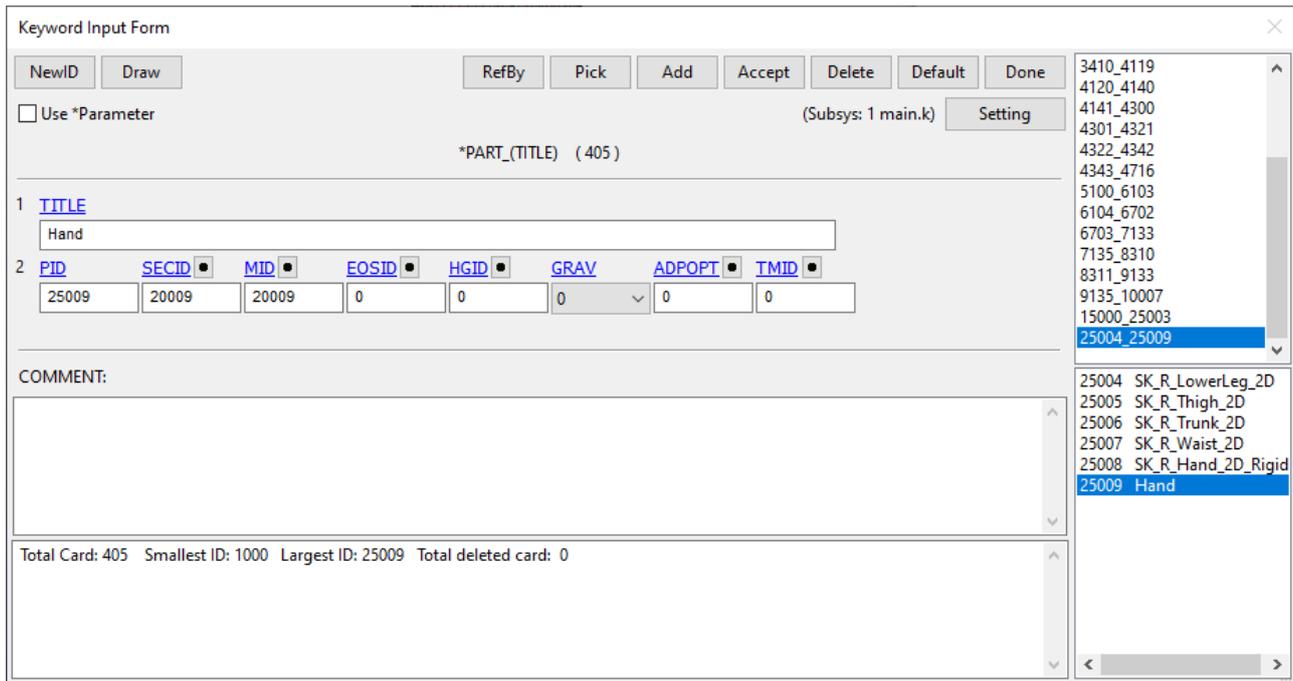
Figure 34 - Definition of the keyword

The section created is a shell type, as previously said, in which a thickness of 1 millimetre is imposed. For what concern the material, the hand is modelled as a rigid body; it means that its material is designed rigid and the motion is given thanks to a card called *prescribed_motion_rigid*. The selected mechanical properties have been taken from the hand of the child model, which is also assumed to be a rigid body. This was done for what concerns density, Young's modulus and Poisson's ratio, so

- $\rho = 2 * 10^{-6} \frac{kg}{mm^3}$
- $E = 2\ GPa$
- $\nu = 0,25$

In addition, to avoid unexpected and unwanted movements, some boundary conditions have been introduced: the only motion permitted to the shell is the one in x-direction, which is the direction along the sagittal plane of the human body [50]. The other 5 degrees of freedom (y-movement, z-movement and all rotations) have been locked. The planes in which the human body is divided are shown in Figure 35, instead the reference system of the finite element model is presented in Figure 36 and Figure 37.
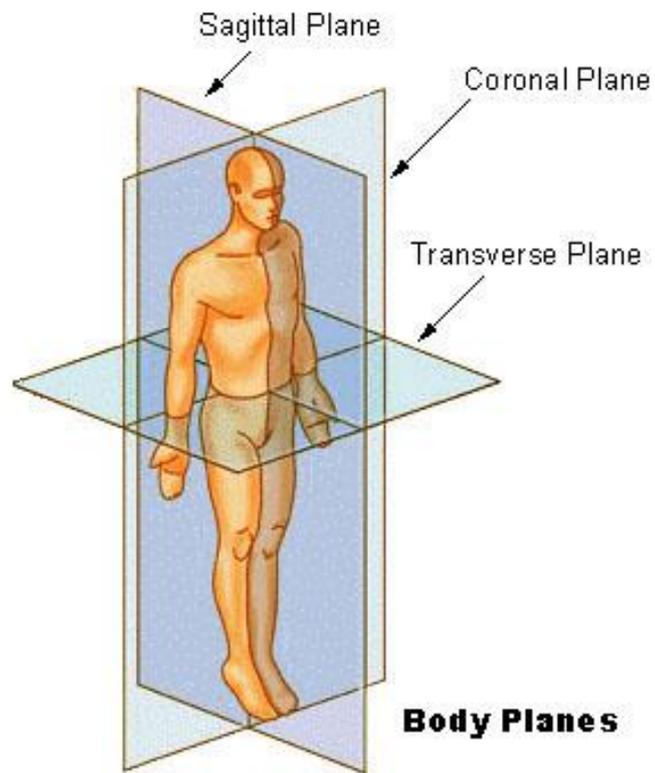
Figure 35 - Planes of motion in which a human body can be divided
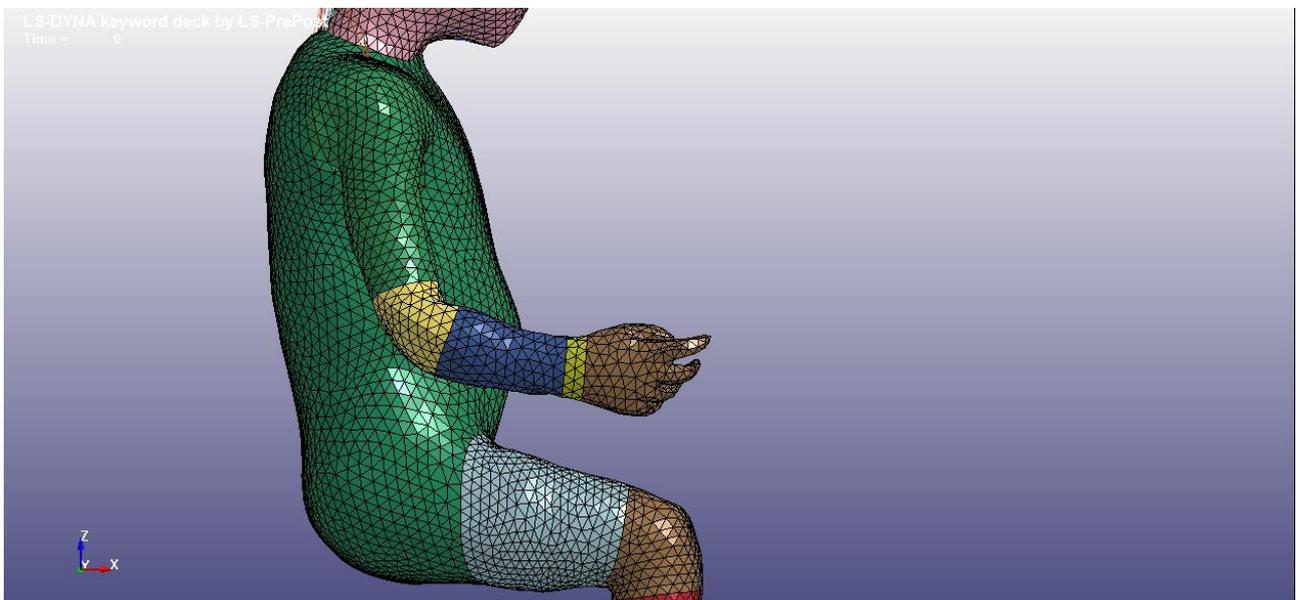
Figure 36 - XZ plane
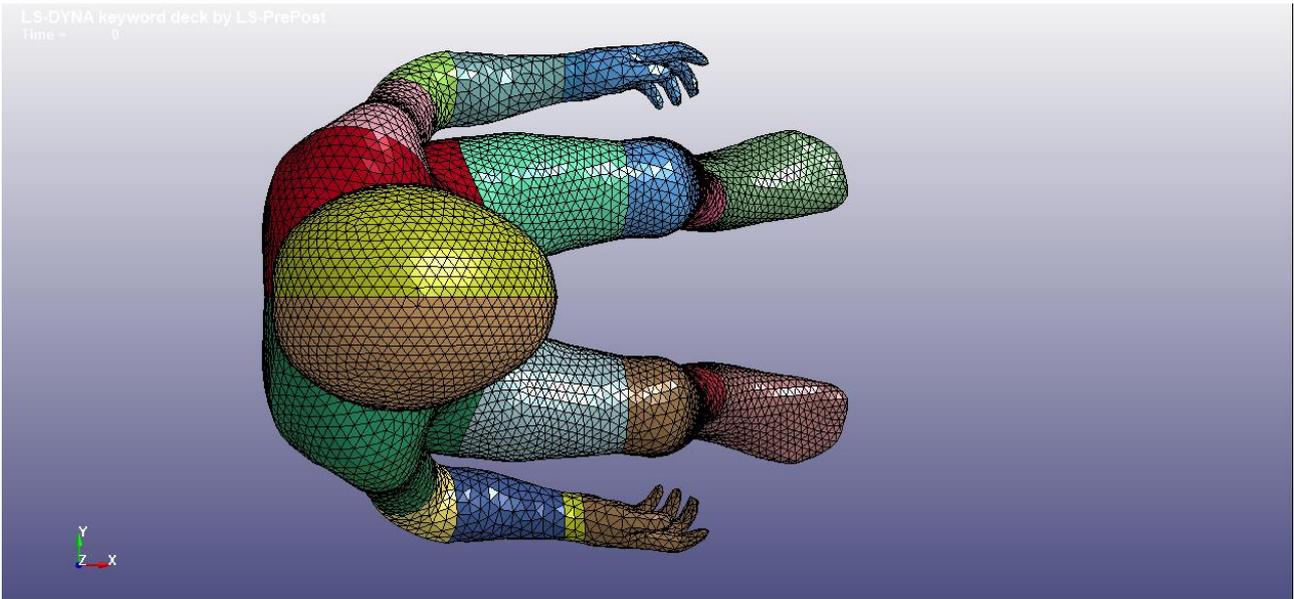
Figure 37 - XY plane

In all the simulations the shell is subjected to a sinusoidal motion law, as the one presented in the previous paragraph. However, the main parameters of the curve have been progressively varied, performing various proofs. Now the main passages of the simulation's evolution will be described.

Step 1

The easiest way to start was to construct a shell with an elliptic form, shown in Figure 38. It wraps the model from the arms.
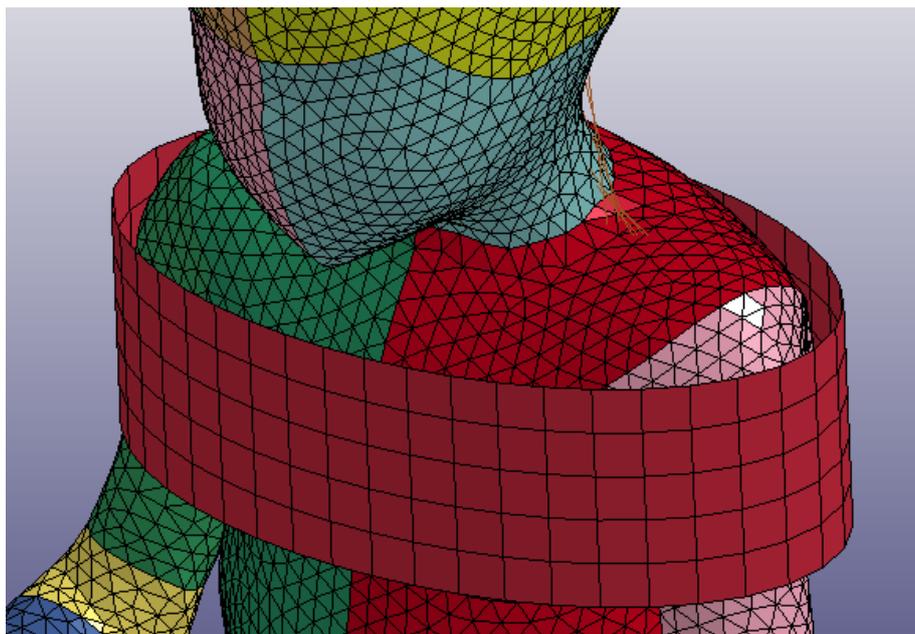
Figure 38 - Elliptic shell

During the pre-processing phase is necessary to impose a contact between parts that interact. Here a type of contact called *automatic_surface_to_surface* is imposed. It requires to define which are the parts involved in the contact and to set some properties. The set coefficients are initially:

- Static friction coefficient $\mu_s = 0,1$
- Dynamic friction coefficient $\mu_d = 0,1$
- Viscous damping coefficient $\zeta = 10\ \%$

The precedent coefficients have been changed subsequently. Initially, this setting was done only between the shell and the skin of arms and trunk, because it represents the exterior part. This solution caused problems of compenetrating between the parts, so an equal kind of contact was also imposed between the shell and the flesh part, to improve the quality of the contact. Doing this, the parts started to interact correctly. Finally, the chosen movement of the shell has an amplitude of 25 millimetres, for a period of 20 milliseconds. The simulation was run and stopped after 40 milliseconds.

In this way the first important result was obtained: the child model started to move for the effect of the "hand". It was possible to appreciate the head's movement.

Step 2

Evolving the model, the shell maintains an elliptic shape, but it has been positioned under the armpits (Figure 39). In the previous solutions there was a strong influence on the model's shoulder, that is an effect unwanted. So, the shell is moved under the armpits of the model. Because of the conformation of the child model, was impossible to avoid the compenetrating phenomenon between the shell and the arms; for this reason, the contact relation between them has been removed.
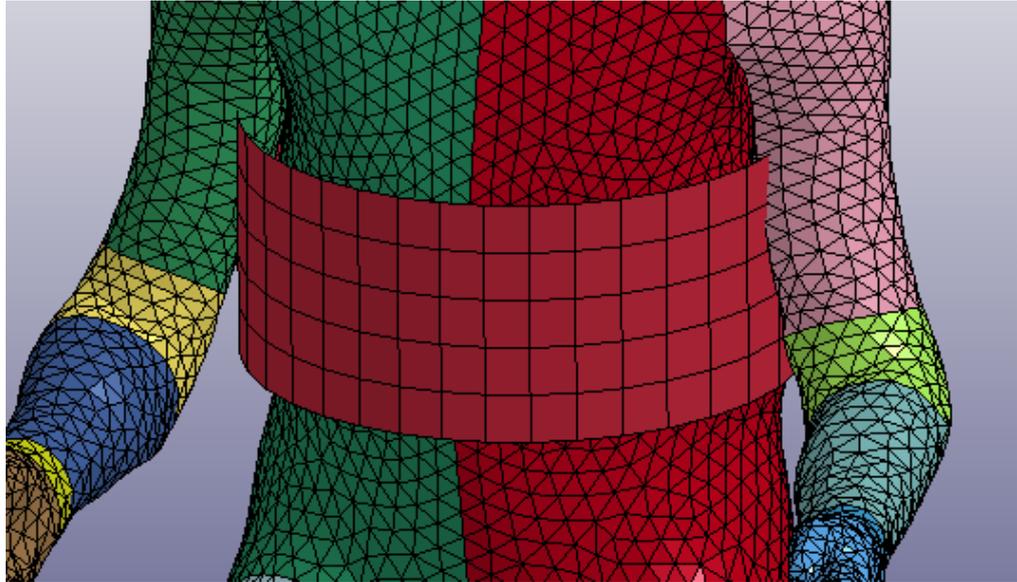
Figure 39 - Elliptic shell; new position

Step 3

Then the model of the shaking hand is creating directly starting from the skin's mesh. It has been copied and scaled with a small offset value (Figure 40). This solution limits the initial impact between shell and body model, which is something not wanted. Ideally, the hands of a man are holding the baby from the starting moment, without any impact. Creating a mesh in this way, this effect is really limited. In a successive step also this small effect will be removed.
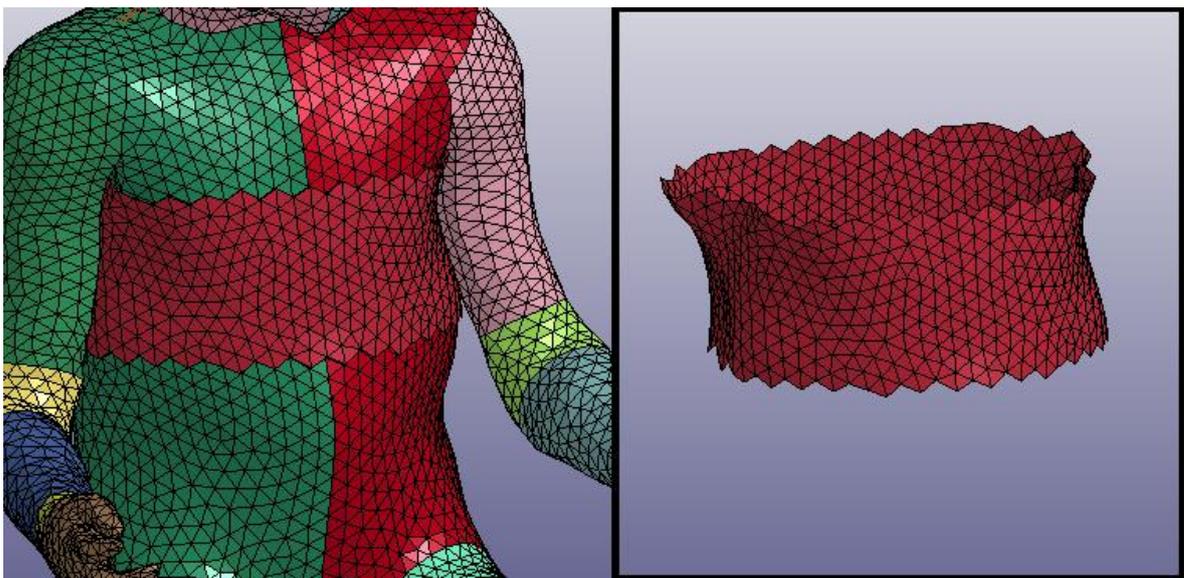
Figure 40 - Shell from the skin's mesh; whole body and detail

<u>Step 4</u>

The fourth step of the evolution process add to the model an initial pressure on the baby's thorax. Obviously, in the act of the shaking, the perpetrator is taking the child from the thorax and he is applying a pressure, which is acting also in the starting time of the simulation (t=0). This will also remove totally the undesired impact between the parts.

In order to obtain this the model should be preloaded in some way, and there are many possibilities to do this. Finally, it is realized with an initial permeation between the hand and the skin's layer. The two parts are both shell type: their offset is chosen small enough so they initially permeate because of their thickness. The type of contact between the parts is changed in *surface_to_surface_inteference* (only the one between skin and shell) and contextually the card *dynamic_relaxation* is added to take into accounts the dynamic phase before the simulation starts. Doing this, in the dynamic phase of the analysis the software tries to remove the initial penetration between the two parts; once that the set tolerance is reached the penetration is removed and an initial state of stress is acting on the child's body.

Then, the effect of gravity is added. To do this, the whole model is loaded with a force produced by the gravity (according to the consistence of units, the gravity's value is set to $9,81 * 10^{-3} mm/ms^2$).

The initial pressure may be high enough to guarantee that the baby is holding in the shell without falling. The same "high-enough" values should be maintained for the whole time. This threshold is simply estimated thanks to a simple equilibrium between the forces acting, modelled in the simplest way: the gravitational force should be balanced from the adult's hand, considering the contact surface and the friction between hand and child's body. This calculus does not pretend to be accurate or precise; it wants only to give a main idea of the order of magnitude, to be sure that the stress values registered are not meaningless.

The necessary pressure was approximated solving this equation, obtained from a force's equilibrium:

$$mg = \mu F$$

where:

- m is the child's mass
- g is the gravitational acceleration
- μ is the friction coefficient
- F is the minimum requested force

Expressing the force as the product of pressure and area in which it is applied, the equation can be easily written as an inequality:

$$p_{min} \geq \frac{mg}{\mu A}$$

In the previous relationship the area called as A is the shell's area, equal to 368,74 cm², that is for sure overestimating the surface of two human's hands. Obviously, the value of minimum pressure changes with the coefficient of friction. In Table 14, for some values of μ are reported the correspondent minima pressures. It is convenient to remember again that these are the results of an extremely simplification, given only to have a main idea of the magnitude of pressures that should be involved.

Friction's coefficient [-]	Minimum pressure [kPa]
0,35	9,52
0,40	8,33
0,45	7,40
0,50	6,66
0,55	6,06
0,60	5,55
0,65	5,12
0,70	4,76

Table 14 - Minimum pressure as function of friction coefficient

After these, some other small modifications have been introduced. First, the offset between the shell and the hand has been varied to understand how it is influencing. It was observed that it is not affecting so strongly the results of the process: so it is definitively maintained at the value of 0,7 millimetres. After this, the friction coefficient is changed. The number chosen until now (0,1) is too low according to the property of human skin [51]. So, it has been modified, also if actually these parameters are not affecting too much the simulation's results.

- Static friction coefficient $\mu_s = 0,6$
- Dynamic friction coefficient $\mu_d = 0,55$

4.2.3 FINAL CONFIGURATION

All the steps and the simulation performed were necessary in order to get the final configuration of the model, that can be used for the last simulations. All the characteristics used finally, introduced little by little, are herein resumed.

- The shaking shell is creating copying the skin's shell. Its area is extended for 368,74 cm² and it is composed of 1429 elements. The mechanical properties are the same as the child model's hand and it can move only in x-direction thanks to the boundary conditions given.

- Gravity is applied to the whole body

- The initial pressure is applied, thanks to initial penetration between moving shell and skin

- The shaking movement follows the next law:

$$x(t) = -30 * \sin(0{,}0314 * t)$$

The sinusoidal law presented has a period of 200 milliseconds (correspondent to a shaking frequency of 5 Hz) and an amplitude of 60 millimetres. Expressing times in milliseconds, the displacement results in millimetres. This law is represented in Figure 41.
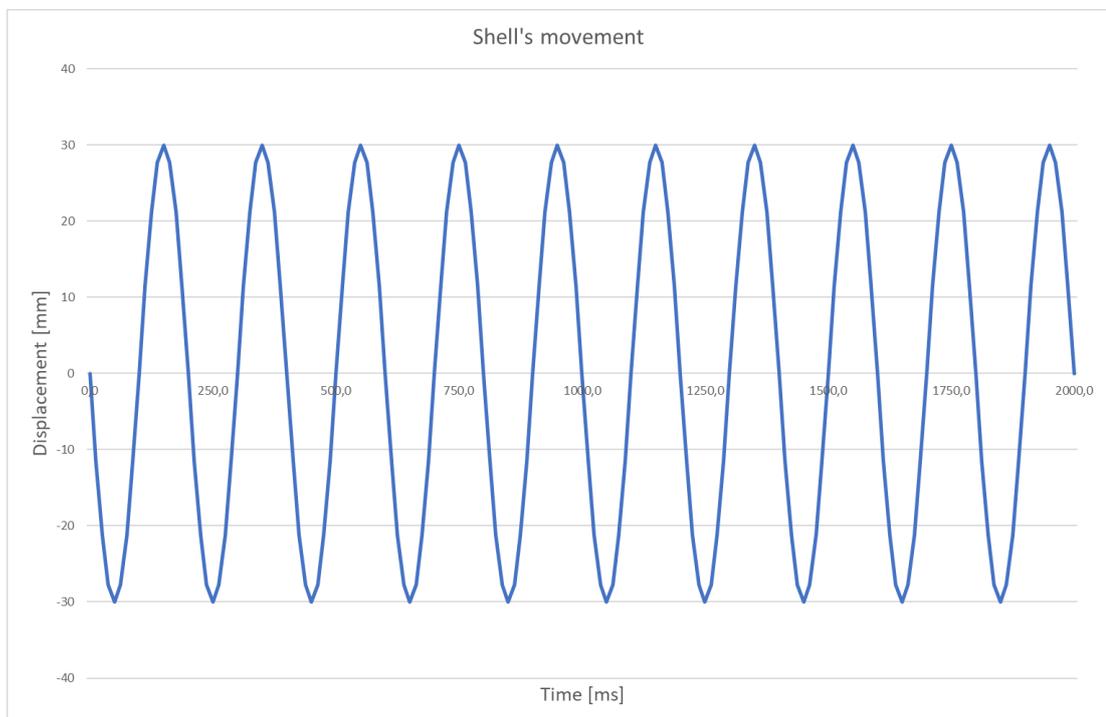
Figure 41 - Sinusoidal displacement law

- Contacts are imposed between moving shell and skin (with an interference) but also between moving shell and flesh.

- The friction coefficients of the contact are set $\mu_s = 0,6$ and $\mu_d = 0,55$ with viscous damping of $\zeta = 10\ \%$

- The termination time is set to 2 seconds

Subsequently Figure 42, Figure 43 and Figure 44 show three different views of the PIPER child model.
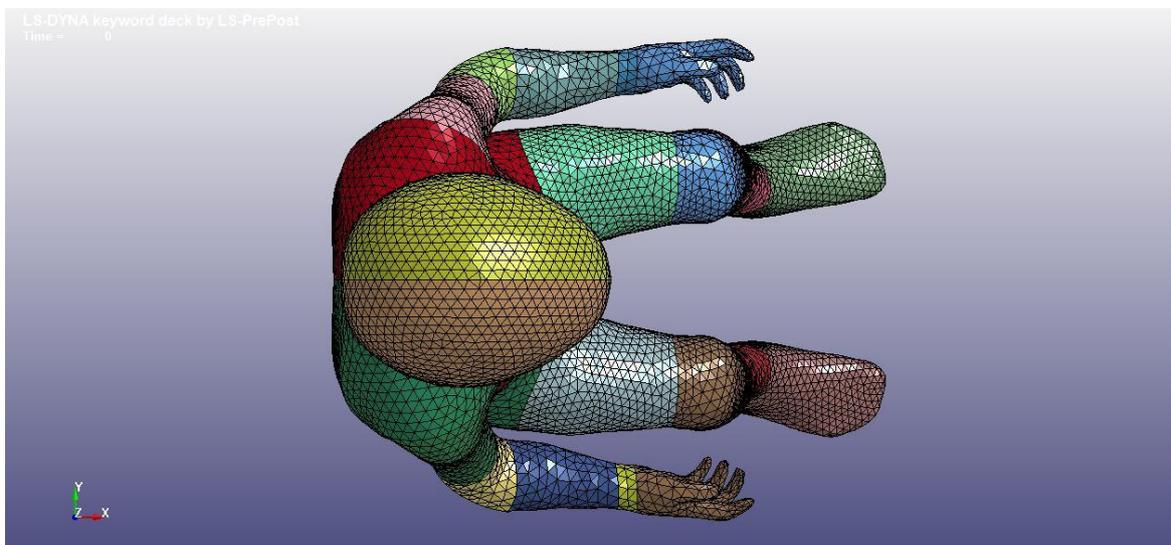
Figure 42 - Child's view
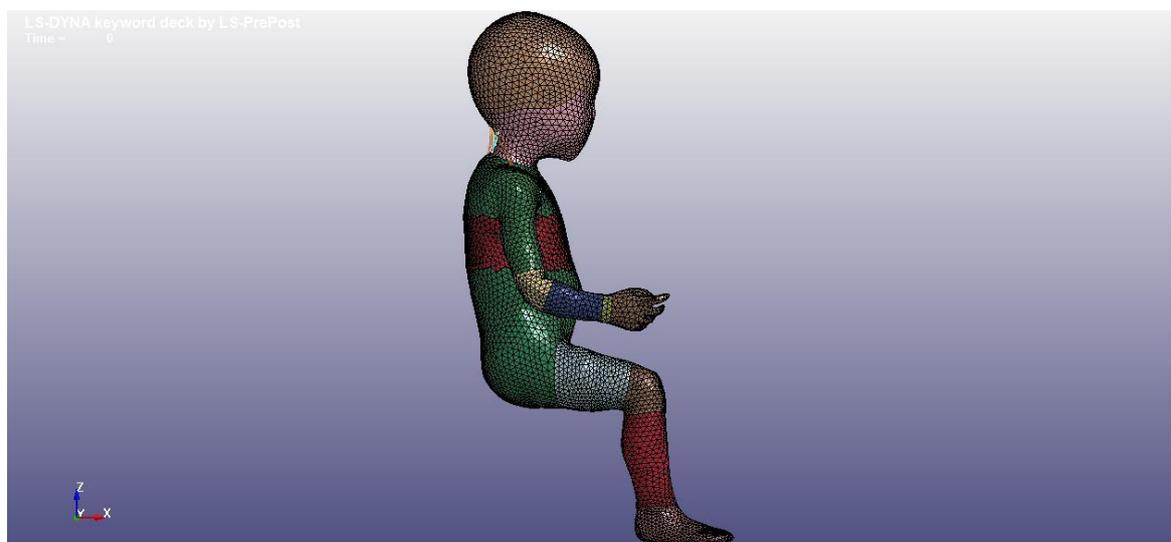
Figure 43 - Child's view

Figure 44 - Child's view

4.3 MEASUREMENTS

Before running the simulation, the desired outputs should be set in the pre-processing phase. Looking at the injury criteria described in chapter 2, the most important parameters are the kinematic angular ones: velocities and accelerations. Correctly measuring these data is a fundamental process to obtain meaningful numbers. The data's collection has been done in two different ways:

1. <u>Using a rigid body inside the head</u>. A small part of the head, normally deformable, is converted into a rigid part, but the original section and material density rest unvaried. In the PIPER child model is already present a rigid element in the head which can conduct this function. It is in a subgroup of the keyword element, called seatbelt accelerometer. It is positioned in the subsystem called sensors, with the number ID 1150. It was obtained by a part of the cerebral cortex. The used card creates an accelerometer fixing it to a rigid body that contains three nodes; in this way, a local reference system will be created, centred in one of these points (in this case the choosing node is 1150000, coincident with the centre of gravity of the head). An accelerometer will usually exhibit considerably less numerical noise than a deformable node [52]. In Figure 45 is shown the position of the accelerometer inside the head.
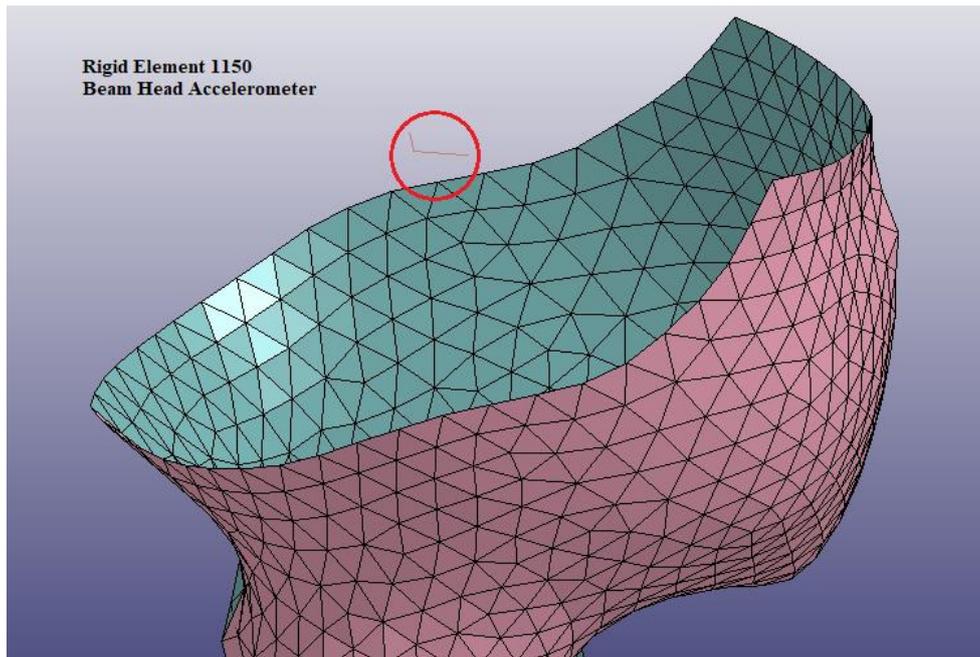
Figure 45 - The accelerometer position inside the head, circled in red

2. Using the centre of gravity. Between all the nodes which are forming the head, is possible to take one of them well-positioned for the measuring function and taking from it the necessary information. The node 155555 (the position is shown in Figure 46) is the one that represents the head's centre of gravity (it is coincident with node 1150000). Then the card *constrained_interpolation* was used. With this keyword, the motion of a single node is interpolated from the motion of a set of nodes [52]. The set used for the interpolation contains nodes which are all taken from the skull, as depicted in Figure 47.
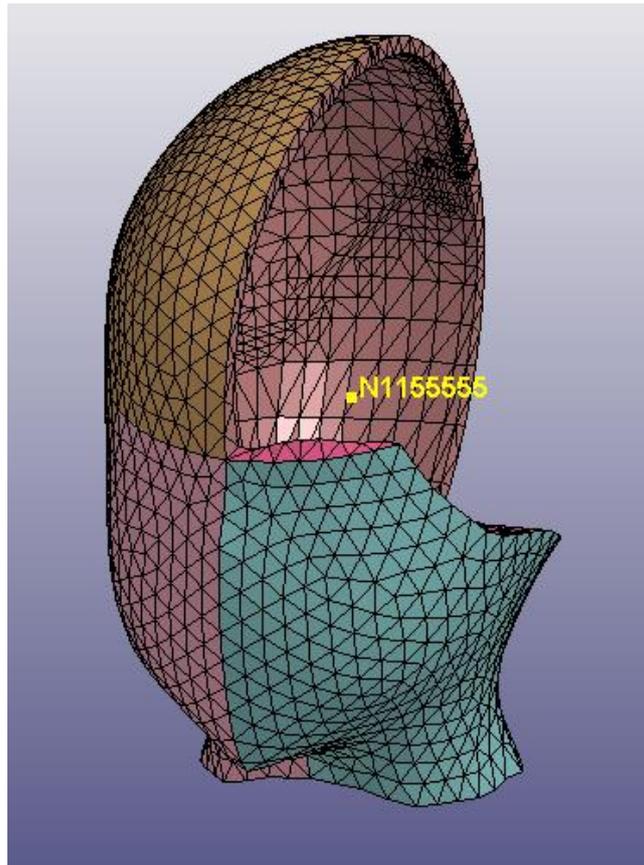
Figure 46 - Position of the node C.O.G. inside the head
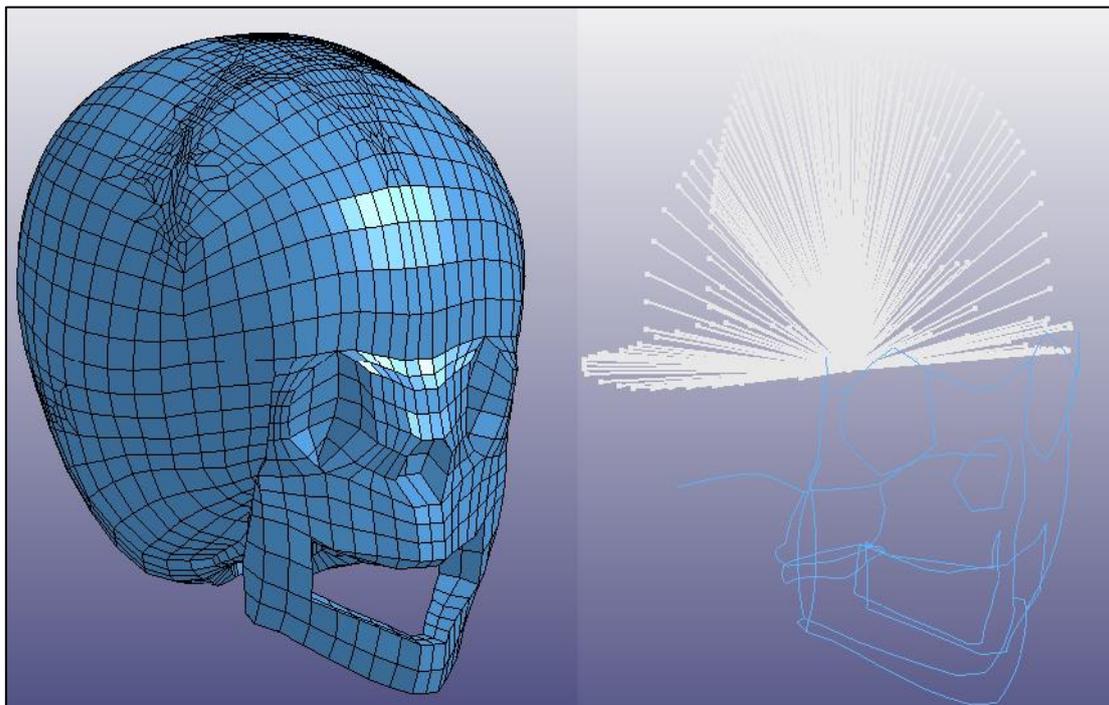
Figure 47 - On the left the skull of the model, on the right the set of nodes used for the constrained interpolation

For what concerns the pressure's measure, the data are obtained setting before the simulation the card *intfor.* which can register forces acting during contacts.

5. POST PROCESSING

The post-processing is the phase in which the outputs of the simulation are analysed and then some conclusions can be figured out. Once that all the necessary parameters are extrapolated, the injury criteria introduced in chapter 2 may be used in this phase to obtain an estimation of the possible damage that can occur, also effectuating a comparison between different criteria which are based on various hypothesis or conditions. In addition, the numerical data can be compared with the results of other studies realized using other child's models, as the ones introduced previously in chapter 3.

In the following paragraphs the most significant parameters are reported and discussed.

5.1 SIMULATION'S RESULTS

So, this simulation replicates a simple shaking episode, without any impact. Considering the conditions imposed step by step (explained in detail in the previous chapter), the simulation has been run for a total time of 2 seconds. The next images (Figure 48, Figure 49, Figure 50, Figure 51, Figure 52) show a sequence of the shaking experiment in various instants of time, starting from the first screenshot at the initial time and then proceeding every 250 ms.
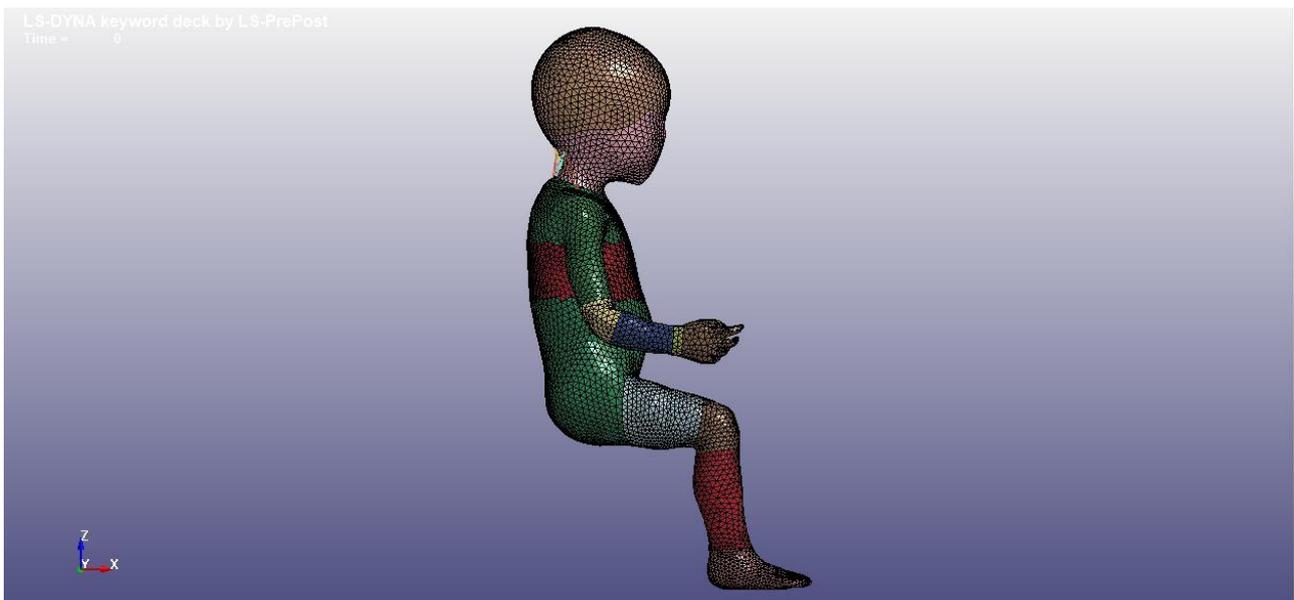
*Figure 48 - Screenshot at t = 0 ms*
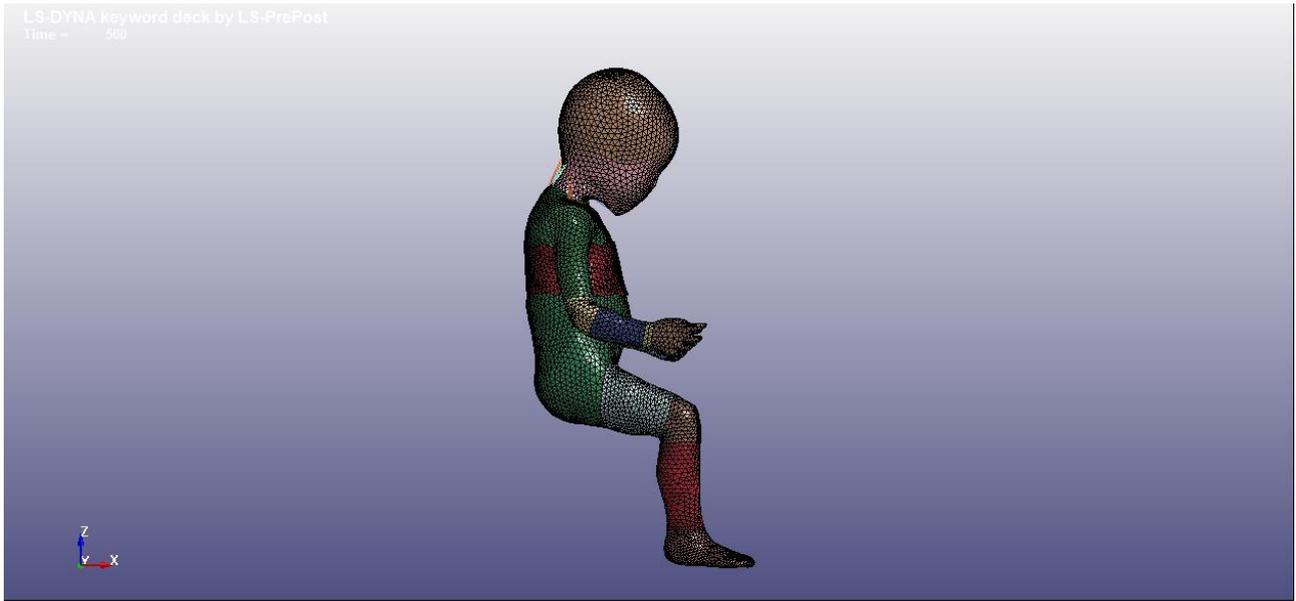
Figure 49 - Screenshot at t = 500 ms


Figure 50 - Screenshot at t = 1000 ms
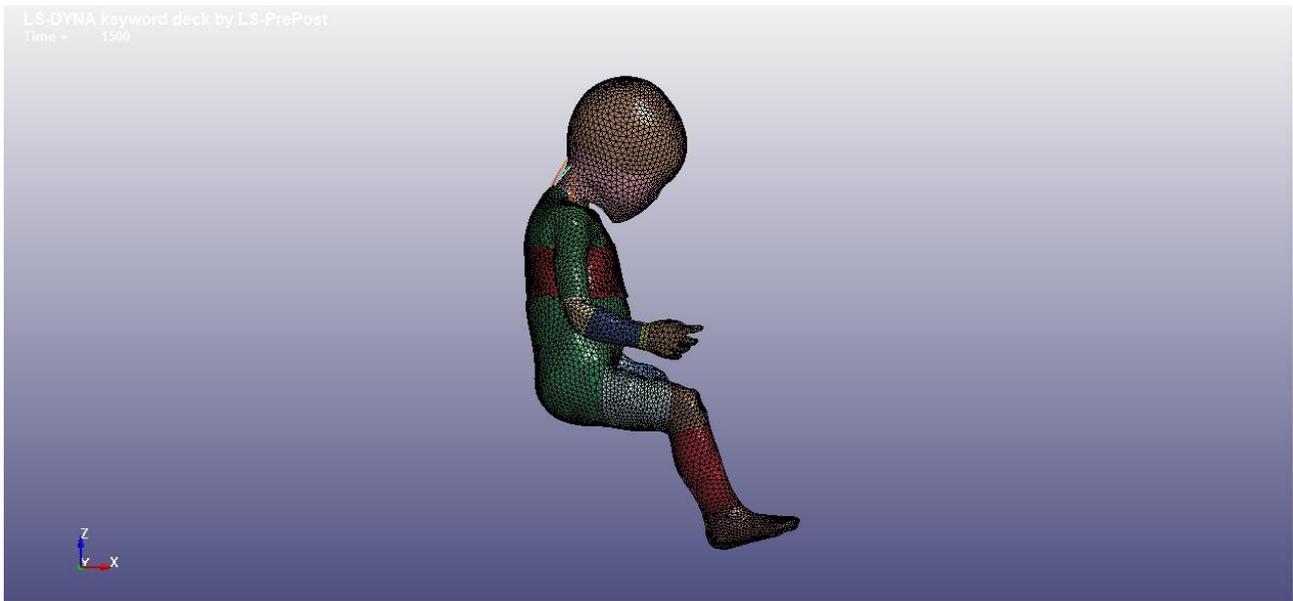
Figure 51 - Screenshot at t = 1500 ms

Figure 52 - Screenshot at t = 2000 ms

Then, all the data necessary for the analysis should be taken. As said, the desired outputs must be requested before the simulation starts (in the pre-processing phase), in the general settings. Therefore, the next cards have been imposed:

- d3plot: every 25 ms, it displays plots of the shaking frequency, allowing to appreciate the movement of the model in a video sequence.

- intfor: every 10 ms, it investigates deeply the contact interactions selected in the pre-processing phase.

- nodout: every 1 ms, it points out the time history of some nodes. Both centre of gravity and accelerometer measures can be read thanks to this card; the first one through the node 1155555, the second one using the central node of the accelerometer 1150000.

5.1.1 CONTACT PRESSURE

As explained in the previous chapter, an interface pressure is present on the baby's thorax at the starting time of the simulation and this value should be almost maintained for all the time, or at least it should not go under an lower threshold. This is necessary to guarantee the hand's grasp on the child's body.

Once that the simulation is run, after a dynamic phase the preload can be applied thanks to the initial penetration between shells. In Figure 53 is depicted which is the situation at t=0 ms on the child's skin. An interface pressure is acting, because a stress state has been left from the initial penetration imposed.
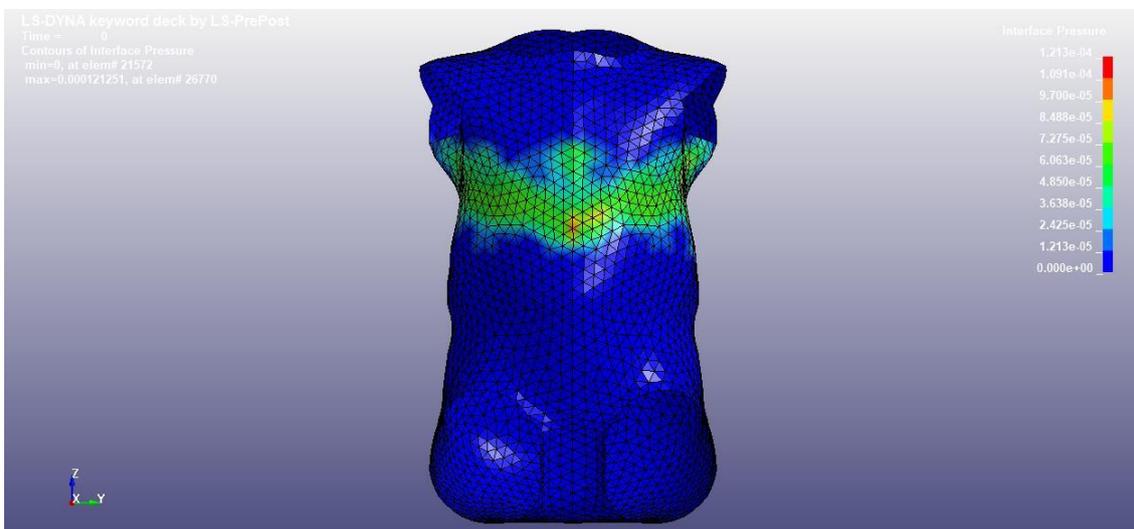

Figure 53 - Interface pressure on the child's skin

During the simulation, an interface pressure is always present in the part in which the contact is operating, as shown by Figure 54 and by Figure 55 taken after 500 and 1000 milliseconds respectively.
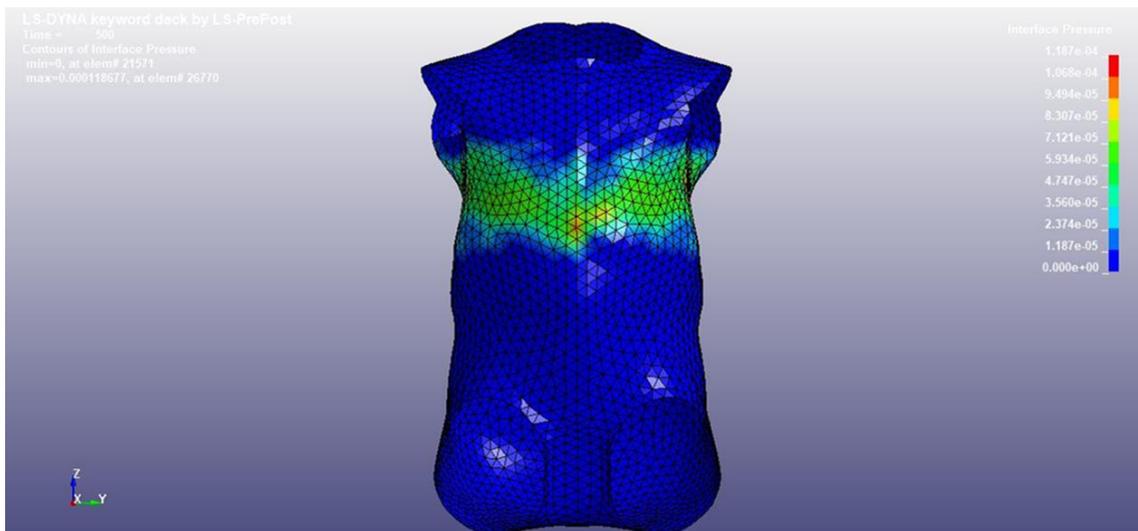
Figure 54 - Screenshot at t = 500 ms
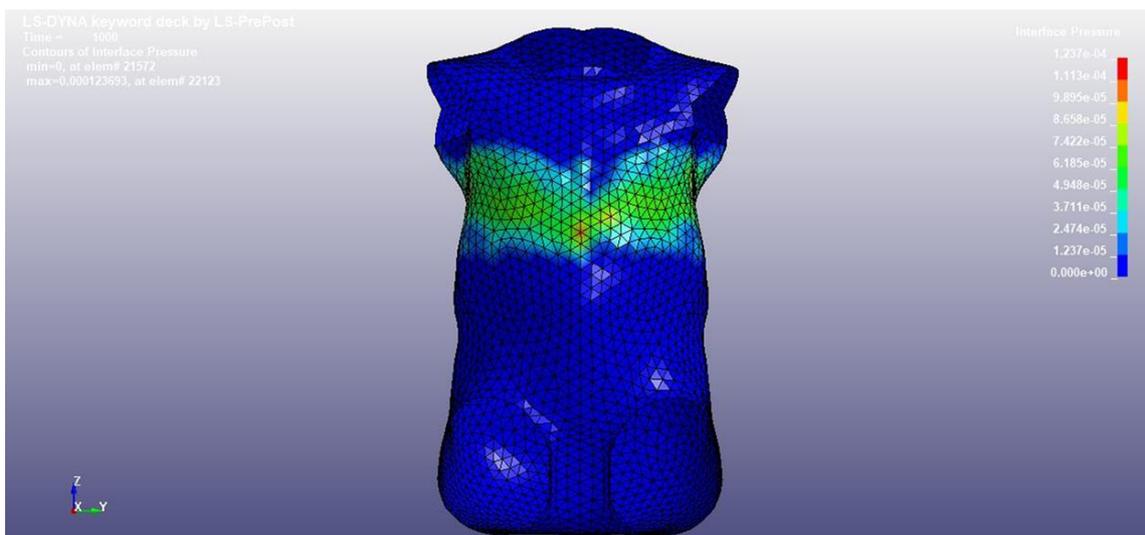
*Figure 55 - Screenshot at t = 1000 ms*

LS-Dyna can register, thanks to the card *intfor*, the interface pressure's value in each element, and also other information about contacts (as shear stresses or interface forces). In Figure 57 is presented a graph showing the average value of pressure over all the interested element which is operating during the time. This value has been calculated instant by instant considering the average of the pressure's value acting on the child's skin, in the area in which it is in contact with the moving shell (Figure 56).
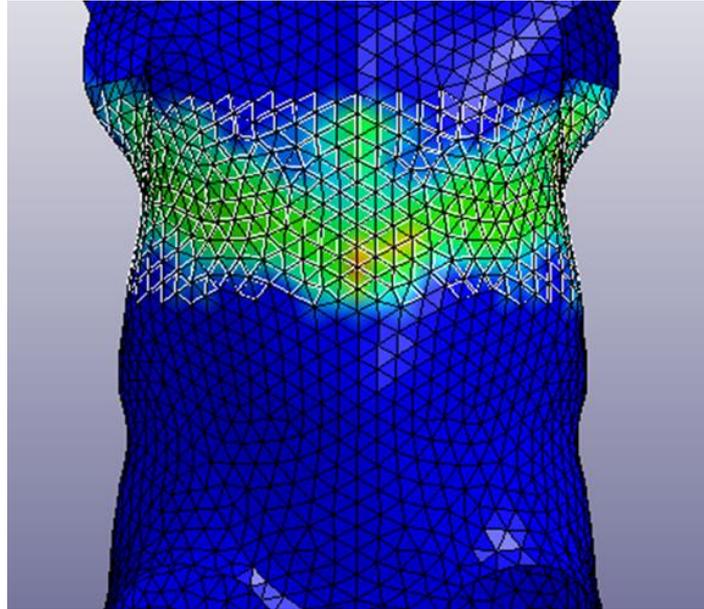
Figure 56 - Selected area on the skin in which the mean pressure has been calculated
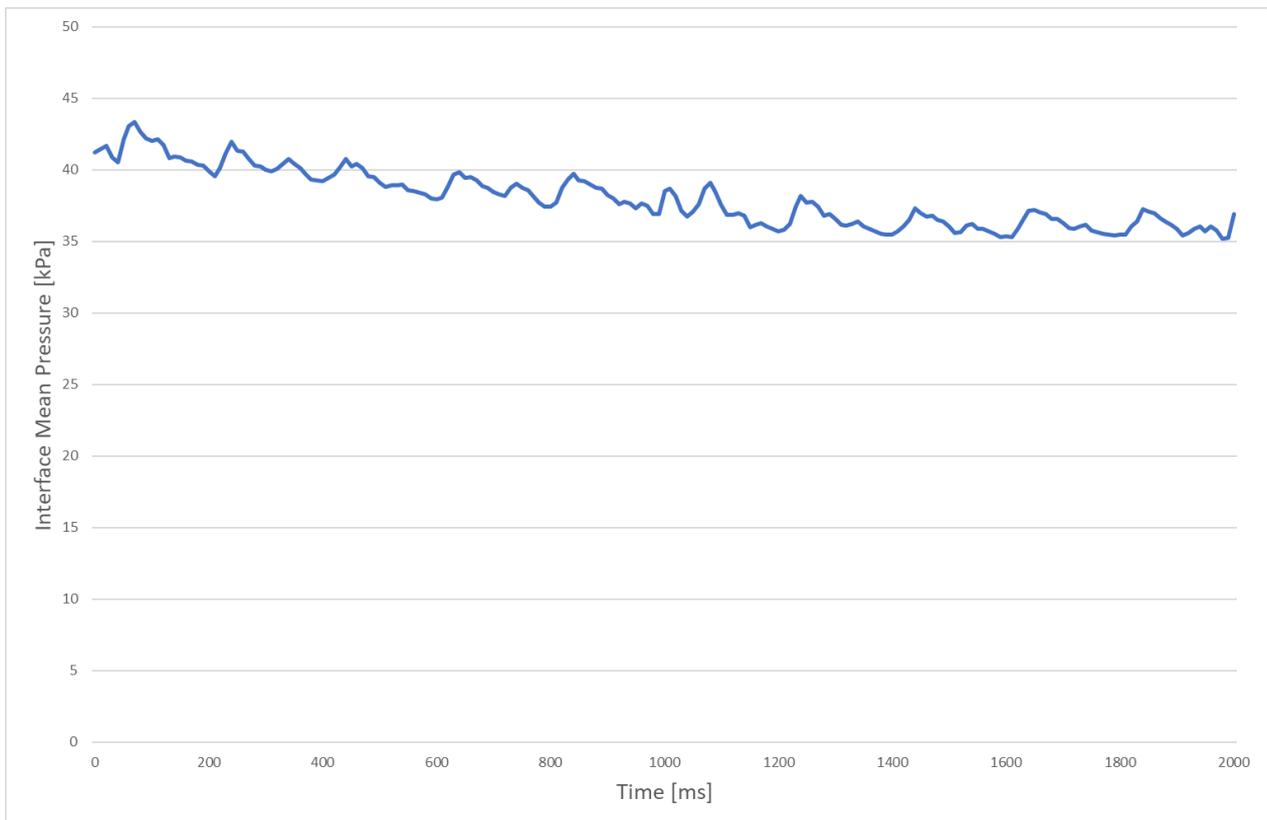

Figure 57 - Interface mean pressure

Considering the global simulation's time, the mean value ranges from a minimum of 35 kPa to a maximum of 43 kPa. According to the simplified model of the contact's interaction presented in paragraph 4.2.2, all these values of mean pressure should guarantee the grasp of the child. Looking at the development of the curve, in the first part of the simulation it seems that the trend is raising down. Then, after almost 1000 ms, the mean pressure value becomes stable, fluctuating around 36,2 kPa.

5.1.2 HEAD'S MOVEMENT

The resultant movement of the head induced by the shake is one of the focal points of the analysis. It can be displayed using the position registered by its centre of gravity, that is node numbered 1155555. Its trend is presented in Figure 58.
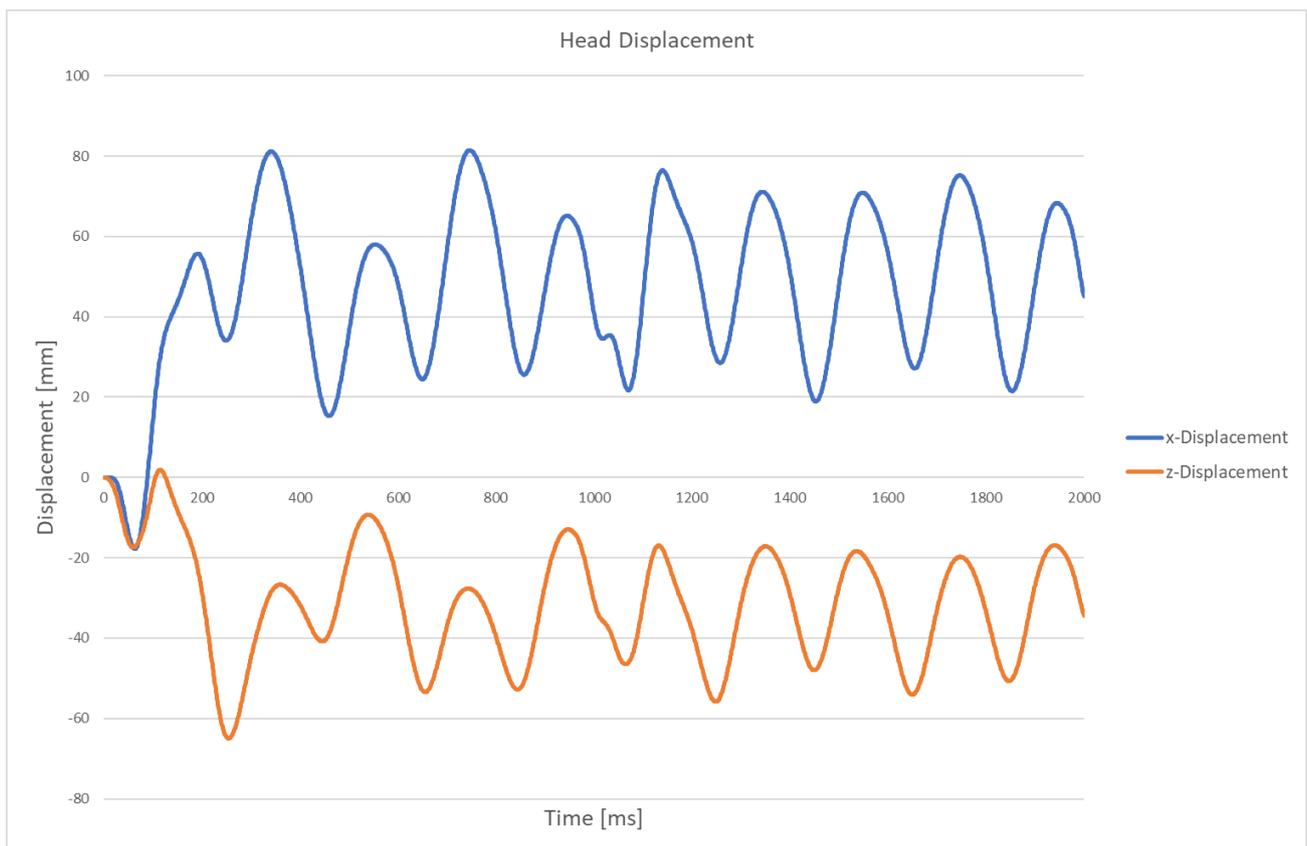

Figure 58 - Head's centre of gravity displacement, in x and z direction

Actually, the obtained trends of the curves are a bit different from the one that was expected before the analysis was completed. In fact, the head is not moving continuously backward and forward, but

it seems that the movement is stabilized after a certain time and after a certain displacement. The head is not able to move forward overcoming a certain position. This is testified to the z-displacement, whose values remain negatives, which indicate that the head does not come back in the restore position. This unexpected result may be a consequence of the relevant difference in terms of mass between the PIPER model and other child's dummy analysed from scientific articles, often lighter and with a smaller inertia. An example of comparison is possible considering the data obtained from Nadarasa et al. [15]. In this work 3 different cases of shaking are introduced, conducted with a shaking frequency of almost 5-6 Hz, similarly to the PIPER's one. The movements in x and z direction (Figure 59 and *Figure 60*) are herein compared, taking into account that the axes of both models are positioned in the same way. It is convenient to remember another time that the two models have relevant differences in terms of age and mass, that can make the comparison difficult.
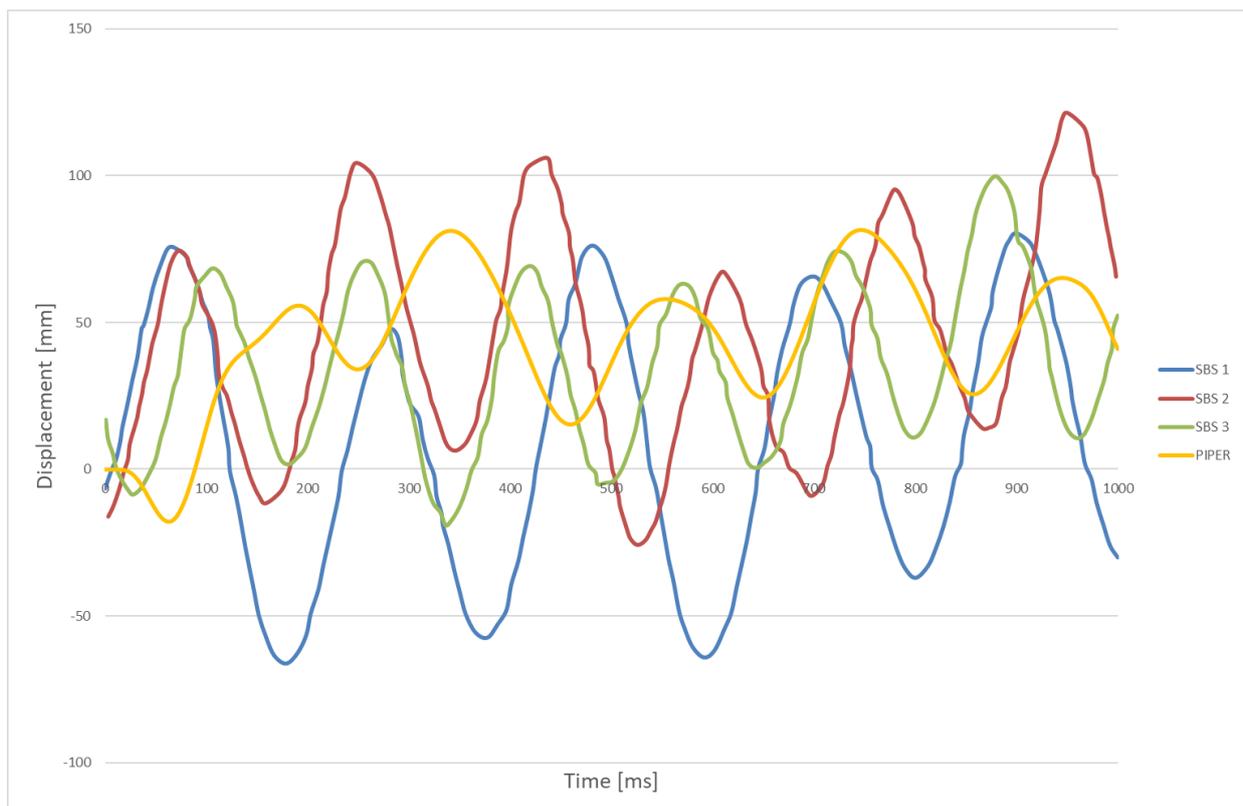

Figure 59 - Displacement of the head in x direction
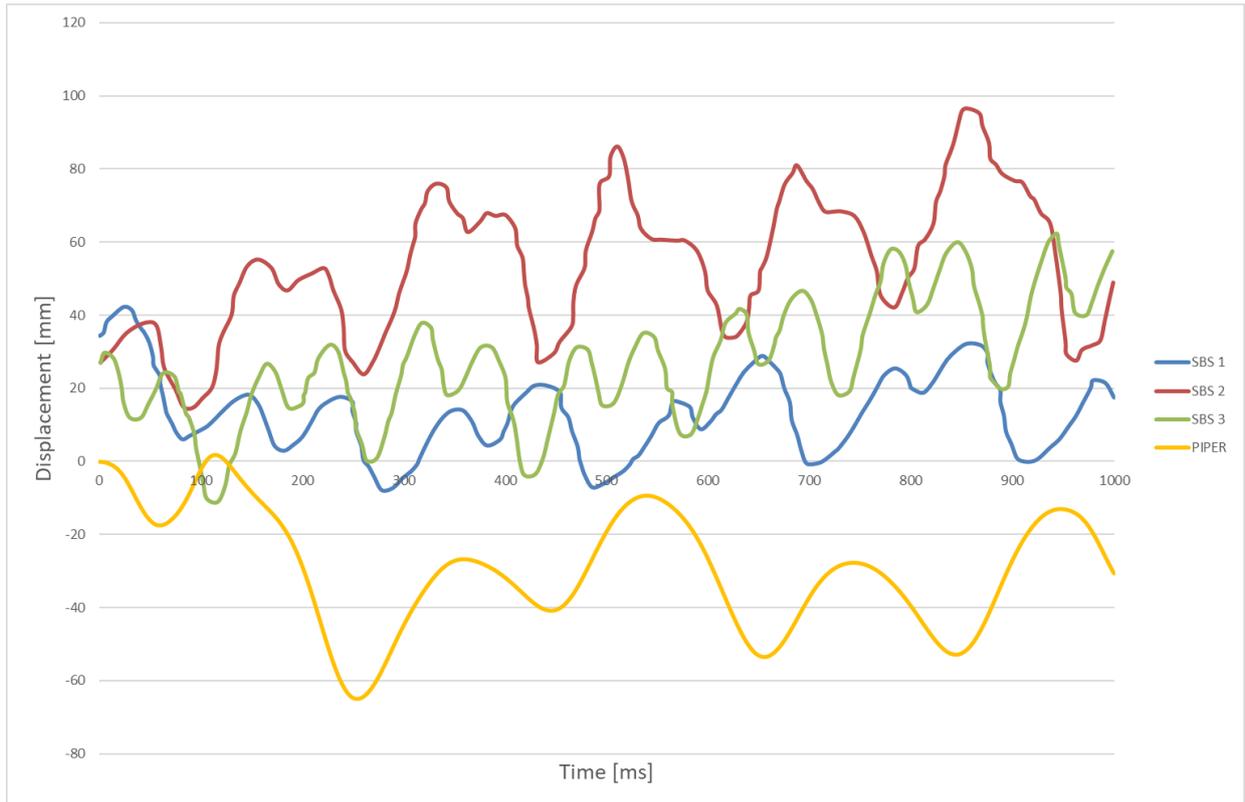
Figure 60 - Displacement of the head in z direction

5.1.3 ANGULAR KINEMATIC PARAMETERS

As often said in the precedent paragraphs, the angular kinematic parameters play probably the most important role in the injury mechanism that can occur after a shaking. In fact, according to many articles in literature, they may be the principal responsible of the presence of subdural hematomas or diffuse axonal injuries, more than other possible parameters. Here, Figure 61 presents the angular accelerations resulted by the simulation, which have been measured in the two different ways already introduced (constrained node interpolation and rigid body accelerometer). The plot shows the resultant acceleration given combining the component in each direction.

$$\alpha = \sqrt{\alpha_x^2 + \alpha_y^2 + \alpha_z^2}$$
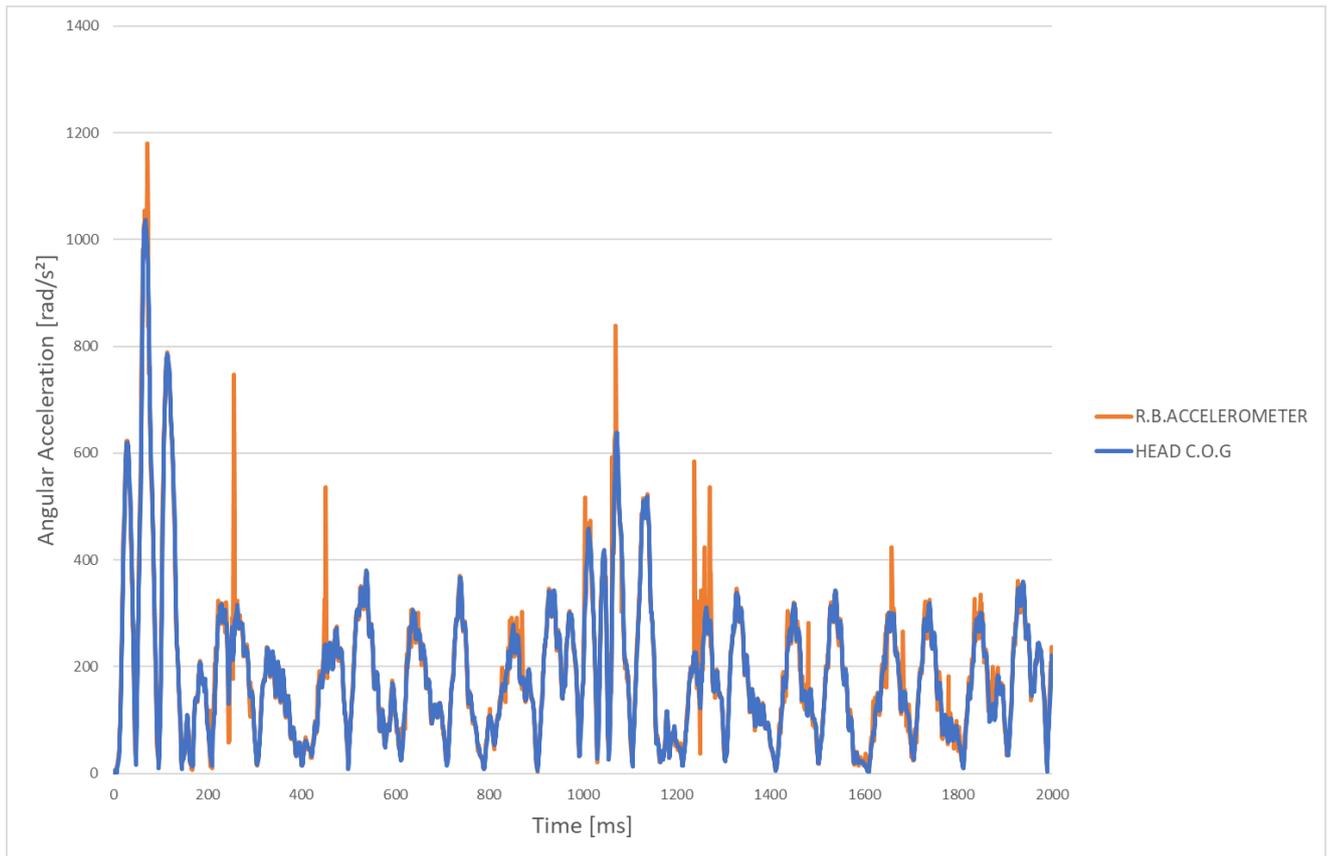
Figure 61 - Angular acceleration

The trend of acceleration continuously goes up and down, reaching the highest value in the early milliseconds of the simulation. After that moment the trend seems to be more stable, reaching a cyclic condition (this is also visible in the chart of head's movement). The pick value can be taken, because it may be useful to analyse the possible injury that the shaking may cause. Both measures register similar values, except that in some instant of times probably because of local numerical errors.

The highest value registered by the signal of the C.O.G. node results 1036 rad/s², measured after 68 milliseconds. Several scientific articles report as limit for head injuries for infants the value of 10.000 rad/s², so the result of the simulation falls 89,6% below. This threshold has been proposed from Depreteire et al. after a cadaveric study; it is associated with a pulse duration shorter than 10 ms and they established also that this limit decreases when pulse duration increase [53]. This limit was also proposed in many articles that specifically discuss about the AHT [54, 55]. This maximum value resulted is coherent with others come out from other studies already cited, which have used similar models in terms of mass and age obtaining accelerations of the same order of magnitude [22, 42]. They have been discussed in chapter 3. To remember them, the experiments performed with the CRABI-12 and with the P3/4 Dummy registered respectively 1068 rad/s² and 830 rad/s².

The precedent cited works discuss only about pick values, no trends of angular acceleration are reported. For what concerns the trend, it can be compared with the one resulting from the studies of Couper et al. [56], which used a finite element model of the infant head. Also in this case, the highest value reached is similar, although the evolution of the curves differs, as Figure 62 shows. These data are compared over a range of 250 milliseconds.
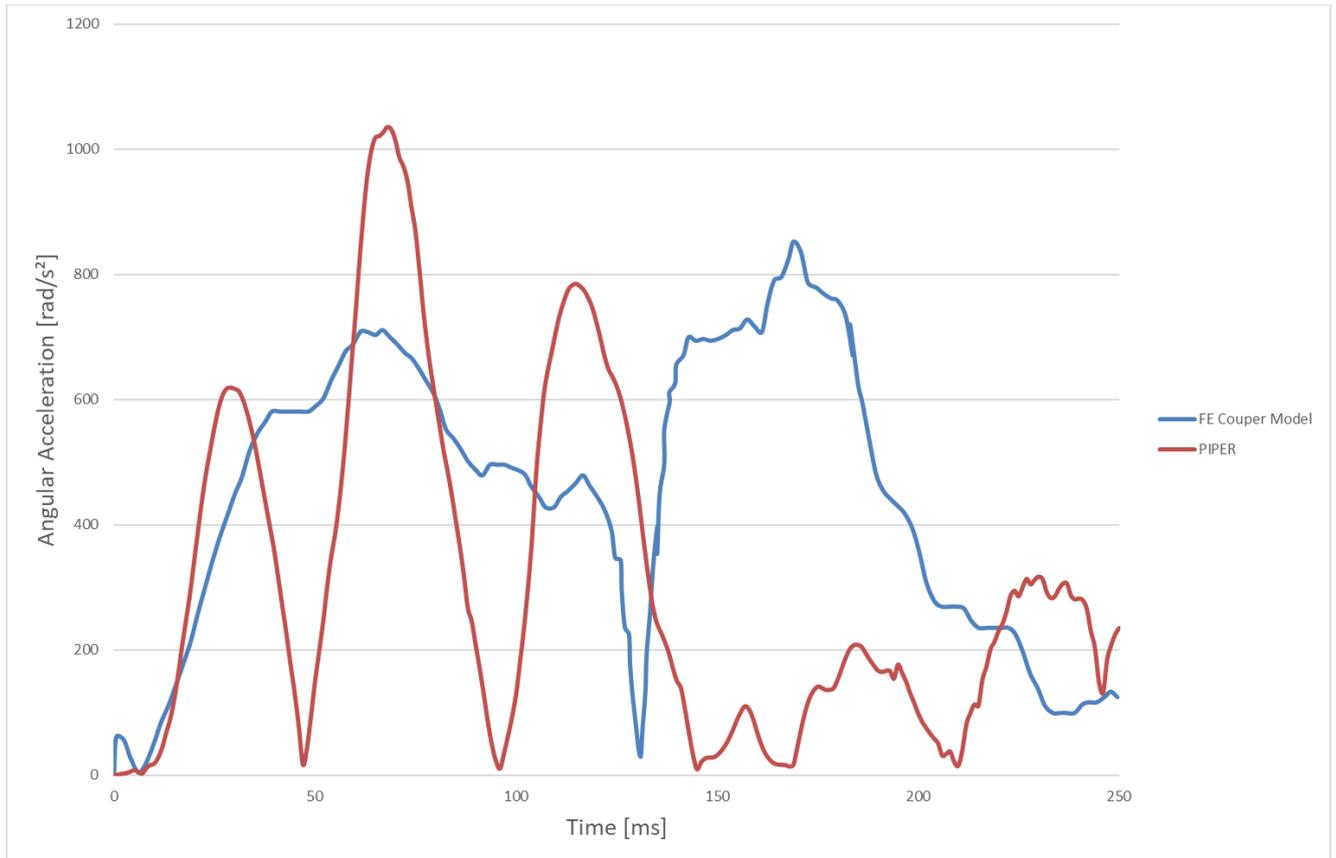

Figure 62 - Comparison between angular accelerations

Another kinematic parameter that has to be considered is the angular velocity. Also for what concerns the angular velocity, the curve replicates an oscillation and the pick value is registered in the first part of the simulation (it corresponds to 13,6 rad/s, registered at t = 95 ms). In Figure 63 the resultant angular velocity is plotted, calculated normally as:

$$\omega = \sqrt{\omega_x^2 + \omega_y^2 + \omega_z^2}$$
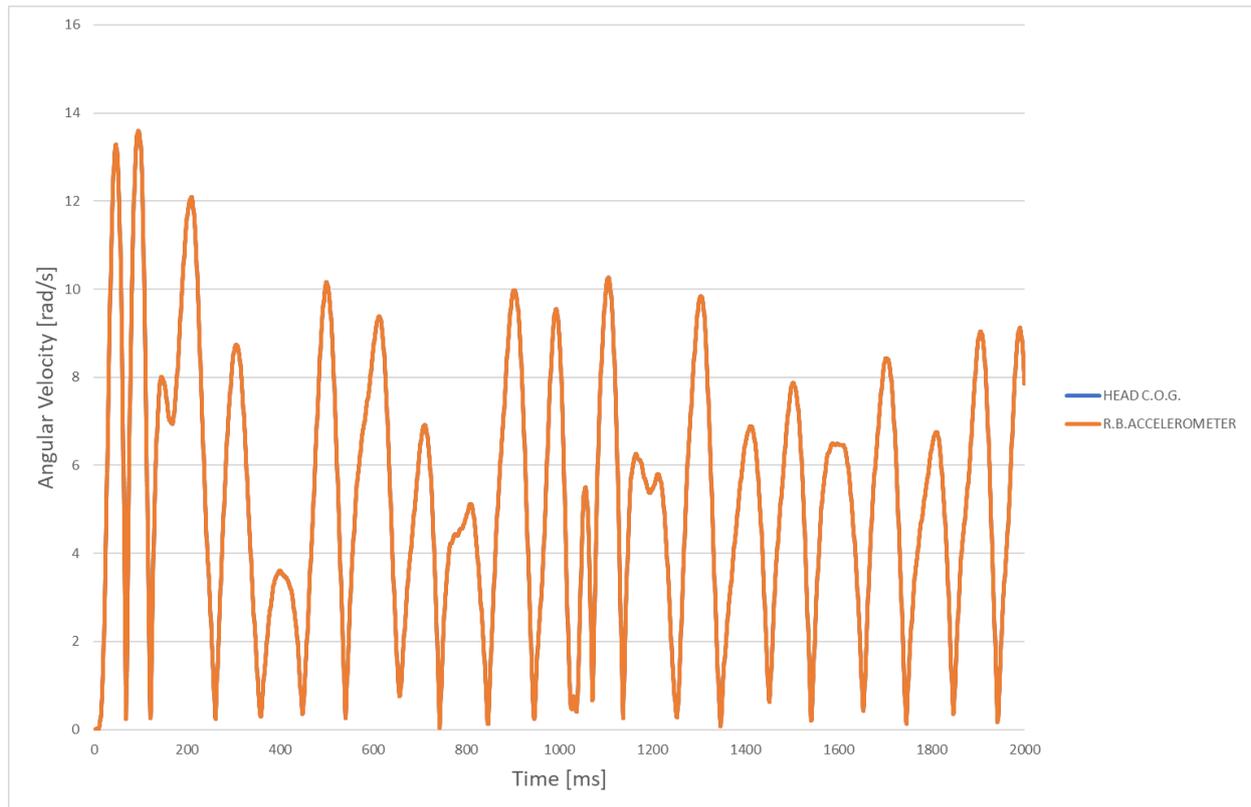
Figure 63 - Angular velocity

For the case of angular velocity, the literature presents as injury criterion the Brain Injury Criterion (Br_IC), that in this case it can be applied. Herein the mathematical formulation already shown is recalled:

$$BrIC = \sqrt{\left(\frac{\omega_x}{\omega_{xcr}}\right)^2 + \left(\frac{\omega_y}{\omega_{ycr}}\right)^2 + \left(\frac{\omega_z}{\omega_{zcr}}\right)^2}$$

The critical values, as explained in paragraph 2.2, have been calculated according to other criteria. Then, it is necessary to have the trend of each component of the angular velocity, that are subsequently reported. In the simulation the component ω_y is much greater than the other two (pick value during time is more than 10 times greater than the others). For this reason, here two different graphs are presented: one with only ω_y (Figure 64) and one with ω_x and ω_z (Figure 65).
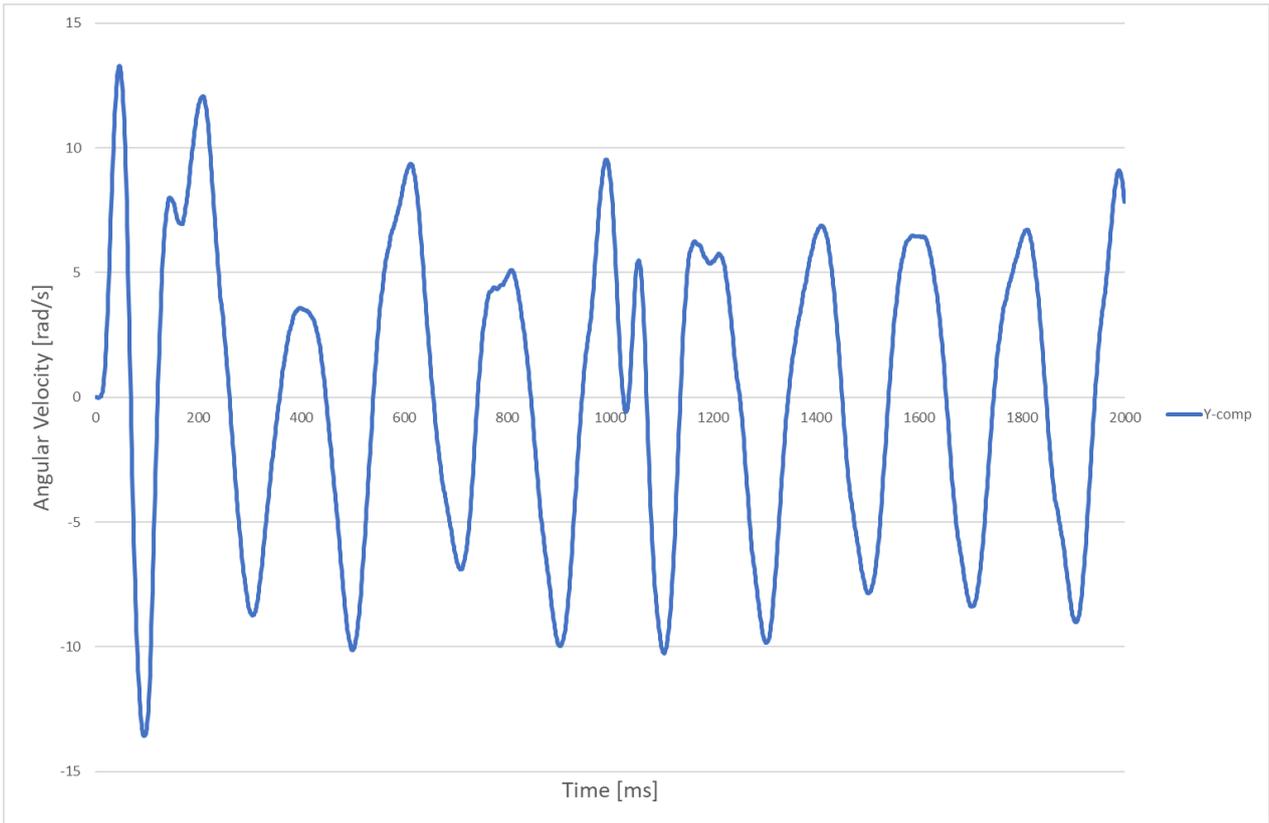
*Figure 64 - Y component of angular velocity*
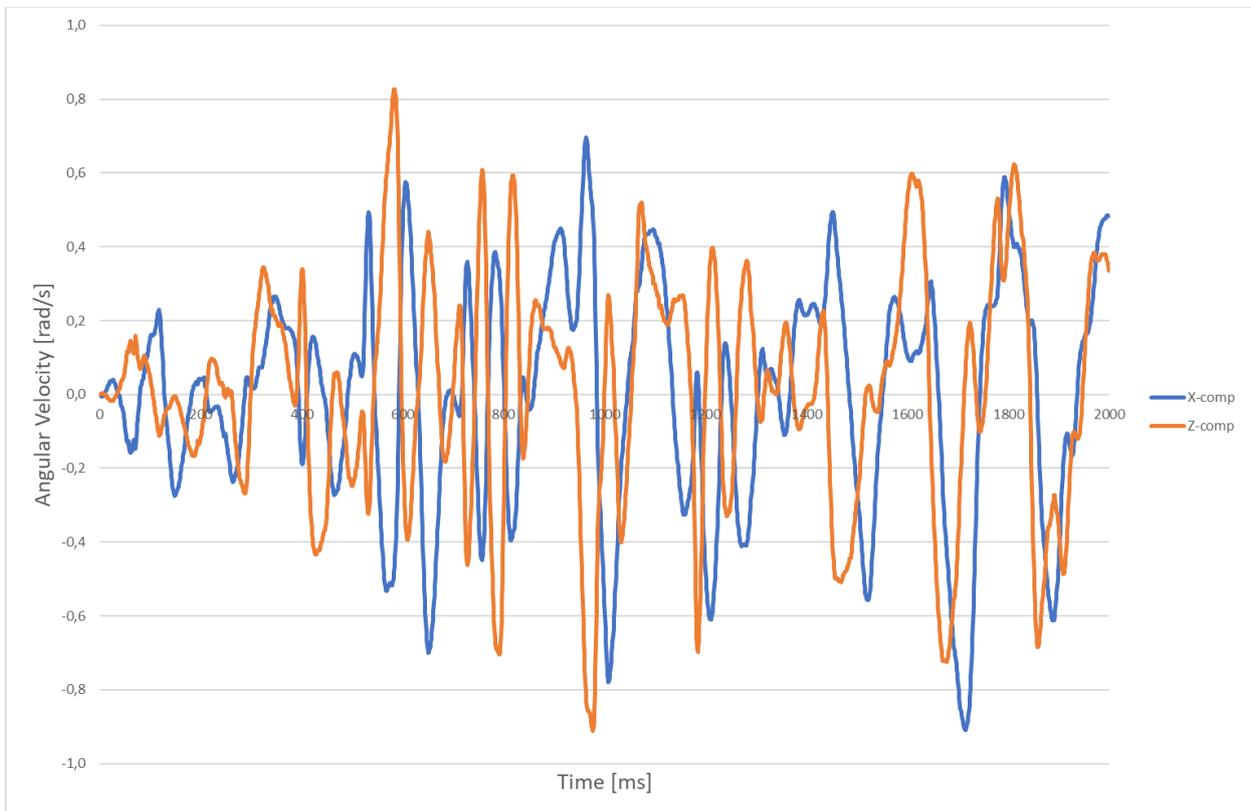
Figure 65 - X and Z components of angular velocity

75

According to the pick values of each component (independently from the instant of time in which they are registered) and considering the critical values estimated, the parameter Br_IC can be computed:

$$BrIC = \sqrt{\left(\frac{0,70}{66,25}\right)^2 + \left(\frac{13,28}{56,45}\right)^2 + \left(\frac{0,83}{42,87}\right)^2} = 0,24$$

The obtained number can be correlated to an injury probability thanks to the graph already introduced in the second chapter, now reported in Figure 66.
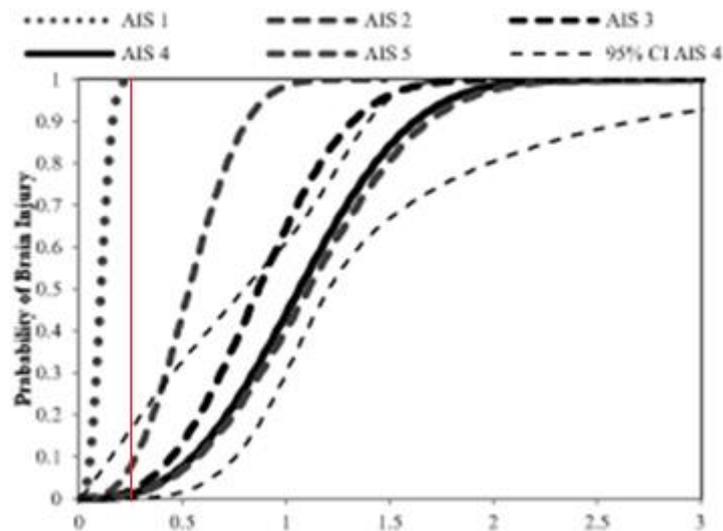

Figure 66 - Br_IC vs Injury Probability

A red line has been drawn in correspondence to the value 0,24 of Br_IC. According to this graph, this angular velocity brings to a damage correspondent to the grade 1 of the AIS (minor damage, light lesions with possible headache, vertigo or lacking consciousness). A certain probability that more serious damages can occur is estimated. The probabilities reach low values; for example, the probability to have an AIS 5 damage (correspondent to a critic situation) seems to be lower than 5 %.

Values of angular velocity and angular acceleration can also be used to obtain an estimation of the strain that the brain's tissue is experiencing. According to the studies already mentioned computed by Takhounts et al. [27, 28] the maximum value of acceleration or velocity is more or less linearly linked with some factors as: maximum principal strain, cumulative strain damage measure (CSDM) and relative motion damage measure (RMDM). It is necessary to remember that these works discuss about impacts and not about AHT, so the next conclusions are only adapted for this study case.

Focusing the attention on one of these parameters (maximum principal strain), this linear correlation is shown in Figure 67, in which the chart has been replicated from the values presented in the referred article.
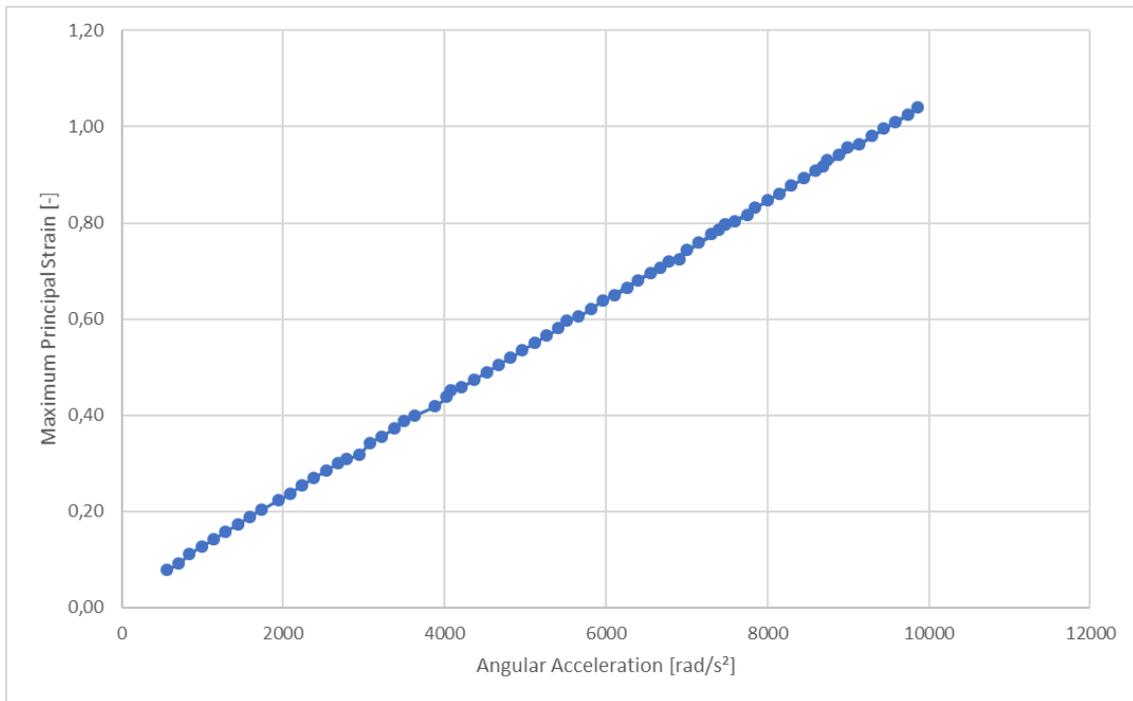

Figure 67 - Relationship between angular acceleration and strain

Considering as maximum value of acceleration 1036 rad/s², the correspondent strain results almost 0,12, due to the linearity of the relationship. Once that the maximum principal strain is estimated, an evaluation of the probability that DAI can occur can be figured out. It is done thanks to the next graph (taken to the mentioned article and presented in Figure 68). It may be described by the equation subsequently reported, used to calculate this probability.

$$probability = \frac{1}{1 + e^{-3,759*\varepsilon_{max}+3,286}} = \frac{1}{1 + e^{-3,759*0,12+3,286}} = 0,055 = 5,5\%$$
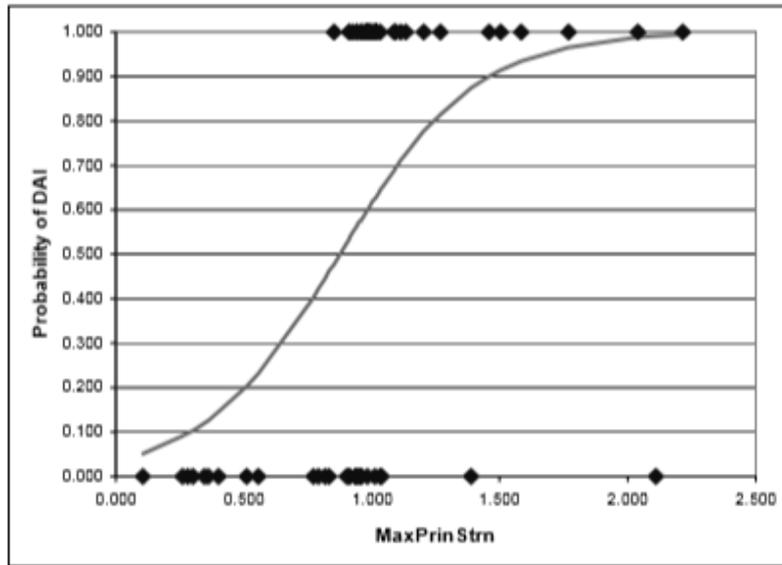
Figure 68 - Injury probability correlated to maximum strain

5.1.4 LINEAR ACCELERATION

The trend of head's linear acceleration is presented in Figure 69
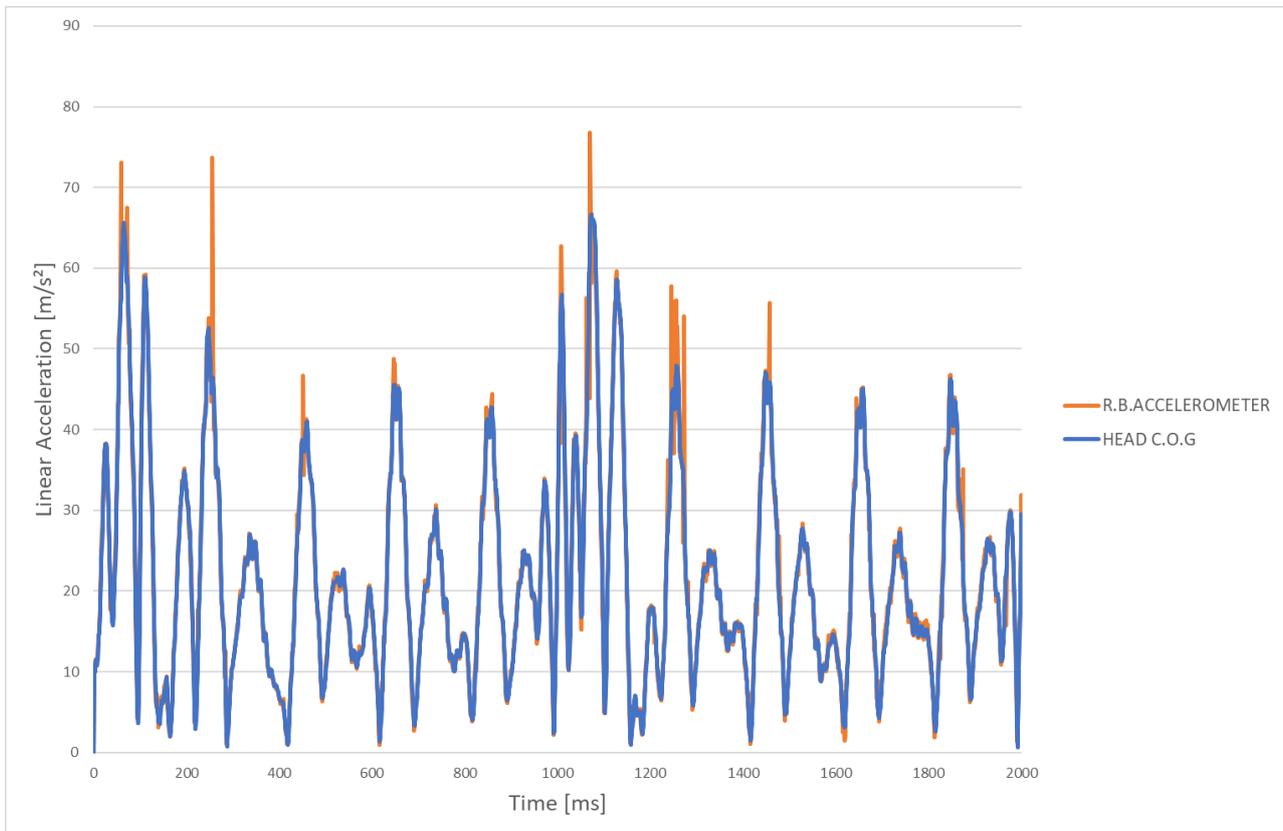
Figure 69 - Linear head's acceleration

A comparison can be done with other maxima values computed in other works. In this simulation, the centre of gravity registers as pick value 66,8 m/s² (equal to 6,8 g). CRABI-12 and P3/4 Dummy experiments have obtained similar values: respectively, they are 7,6 g and 5,8 g. In opposition, the experiment conducted over the Q0 Dummy procure a higher value (12,2 g). As results, between all the models analysed, the ones with similar masses (global and of the head) register comparable pick values.

Then, components' trends of linear acceleration can be analysed. The research of Cirovic et al., done using the child's mannequin P3/4 Dummy [42], has also produced the charts relative to these trends. After having collected and organized all the data, values along x (motion direction), y and z can be compared each by each in three different charts, presented in Figure 70, Figure 71 and Figure 72.
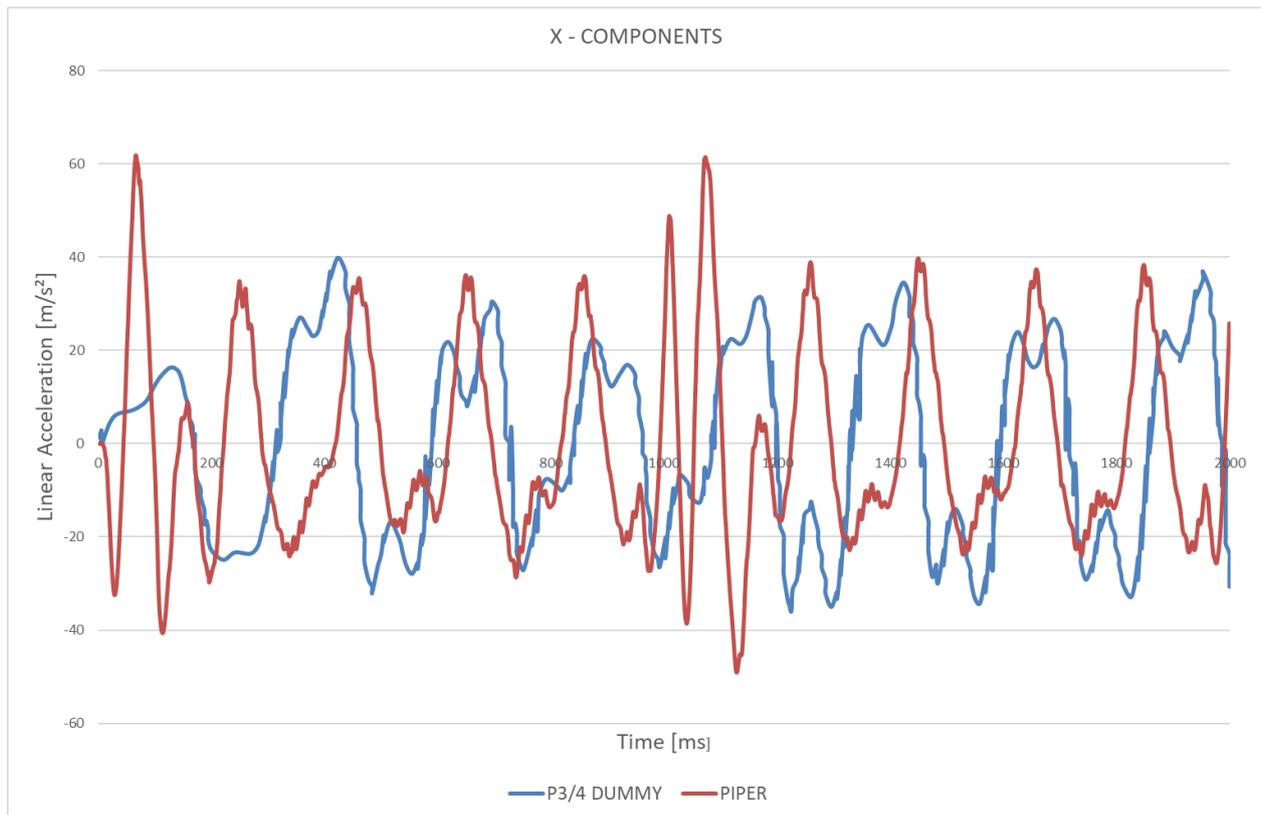


Figure 70 - Comparison between x components of linear acceleration; this is the motion direction
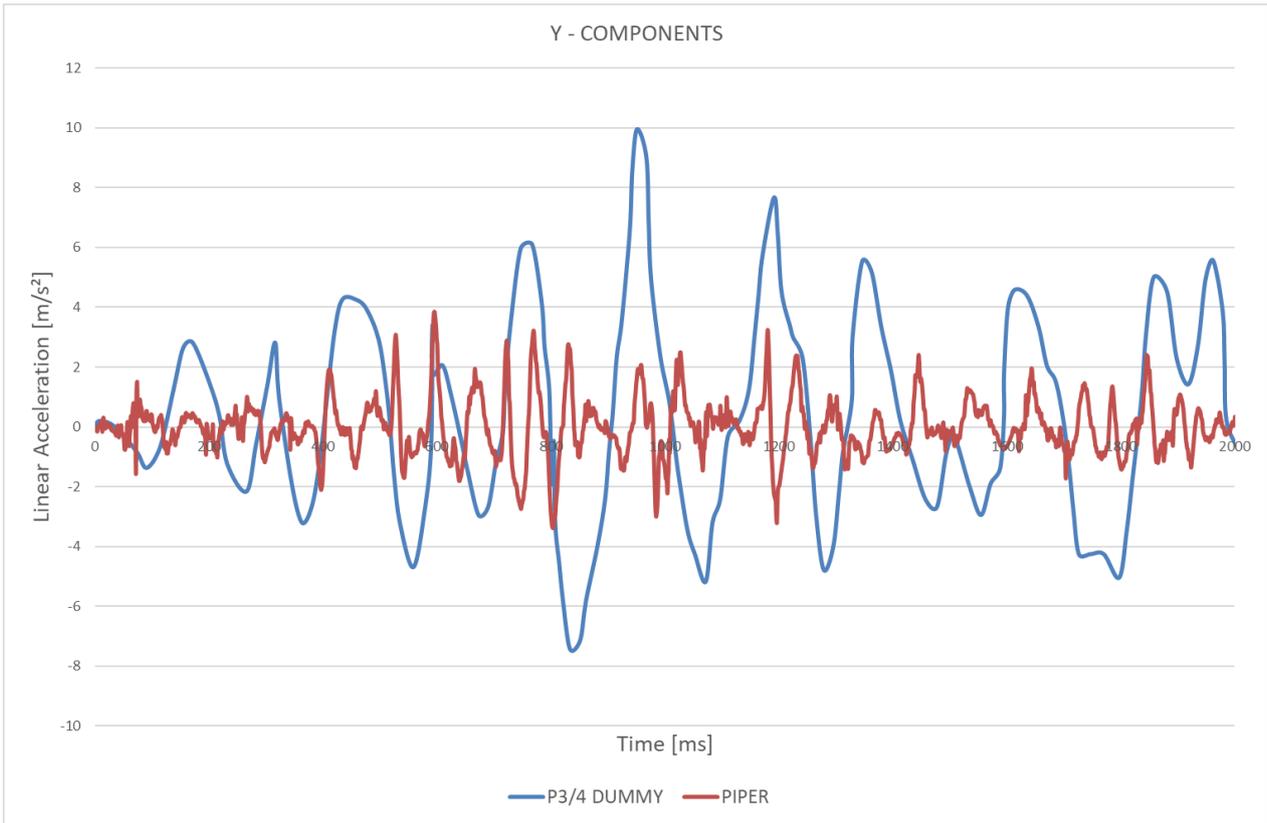
Figure 71 - Comparison between y components of linear acceleration
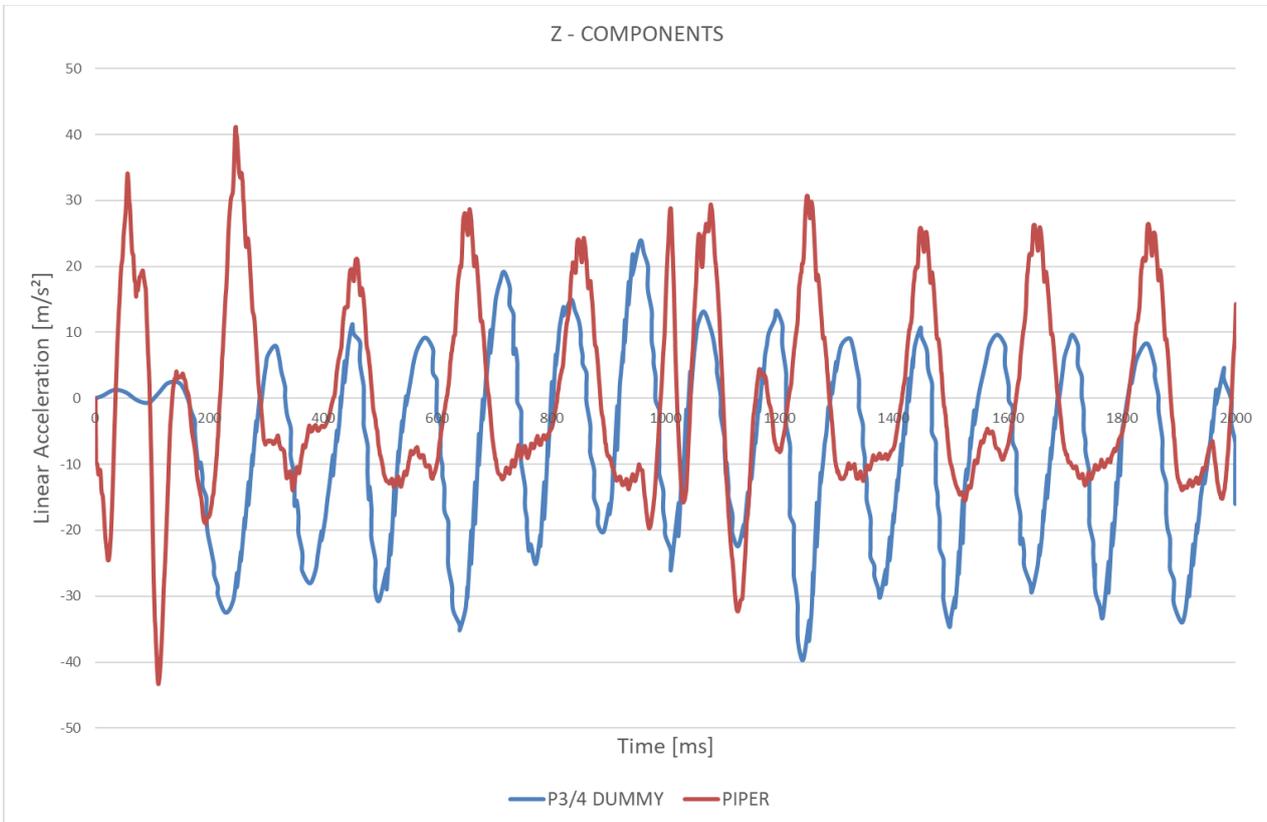
Figure 72 - Comparison between z components of linear accelerations

80

In these charts is possible to see that trends are similar and in both cases values in y direction are more or less 10 times lower than the ones in x and z direction.

As said when the head's injuries were introduced, linear accelerations are not so important in the evaluation of these kind of injuries, because they are not generally responsible for diffuse lesions but only for focal lesion [13].

5.1.5 COMPARISON: RESUME

In order to have a schematic comparison between all the available data, here in Table 15 the values registered in the PIPER simulation and in other cases are again reported.

MODEL	AGE [months]	TOTAL MASS [kg]	HEAD MASS [kg]	MAX.LIN. ACCELER. [g]	MAX.ANG. ACCELER. [rad/s²]	MAX.ANG. VELOC. [rad/s]
PIPER	18	12,5	2,98	6,8	1036	13,6
Q0 Dummy [15]	1,5	3,5	1,13	12,2	4962	\
P3/4 Dummy [42]	9	9	2,20	5,8	830	32,0
CRABI-12 [22]	12	10	2,64	7,6	1068	25,5

Table 15 - Resume of the results

Between these models, three of them have similar results in terms of acceleration. Especially, the PIPER and the CRABI-12 model are, between all, the most similar in these terms, also because of their characteristics. In particular, in both models the weight of the head is almost ¼ of the total weight. The accelerations measured in the PIPER's simulation are a bit lower than the one in the CRABI-12 (-3% for the angular, -10% for the linear). A greater difference is for what concern the angular velocity (-46% in the PIPER).

On the other hand, accelerations and velocities given by the Q0 Dummy present relevant differences. This seems to be an effect of the global mass (in particular the head's one); it plays an important role in the outputs of the shaking mechanism. Obviously, the simulated ages are important, especially because the grow rate of a child is very fast in the first year of age: a great difference can be present in a model of 18 months in respect than a model of 1 month.

Also, the analysed trend sometimes present relevant difference (for example looking at the head's movement). This can be also a consequence not only of the mass difference, but more in general of the shaking movement which has been impressed. In addition, it is important to remember that the other models analysed are mannequins, shaken by real person, in opposition with the PIPER which is a finite element model shaken by a shell.

6. CONCLUSIONS

The main task of the thesis's work was performing a simulation of a shaking episode to analyse the phenomenon of Abusive Head Trauma (AHT). This was done using a finite element model, the PIPER Child Model, that replicates an 18-months-old baby.

The simulations gave many outputs that can be seen thanks to LS-PrePost. The ones analysed deeply regarded especially velocities and accelerations of the head. What resulted was a stabilized trend after a certain time, also if some curves were different from the ones expected (after having considered several literature's articles). In particular, the displacement of the head did not replicate a backward-forward movement and probably this is due to the weight of the head. Moreover, the comparison with other child models was for sure a critical point, because of the little amount of data (in particular about trends) found in literature papers. Nevertheless, a comparison with some child models was made, verifying that usually models with similar weights and with similar boundary conditions register comparable maxima values of the kinematic parameters.

For what concerns the injury damages' estimation, what comes from this study was that the reached values of accelerations and velocities are below the thresholds established by some medical and biomechanical works. This should suggest that the Abusive Head Trauma is not normally the first cause of diffuse axonal injury or subdural hematomas, at least if no impacts against any surface are present. Despite this, obviously shaking an infant is potentially dangerous and unsafe, as the evidence of many real cases state. In addition, for what regards the finite element simulation, these results are strictly related with the condition given in terms of shaking law (amplitude and phase), total mass of the body, head's weight and complexity of the model used. It is reasonable to think that different results can come out changing these conditions or introducing an impact, remembering that about it much more articles and researches have been done in literature's work.

REFERENCES

[1] S. Amagasa, H. Matsui, S. Tsuji, S. Uematsu, T. Moriya and K. Kinoshita, "Characteristics distinguishing abusive head trauma fra accidental head trauma in infants with traumatic intracranial hemorrage in Japan," 2018.

[2] M. Niola, C. Musella, L. Paciello, P. Siani, M. Paternoster and P. Di Lorenzo, "Abusive head trauma: aspetti clinici e medico-legali," 2016.

[3] A. Iqbal O'Meara, J. Sequiera and N. Miller Ferguson, "Advances and Future Directions of Diagnosis and Management of Pediatric Abusive Head Trauma: A Rewiew of the Literature," 2020.

[4] J. Caffey, The whiplash shaken infant syndrome: manual shaking by the extremities with whiplash-induced intercranial and intraocular bleedings, linked with residual permanent brain damage and mental retardation, 1974.

[5] F. Testi, "Abusive Head Trauma:casistica clinicae sviluppo di un modello numerico di manichino antropomorfo," Politecnico di Torino, 2018.

[6] P. Gerber and K. Coffman, "Nonaccidental head trauma in infants".

[7] American Academy of Pediatrics, "Committee on Child abuse and neglect".

[8] K. M. Barlow and R. A. Minns, "Lancet," May 2018. [Online]. Available: http://www.ncbi.nlm.nih.gov/pubmed/11075773.

[9] J. Nadarasa, C. Deck, F. Meyer, R. Willinger and R. S. Rau, "Update on injury mechanisms in abusive head trauma - shaken baby syndrome," 2014.

[10] FAMILYDOCTOR.org, "Abusive head trauma," [Online]. Available: https://myhasslefreehomebasebusiness.wordpress.com/diseases-conditions-4/.

[11] D. R. Fulton, "Shaken Baby Syndrome. Critical Care Nurs.".

[12] J. Smith, "Shaken Baby Syndrome. Orthop Nurs".

[13] R. J. Castellani and C. J. Schmidt, "Brain Injury Biomechanics and Abusive Head Trauma," J Forensic Sci Med 2018, 2018.

[14] Wikipedia, "Subdural Hematoma," [Online].

[15] J. Nadarasa, C. Deck, F. Meyer, N. Bourdet, J. S. Raul and R. Willinger, "Development of a finite-element eye model to investigate retinal hemorrhages in shaken baby syndrome," 2017.

[16] D. Graham and T. A. Gennarelli, "Trauma In: Greenfiel's Neuropatology," London, 1997.

[17] S. Klevein, "Head Injury Biomechanics & Criteria".

[18] E. W. Matshes, R. M. Evans, J. K. Pinckard, J. T. Joseph and E. O. Lew, "Shaken infants die of neck trauma, not of brain trauma," 2011.

[19] C. Berardi, "Il maltrattamento fisico: quali conoscenze per il pediatra".

[20] T. Joyce and M. R. Hueker, Pediatric Abusive Head Trauma, 2019.

[21] A. C. Duhaime, T. A. Gennarelli, L. E. Thibault, D. A. Bruce, S. S. Marguiles and R. Wiser, "A clinical, pathological, and biomechanical stud," Philadelphia, Pannsylvania (USA), 1987.

[22] J. Lloyd, E. N. Willey, J. G. Galaznik, W. E. LeeIII and S. E. Luttner, "Biomechanical Evaluation of Head Kinematics During Infant Shaking Versus Pediatric Activities of Daily Living," 2011.

[23] S. Roth, J. Vappou, J. S. Raul and R. Willinger, "Child head injury criteria investigation through numerical simulation of real world data," 2008.

[24] E. G. Takhounts, M. J. Craig, K. Moorhouse, J. McFadde and V. Hasija, "Development of the Brain Injury Criteria (BrIC)," 2013.

[25] M. Shojaati, "Correlation between injury risk and impact severity index ASI," Zurich, 2003.

[26] K. H. Digges, "Injury Measurements and Criteria," Ashburn (USA).

[27] E. G. Takhounts, R. H. Eppinger, J. Q. Campbell, R. E. Tannous, E. D. Power and L. S. Shook, "On the Development of the SIMon Finite Element Head Model," 2003.

[28] E. G. Takhounts, S. A. Ridella, V. Hasija, R. E. Tannous, J. Q. Campbell, D. Malone, K. Danelson, J. Stitzel, S. Rowson and S. Duma, "Investigation of Traumatic Brain Injuries Using the Next Generation of Simulated Injury Monitor (SIMon) Finite Element Head Model," 2008.

[29] F. Meyer, C. Deck and R. Willinger, "Child Head-Neck Finite Element Modelling: towards improved child head injury criteria," Strasburgo, Francia, 2012.

[30] A. Harish, "Finite Element Method - What is it? FEM and FEA explained," [Online].

[31] P. Beillas, C. Giordano, V. Alvarez, X. Li, X. Ying, M.-C. Chevalier, S. Kirscht and S. Kleiven, "Development and performance of the PIPER scalable child human body models".

[32] C. Giordano and S. Klevein, "Development of a 3-year-old Child FE Head Model, Continously Scalable fre 1.5- tp 6-years-old.," Malaga, 2016.

[33] M. T. Davis, A. M. Loyd, H. H. Shen, M. H. Mulroy, R. W. Nightingale, B. S. Myers and C. D. Bass, "The mechanical and morphological properties of 6 year-old cranial bone," in *Journal of Biomechanics*, 2012.

[34] M. Prange and S. Marguiles, "Regional, directional, and age-dependent properties of the brain undergoing large deformation," in *Journal of Biomechanical Engineering*, 2002.

[35] A. Gefen, N. Gefen, Q. Zhu, R. Raghupathi and S. Marguiles, "Age-Dependant Changes in Material Properties of the Brain and Braincase of the Rat," in *Journal of Neurotrauma*, 2003.

[36] S. Chatelin, J. Vappou, S. Roth, J. S. Raul and R. Willinger, "Towards child versus adult brain mechanical properties," in *Journal of Mechanical Behavior of Biomedical Materials*, 2012.

[37] M. MSD, "www.msdmanuals.com," [Online].

[38] EEVC, "Q-dummies Report: Advanced Child Dummies and Injury Criteria for Frontal Impact".

[39] Humanetics, "Q0 (6 week old, Newborn) User Manual".

[40] Humanetics, "CRABI 12M Child Dummy 921022-000-H FMVSS213, 49CFR Part 572, Subpart R".

[41] B. Depreitere, C. Van Lierde, J. V. Sloten, V. A. R. Audd, G. Van der Perre and C. Plets, "Mechanics of acute subdural hematomas resulting from bridging vein rupture," 2006.

[42] S. Cirovic, M. Freddolini, R. Goodwin and D. Zimarev, "Shaken Mannequin Experiments: Head Motion Pattern and Its Potential Effect on Blood Pressure," 2012.

[43] D. R. Wolfson, D. S. McNally, M. J. Clifford and M. Vloebergh, "Rigid-body modelling of shaken baby syndrome," 2005.

[44] M. D. Jones, P. S. Martin, J. M. Williams, A. M. Kemp and P. Theobald, "Development of a computational biomechanical infant model for the investigation of infant head injury by shaking," 2014.

[45] C. A. Jenny, G. Bertocci, T. Fukuda, N. Rangarajan and T. Shams, "Biomechanical Response of the Infant Head to Shaking: An Experimental Investigation," 2017.

[46] R. J. Reimann, "Ph D. Fundamental limits of shaken baby," 2018.

[47] J. Nadarasa, C. Deck, F. Meyer, N. Bourdet, J. S. Raul and R. Willinger, "Development of a finite-element eye model to investigate retinal hemorrhages in shaken baby syndrome," 2017.

[48] W. H. Organization, "www.who.int," [Online].

[49] F. Tosi, A. Brischetto, I. Bruni and D. Busciantella, "La componente dimensionale: le misure antropometriche".

[50] Athlepedia, "Planes of Motion," [Online].

[51] M. Zhang and A. F. T. Mak, "In vivo friction properties of human skin," 1999.

[52] LSTC, LS-Dyna Keyword User Manual Volume I, 2018.

[53] B. Depreteire, C. Van Lierde, J. Vander Sloten, R. Van Audekercke, G. Van Der Perre, C. Plets and J. Goffin, "Mechanism of acute subdural hematomas resulting from bridging vein rupture," 2006.

[54] A. K. Ommaya, W. Goldsmith and L. Thibault, "Biomechanics and neuropathology of adult and paediatric head injury," 2002.

[55] W. P. J. Goldsmith, " A biomechanical analysis of the causes of traumatic brain injury in infants and children," 2004.

[56] Z. Couper and F. Albermani, "Mechanical response of infant brain to manually inflicted shaking," 2009.